
IMPACT OF THE EURO 2020 CHAMPIONSHIP ON THE SPREAD OF COVID-19

Jonas Dehning^{1,¶}, Sebastian B. Mohr^{1,¶}, Sebastian Contreras¹, Philipp Dönges¹, Emil N. Iftekhar¹, Oliver Schulz², Philip Bechtle^{3*a}, and Viola Priesemann^{1,4,5*b}

¹Max Planck Institute for Dynamics and Self-Organization, 37077 Göttingen, Germany.

²Max Planck Institute for Physics, 80805 München, Germany

³Physikalisches Institut, Universität Bonn, 53115 Bonn, Germany

⁴Institute for the Dynamics of Complex Systems, University of Göttingen, 37077 Göttingen, Germany.

⁵Institute of Computer Science and Campus Institute Data Science, University of Göttingen, 37077 Göttingen, Germany

¶These authors contributed equally

* Corresponding authors:

^abechtle@physik.uni-bonn.de

^bviola.priesemann@ds.mpg.de

Abstract

Large-scale events like the UEFA Euro 2020 football (soccer) championship offer a unique opportunity to quantify the impact of gatherings on the spread of COVID-19, as the number and dates of matches played by participating countries resembles a randomized study. Using Bayesian modeling and the gender imbalance in COVID-19 data, we attribute 840,000 (95% CI: [0.39M, 1.26M]) COVID-19 cases across 12 countries to the championship. The impact depends non-linearly on the initial incidence, the reproduction number R , and the number of matches played. The strongest effects are seen in Scotland and England, where as much as 10,000 primary cases per million inhabitants occur from championship-related gatherings. The average match-induced increase in R was 0.46 [0.18, 0.75] on match days, but important matches caused an increase as large as +3. Altogether, our results provide quantitative insights that help judge and mitigate the impact of large-scale events on pandemic spread.

Introduction

Passion for competitive team sports is widespread worldwide. However, the tradition of watching and celebrating popular matches together may pose a danger to COVID-19 mitigation, especially in large gatherings and crowded indoor settings (see, e.g., [1–6]). Interestingly, sports events taking place under substantial contact restrictions had only a minor effect on COVID-19 transmission [7–11]. However, large events with massive media coverage, stadium attendance, increased travel, and viewing parties can play a major role in the spread of COVID-19 — especially if taking place in settings with few COVID-19-related restrictions. This was the case for the UEFA Euro 2020 Football Championship (Euro 2020 in short), staged from June 11 to July 11, 2021. While stadium attendance might only have a minor effect [12–14], it increases TV viewer engagement [15–17] and encourages additional social gatherings [18]. These phenomena and previous observational analyses [19] suggest that the Euro 2020’s impact may have been considerable. Therefore, we used this championship as a case study to quantify the impact of large events on the spread of COVID-19. Counting with quantitative insights on the impact of these events allows policymakers to determine the set of interventions required to mitigate it.

Two facts make the Euro 2020 especially suitable for the quantification. First, the Euro 2020 resembles a randomized study across countries: The time-points of the matches in a country do not depend on the state of the pandemic in that country and how far a team advances in the championship has a random component as well [20]. This independence between the time-points of the match and the COVID-19 incidence allows quantifying the effect of football-related social gatherings without classical biasing effects. This is advantageous compared to classical inference studies quantifying the impact of non-pharmaceutical interventions (NPIs) on COVID-19 where implementing NPIs is a typical reaction to growing case numbers [21–23]. Second, the attendance at match-related events, and thus the cases associated with each match, is expected to show a gender imbalance [24]. This was confirmed by news outlets and early studies [25–28]. Hence, the gender imbalance presents a unique opportunity to disentangle the impact of the matches from other effects on pathogen transmission rates.

Here we build a Bayesian model to quantify the effect large-scale sports events on the spread of COVID-19, using the Euro 2020 as case study. In the following, we use “case” to refer to a confirmed case of a SARS-CoV-2 infections in a human and “case numbers” to refer to the number of such cases. Not all infections are detected and represented in the cases and cases come with a delay after the actual infection. Our model simulates COVID-19 spread in each country using a discrete renewal process [22, 29] for each gender separately, such that the effect of matches can be assessed through the gender imbalance in case numbers. This is defined as “(male incidence - female incidence) / total incidence”, and through the temporal association of cases to match dates of the countries’ teams. Regarding the expected gender imbalance at football-related gatherings, we chose a prior value of 33% (95% percentiles [18%, 51%]) female participants, which is more balanced than the values reported for national leagues (about 20%) [24]. However, this agrees with the expected homogeneous and broad media attention of events like the Euro 2020. For the effective reproduction number R_{eff} we distinguish three additive contributions; the base, NPI-, and behavior-dependent reproduction number R_{base} , a match-induced boost on it $\Delta R_{\text{football}}$, and a noise term ΔR_{noise} , such that $R_{\text{eff}} = R_{\text{base}} + \Delta R_{\text{football}} + \Delta R_{\text{noise}}$. We assume R_{base} to vary smoothly over time, while the effect of single matches $\Delta R_{\text{football}}$ is concentrated on one day and allows for a gender imbalance. The term ΔR_{noise} allows the model to vary the relative reproduction number for each gender independent of the football events smoothly over time. We analyzed data from all participating countries in the Euro 2020 that publish daily gender-resolved case numbers (n=12): England, the Czech Republic, Italy, Scotland, Spain, Germany, France, Slovakia, Austria, Belgium, Portugal, and the Netherlands (ordered by resulting effect size). We retrieved datasets directly from governmental institutions or the COVerAGE-DB [30]. See Supplementary Section S1 for a list of data sources. Our analyses were carried out following FAIR [31] principles; all code, including generated datasets, are publicly available (https://github.com/Priesemann-Group/covid19_soccer).

Results

The main impact arises from the subsequent infection chains

We quantified the impact of the Euro 2020 matches on the reproduction number for the 12 analyzed countries (Fig. 1a) and for every single match (Supplementary Fig. S8). On average, a match increases the reproduction number R by 0.46 (95% CI [0.18, 0.75]) (Fig. 1a and Supplementary Table S4) for a single day. In other words, when a country participated in a match of the Euro 2020 championship, every individual of the country infected on average ΔR_{match} extra persons (see Supplementary Section S2 for more details). The cases resulting from these infections occurring at gatherings on the match days are referred to as primary cases.

However, primary cases are only the tip of the iceberg; any of these cases can initiate a new infection chain, potentially spreading for weeks (see Supplementary Section S2 for more details). We included all subsequent cases until July 31, which is about two weeks after the final. As expected, subsequent cases outnumber the primary cases considerably at a ratio of about 4 : 1 on average (Supplementary Table S3). As a consequence, on average, only 3.2%, [1.3%, 5.2%] of new cases are directly associated with the match-related social gatherings throughout that analysis period (Fig. 1b). This surge of subsequent cases highlights the long-lasting impact of potential single events on the COVID-19 spread (see Supplementary Table S2).

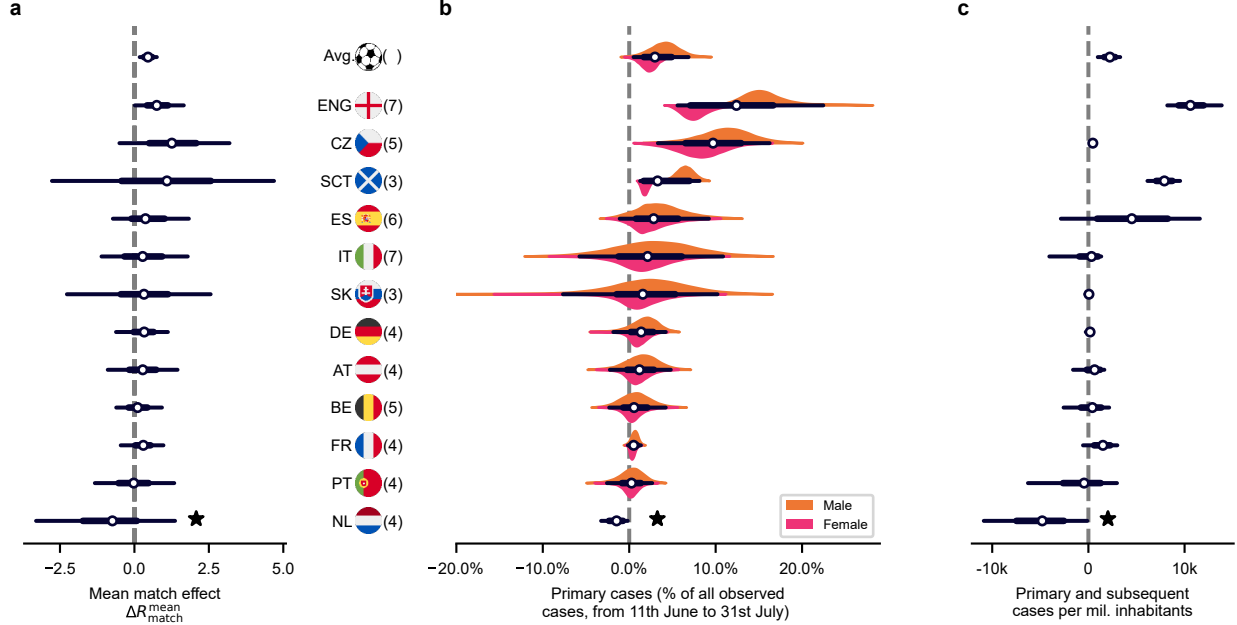


Figure 1: **Quantifying the impact of the Euro 2020 on COVID-19 spread.** **a.** Using Bayesian inference and an SEIR-like model, we infer the mean increase on the reproduction number associated with Euro 2020 matches, $\Delta R_{\text{match}}^{\text{mean}}$, in each analyzed country ($n = 12$ countries). Almost all countries show a median increase larger than zero (cf. Supplementary Table S4). Note that in the Netherlands (★) a complete lifting of restrictions was implemented on 26th of June 2021 (“freedom day”). Apparently, its impact also had the opposite gender imbalance, making it hard for the model to extract the Euro 2020’s effect (Supplementary Fig. S31). **b.** The $\Delta R_{\text{match}}^{\text{mean}}$ enables us to quantify the primary cases, i.e., cases associated directly with the match days (as percentage of all cases from 11th June to 31st July 2021). **c.** Any primary infection at a match can start an infection chain. The total number of primary and subsequent cases that were inferred to be causally related to the Euro 2020 from its start until 31st July depend on the COVID-19 prevalence and the base spread during the analysis period. In parentheses are the number of matches played by the respective team. White dots represent median values, black bars and whiskers correspond to the 68% and 95% credible intervals (CI), respectively, and the distributions in color (truncated at 99% CI) represent the differences by gender (Supplementary Table S2). The Netherlands is left out from the average calculations and subsequent analyses.

We find an increase in COVID-19 spread at the Euro 2020 matches in all countries we analyzed, except for the Netherlands. In the Netherlands, a “freedom day” coincided with the analysis period [32] and was accompanied by the opposite gender imbalance compared to the football matches, thereby apparently inverted the football effect. Therefore, we exclude the Netherlands from general averages and correlation studies, but still display the results for completeness.

The primary and subsequent cases on average amounted to 2.200 (95% CI [986, 3308]) cases per million inhabitants (Fig. 1c, Supplementary Table S2). This amounts to about 0.84 million (CI: [0.39M, 1.26M]) cases related to the Euro 2020 in the 12 countries (cf. Supplementary Table S3). With the case fatality risk of that period, this corresponds to about 1700 (CI: [762, 2470]) deaths, assuming that the primary and subsequent spread affects all ages equally. Most likely this is slightly overestimated since the age groups most at risk from COVID-19 related death are probably underrepresented in football-related social activities and thus more unlikely to be affected by primary championship-related infections. However, the overall number of primary and subsequent cases attributed to the championship is dominated by the subsequent cases, and the mixing of individuals of different age-groups then mitigates this bias. Individually, three countries, England, the Czech Republic, and Scotland showed a significant increase in COVID-19 incidence associated with the Euro 2020, and Spain and France show an increase at the one-sided 90% significance threshold. In other countries such as Germany, only a relatively small contribution of primary cases was associated with the Euro 2020 championship, and a small gender imbalance was observed. Low COVID-19 incidence during the

championship or imprecise temporal association between infection and confirmation of it as a case can lead to a loss of sensitivity and hinder the detection of an effect, as can be seen from the large width of several posterior distributions (e.g., Italy and Slovakia, which had particularly low incidence).

The strongest effect is observed in England and Scotland

Overall, the effect of the Euro 2020 was quite diverse across the participating countries, ranging from almost no additional infections to up to 1% of the entire population being infected (i.e., from Portugal to England, Fig. 1). To illustrate this diversity, the comparison between England, Scotland, and the Czech Republic is particularly illustrative (Fig. 2). For all countries, we disentangled the cases that are considered to happen independently of the Euro 2020 (Fig. 2a, gray), the primary cases directly associated with gatherings on the days of the matches (red), and the subsequent infection chains started by the primary cases (yellow; see Supplementary Fig. S24–S36 for all countries).

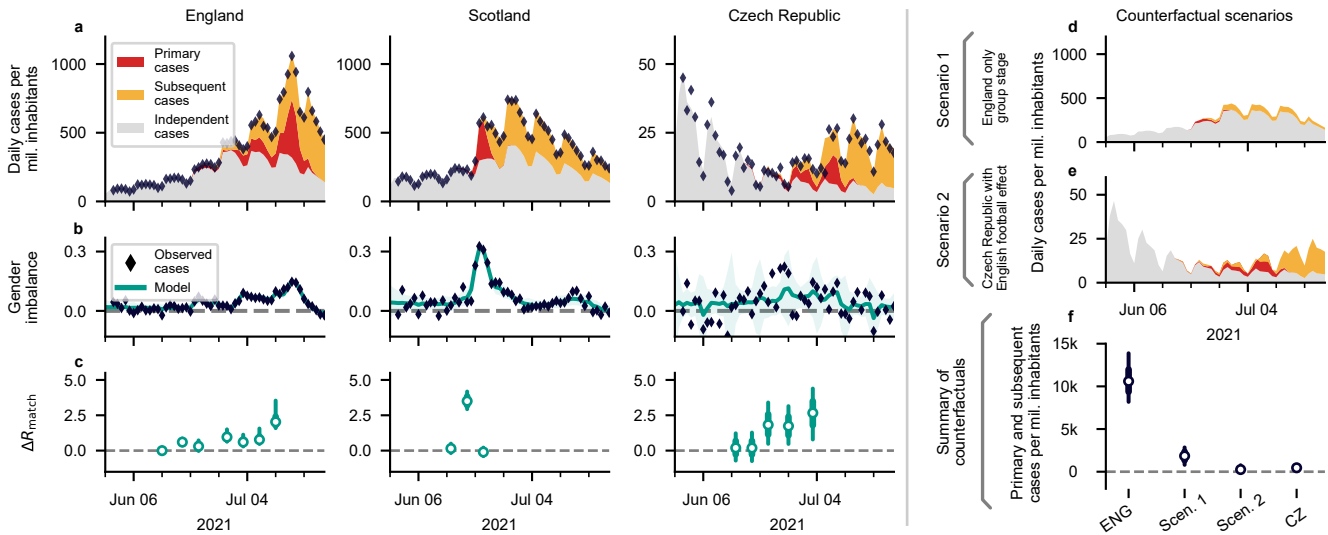


Figure 2: **Example cases illustrate that the spread associated with the Euro 2020 can encompass a substantial fraction of the observed cases.** **a.** The model enables one to split the observed incidence (black diamonds) into: cases independent of Euro 2020 matches (gray area), primary cases (directly associated with Euro 2020 matches, red area), and subsequent cases (additional infection chains started by primary cases, orange area). See supplementary information for all countries (Supplementary Fig. S24–S36). Here and in all following figures, the light blue shaded area signifies the time span of the Euro 2020. **b.** Football-related gatherings, and hence the case numbers, show a gender imbalance. This facilitates the inference of the football-related increase in COVID-19 spread. Here the turquoise shaded areas correspond to 95% CI. **c.** The effect of social gatherings at match days is modeled as a single additive increase in the reproduction number ΔR_{match} concentrated on the day of each match. For example, $\Delta R_{\text{match}} = 2$ means that, on the day of the match, each infected individual on average infected two additional persons (on top of the base trend). **d, e.** The counterfactual scenario assumes that England would not have reached the knockout phase (d, Scen. 1), or that the Czech fans and matches would have been equal to the English by their impact on disease spread; e, Scen. 2). **f.** In the counterfactual scenarios, the Euro 2020 would have had much smaller impact with fewer matches (Scen. 1), or with an overall more favorable pandemic situation as in the Czech Republic (Scen. 2). White dots represent median values, bars and whiskers correspond to the 68% and 95% credible intervals (CI).

England, being the runner-up of the championship and thus played the maximum number of matches, displays the strongest effect over the longest duration, with a substantial increase in reproduction number ΔR_{match} towards the last matches of the championship. This reflects the increasing popularity of the later matches, as e.g., quantified by the increase of the search term on Google (Supplementary Fig. S20). Scotland shows a particularly strong effect of a single match (Scotland vs England) staged in London during the group phase, with $\Delta R_{\text{match}} = 3.5 [2.9, 4.2]$ (Fig. 2c). This means that on average over the total Scottish population, every

single person infected additional 3.5 persons at or around that single day. These are very strong effects. As a consequence, in Scotland the subsequent cases from the single match accounted for about 30% of the cases in the following weeks, illustrating the impact of such gatherings on public health.

Low overall incidence prevents large match-related spread

In the Czech Republic, the situation was different compared to England and Scotland, although the analyses point to similarly strong gatherings on the match days (i.e., large ΔR_{match} , Fig. 1a). However, because of the overall low incidence much fewer people were infected throughout the championship. The advantage of low incidence or fewer games is illustrated in two counterfactual scenarios. Even under the assumption that the Czech team had continued to the final and the population had gathered exactly like the English (i.e., showing the same ΔR_{match} in the matches they played), the total number of cases (per million) would have been more than 40 times lower than in England, owing to the lower base incidence and a lower base reproduction number (Fig. 2d). Assuming, as a counterfactual scenario, that England had dropped out in the group stage, the number of cases associated with the Euro 2020 would have been much lower. This suggests that both the success in the championship and the base incidence and behavior in a country influence the public health impact of such large-scale events.

To better understand the impact of the Euro 2020, we quantified the determinants of the spread across countries. From theory, we expect the absolute number of infections generated by Euro 2020 matches to depend non-linearly on a country's base incidence N_0 , which determines the probability to meet an infected person, and on the effective reproduction number prior to the championship R_{pre} , as a gauge for the underlying infection dynamics generating the subsequent cases, which determines how strongly an additional infection spreads in the population. We can then define the potential for COVID-19 spread as the number of COVID-19 cases that would be expected during the time T a country is playing in the Euro 2020 ($N_0 \cdot R_{\text{pre}}^{T/4}$), assuming a generation interval of 4 days. Indeed, we find a clear correlation between the observed and the expected incidence Fig. 3a, $R^2 = 0.77$ (95% CI [0.39, 0.90]), $p < 0.001$, with a slope of 1.62 (95% CI [1.0, 2.26]). The strong significance of this correlation relies mainly on England and Scotland. However, the observed slope in an analysis without these two countries (0.76, 95% CI: [-1.46, 3.04]), while not significant at the 95% confidence level, is consistent with the findings including all countries. This is shown in Supplementary Fig. S7.

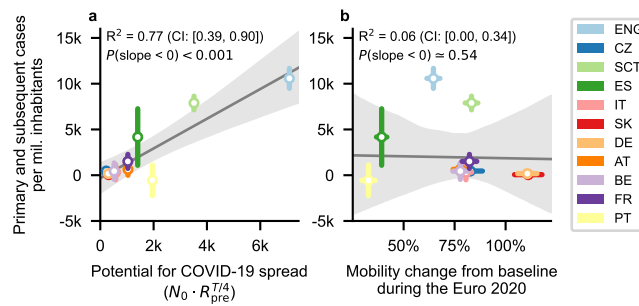


Figure 3: **Which variables can predict the extent of the impact of Euro 2020 matches?** **a.** The potential for spread, i.e., the number of COVID-19 cases that would be expected during the time T a country is playing in the Euro 2020 ($N_0 \cdot R_{\text{pre}}^{T/4}$), is strongly correlated with the number of Euro 2020-related cases. Therefore, policymakers should simultaneously consider the initial incidence N_0 , reproduction number prior to the event R_{pre} , and expected duration of an event T to assess whether it is pertinent to allow it (The correlation is not significant if England and Scotland are left out, but the slope is still consistent with this result.) **b.** Mobility changes from baseline during the Euro 2020 are not correlated with the number of COVID-19 cases associated with the championship in each country. Furthermore, the direction of the effect of mobility per se in this context is unclear. The gray line and area are the median and 95% CI of the linear regression ($n = 11$ countries; The Netherlands was excluded for this analysis). Whiskers denote one standard deviation.

Furthermore, quantifying correlations between N_0 and R_{pre} and the number of primary and subsequent cases related to the Euro 2020, we see a trend for each (Supplementary Fig. S6a and S6b). However, these are weak and statistically significant only for R_{pre} . Altogether, our data suggest that a favorable pandemic situation (low R_{pre} and low N_0) before the gatherings, and low R_{base} during the period of gatherings jointly minimize the impact of the Euro 2020 on community contagion. A prerequisite for this is that the known preventive measures, such as reducing group size, imposing preventive measures, and minimizing the number of encounters remain encouraged.

Independently on the epidemic situation, Euro 2020’s effect might be influenced by people’s prudence and the team’s popularity and success during the championship. While we do not observe any obvious effect of local mobility as a measure of the prudence of people (Fig. 3b, $R^2 = 0.06$ (95% CI [0.00,0.34]), $p=0.54$, and Supplementary Fig. S4), the potential popularity —represented by the number of matches played and hosted by a given country— had a more notable trend (Supplementary Fig. S6c). Still, this correlation was not statistically significant. Moreover, we found no relationship between the effect size and the Oxford governmental response tracker [33] (Supplementary Fig. S5).

Discussion

Large international-scale sports events like the Euro 2020 Football Championship have the potential to gather people like no other type of event. Our quantitative insights on the impact of such gatherings on COVID-19 spread provide policymakers with tools to design the portfolio of interventions required for mitigation (using, e.g., results of [22, 23, 34]). Thereby, our quantification can support society in carefully weighing the positive social, psychological, and economic effects of mass events against the potential negative impact on public health [35]. Our analysis attributes about 0.84 million (95% CI: [0.39M, 1.26M]) additional infected persons to the Euro 2020 championship. Assuming that the primary and subsequent spread affects all ages equally, this corresponds across the 12 countries to about 1700 (CI: [762, 2470]) deaths. Thus, the public health impact of the EURO 2020 was not negligible.

To prevent the impacts of these events, measures, such as promoting vaccination, enacting mask mandates, and limiting gathering sizes, can be helpful. Besides, the effectiveness of such interventions has already been quantified in different settings (e.g., [22, 23]) so that policymakers can weigh them according to specific targets and priorities. Furthermore, focused measures that aim to mitigate disease spread in situ, such as testing campaigns and requiring COVID passports to attend sport-related gatherings and viewing parties, present themselves as helpful options. In addition, one could encourage participants of a large gathering to self-quarantine and test themselves afterward. Moreover, the championship distribution of matches every 4 to 5 days coincides with the mean incubation period and generation interval of COVID-19. This means that individuals who get infected watching a match can turn infectious by the subsequent while potentially pre-symptomatic. Such resonance effects between gathering intervals and incubation time can increase the spread considerably [34]. It thus depends on the design of the championships, on the precautionary behavior of individuals, and on the basic infection situation how much large-scale events threaten public health, even if the reproduction number is transiently increased during these events.

Previous studies that evaluated the impact of sports events on the spread of COVID-19 and considered the spectator gatherings at match venues were not conclusive [7, 8, 36]. This agrees with our results as we find the impact of hosting a match to be small to non-existent (Supplementary Fig. S9). However, location having little effect may well be specific to the Euro 2020, where matches were distributed across different countries. In the traditional settings of the UEFA European Football Championship or the FIFA World Cup, a single country or a small group of countries hosts the entire championship, and the championship is accompanied by elaborate supporting events, public viewing, and extensive travel of international guests. Hence, for future championships, such as, e.g., the World Cup 2022 in Qatar or the Euro 2024 in Germany, the impact of location might be considerably larger.

Our model accounts for slow changes in the transmission rates that are unrelated to football matches through the gender-independent reproduction number R_{base} . We find R_{base} to increase at least transiently during the championship in all 12 countries except for England and Portugal (Supplementary Fig. S24 to Supplementary Fig. S35). The above may suggest that our estimate of the match effect ΔR_{match} is conservative: The overall

increase of COVID-19 spread might in part be attributed to R_{base} , but will not be incorrectly associated with football matches. Our results might further be biased if the incidence and the teams’ progression in the Euro 2020 are correlated. It is conceivable that high incidence would negatively correlate with team progression through ill or quarantined team members. However, there were only few such cases during the Euro 2020 [37], and the correlation might also be positive: At higher case numbers the team might be more careful. Hence, the correlation is unclear and probably negligible.

The COVID-19 spread obviously depends on many factors. However, many of those parameters, such as the vaccination rate, the contact behavior or motivation to be tested, are changing slowly over time and hence can be absorbed into the slowly changing base reproduction rate R_{base} and the gender-asymmetric noise ΔR_{noise} ; other parameters, like social and regional differences, age-structure or specific contact networks are expected to be constant over time and average out across a country. To further test the robustness of our model, we systematically varied the prior assumptions on the central model parameters, among them the delay (Supplementary Fig. S12), the width of the delay kernel (Supplementary Fig. S13), the change point interval (Supplementary Fig. S14), the generation interval (Supplementary Fig. S16) and a range of other priors (Supplementary Fig. S17). Furthermore, when using wider prior ranges for the gender imbalance, football-related COVID-19 cases remain unchanged but the uncertainty increases (Supplementary Fig. S15), thus validating our choice. Even for the case of prior symmetric gender imbalance assumptions, the posterior distribution of the female participation converges for the three most significant countries to median values between 20% – 45%. As last cross-check, we made sure that we found no effect when shifting the match dates by 2 weeks relative to the case numbers (Supplementary Fig. S10) nor by shifting match dates outside the championship range, by more than ± 30 days (Supplementary Fig. S11).

Besides quantifying the impact of matches on the reproduction number, our methodology allowed us to estimate the delay between infections and confirmation of positive tests D without a requirement to identify the source of each infection (Supplementary Fig. S19). Our estimates for D in the participating countries were around 3-5 days (England: 4.5 days (95% CI [4.3, 5]), Scotland: 3.5 days (95% CI [3.3, 3.8]), Supplementary Fig. S24, Supplementary Fig. S33g, and Supplementary Table S4). This agrees with available literature and is an encouraging signal for the feasibility of containing COVID-19 with test-trace-and-isolate [38–42]. However, we expect that some individuals would actively get tested right after a match, thereby increasing the case finding and reporting rates. This can slightly affect our estimates for the delay distribution D and would require additional information to be corrected. Altogether, analyzing large-scale events with precise timing and substantial impact on the spread presents a promising, resource-efficient complement to classical quantification of delays.

Understanding how popular events with major in-person gatherings affect the spreading dynamics of COVID-19 can help us design better strategies to prevent new outbreaks. The Euro 2020 had a pronounced impact on the spread despite considerable awareness of the risks of COVID-19. We estimate that e.g. about 48% of all cases in England until July 31st are related to the championship. In future, with declining awareness about COVID-19 but potentially better immunity, similar mass events, such as the football world cups, the Super Bowl, or the Olympics, will still unfold their impact. Acute, long- and post-COVID-19 will continue to pose a challenge to societies in the years to come. Our analysis suggest that a combination of low R_{pre} and low initial incidence at the beginning of the event, together with the known preventive measures, can strongly reduce the impact of these events on community contagion. Fulfilling these preconditions and increasing health education in the general population can substantially reduce the adverse health effects of future mass events.

Methods

To estimate the effect of the championship in different countries we constructed a Bayesian model which uses the reported case numbers in twelve countries. Ethical approval was not sought as we only worked with openly available data. A graphical overview of the inference model is given in Fig. 4 and model variables, prior distributions, indices, country-dependent priors, and sampling performance are summarized in Tables 1, 2, 3, 4, and 5, respectively.

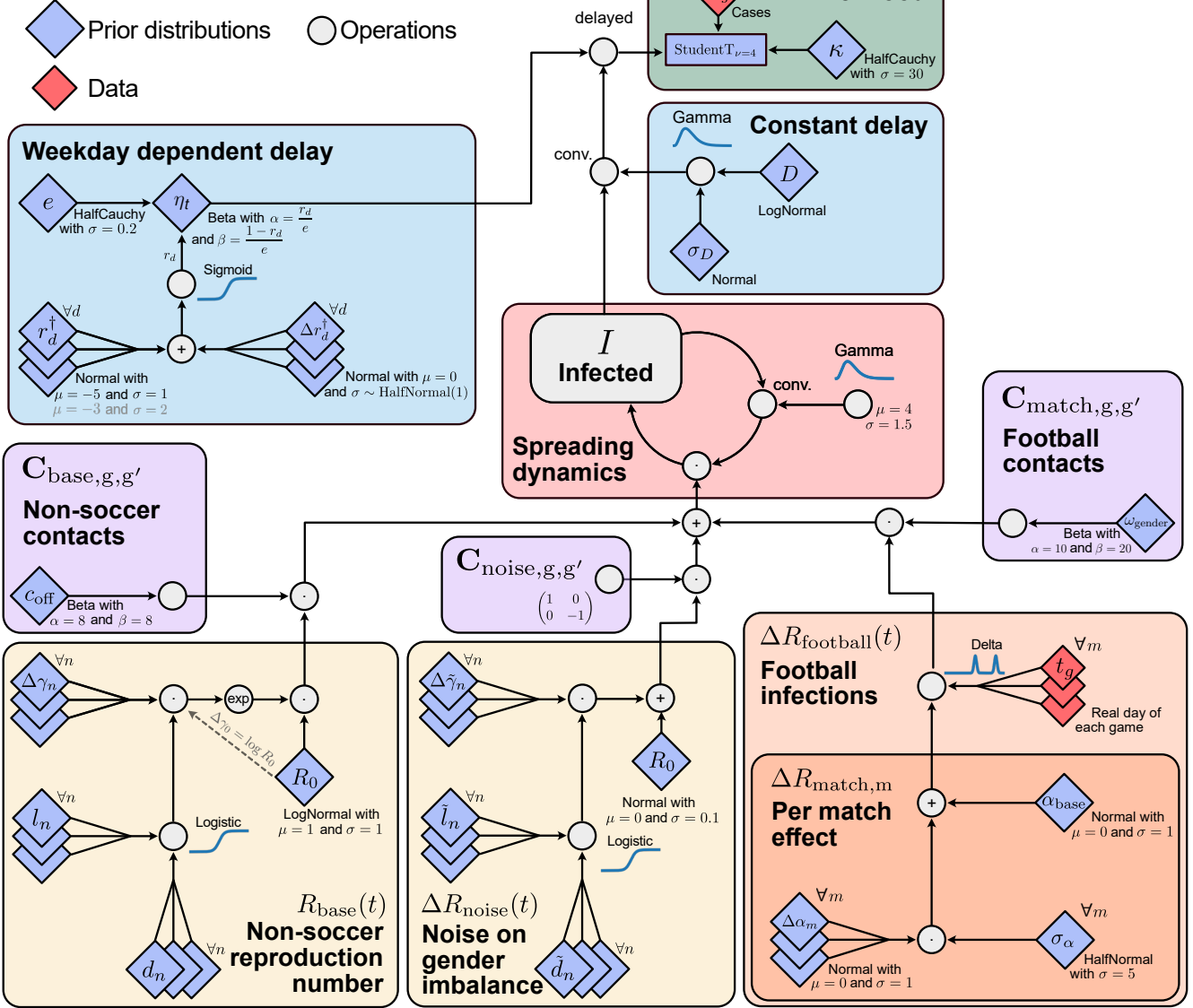
Model Overview


Figure 4: **Model Overview**, illustrating the relationship between the chosen prior distributions and the disease dynamics. Boxes in the flowchart are color-coded according to what they describe; Light blue boxes: delay modulations. Green boxes: likelihoods. Red boxes: spreading dynamics. Purple boxes: contact matrices. Yellow boxes: effects independent of football matches. Orange boxes: effects of the football matches. Diamonds show prior distributions (blue) or incorporated data (red), and gray circles denote any mathematical operation.

Modelling the spreading dynamics including gender imbalance

The model simulates the spread of COVID-19 in each country separately using a discrete renewal process [22, 29, 43]. We infer a time-dependent effective reproduction number with gender interactions between genders g and g' , $R_{eff,g,g'}(t)$, for each country [21].

Even though participation of women in football fan activity has increased in the last decades [44], football fans are still predominantly male [24]. Hence one expects a higher infection probability at the days of the match for the male compared to the female population. Integrating this information into the model by using gender resolved case numbers, allows improved inference of the Euro 2020's impact. In the following, genders

“male” and “female” are denoted by the subscripts $\cdot_{g=1}$ and $\cdot_{g=2}$, respectively. Furthermore, we modeled the spreading dynamics of COVID-19 in each country separately.

In the discrete renewal process for disease dynamics of the respective country, we define for each gender g a susceptible pool S_g and an infected pool I_g . With N denoting the population size, the spreading dynamics with daily time resolution t reads as

$$I_g(t) = \frac{S_g(t)}{N} \sum_{g'=1}^2 \mathbf{R}_{\text{eff},g,g'}(t) \sum_{\tau=0}^{10} I_{g'}(t-1-\tau) G(\tau), \quad (1)$$

$$S_g(t) = S_g(t-1) - E_g(t-1), \quad (2)$$

$$G(\tau) = \text{Gamma}(\tau; \mu = 4, \sigma = 1.5). \quad (3)$$

We apply a discrete convolution in equation (1) to account for the latent period and subsequent infection (red box in Fig. 4). This generation interval (between infections) is modeled by a Gamma distribution $G(\tau)$ with a mean μ of four days and standard deviation σ of one and a half days. This is a little longer than the estimates of the generation interval of the Delta variant [45, 46], but shorter than the estimated generation interval of the original strain [47, 48]. The impact of the choice of generation interval has negligible impact on our results (Supplementary Fig. S16). The infected compartment (commonly I) is not modeled explicitly as a separate compartment, but implicitly with the assumed generation interval kernel.

The effective spread in a given country is described by the country-dependent effective reproduction numbers for infections of individuals of gender g by individuals of gender g'

$$\mathbf{R}_{\text{eff},g,g'}(t) = R_{\text{base}}(t)C_{\text{base},g,g'} + \Delta R_{\text{football}}(t)C_{\text{match},g,g'} + \Delta R_{\text{noise}}(t)C_{\text{noise},g,g'}, \quad (4)$$

where $C_{\text{base},g,g'}$, $C_{\text{match},g,g'}$, and $C_{\text{noise},g,g'}$ describe the entries of the contact matrices \mathbf{C}_{base} , $\mathbf{C}_{\text{match}}$, $\mathbf{C}_{\text{noise}}$ respectively (purple boxes in Fig. 4).

This effective reproduction number is a function of three different reproduction numbers (yellow and orange boxes in Fig. 4):

1. a slowly changing base reproduction number R_{base} (22) that has the same effect on both genders; besides incorporating the epidemiological information given by the basic reproduction number R_0 , it represents the day-to-day contact behavior, including the impact of non-pharmaceutical interventions (NPIs), voluntary preventive measures, immunity status, etc.
2. the reproduction number associated with social gatherings in the context of a football match $R_{\text{match}}(t)$ (11); this number is only different from zero on days with matches that the respective country's team participates in and it has a larger effect on men than on women.
3. a slowly changing noise term $\Delta R_{\text{noise}}(t)$ (31), which subsumes all additional effects which might change the incidence ratio between males and females (gender imbalance).

The interaction between persons of specific genders is implemented by effective contact matrices $\mathbf{C}_{\text{match}}$, \mathbf{C}_{base} and $\mathbf{C}_{\text{noise}}$. All three are assumed to be symmetric.

\mathbf{C}_{base} describes non-football related contacts outside the context of Euro 2020 matches (left purple box in Fig. 4):

$$\mathbf{C}_{\text{base}} = \begin{pmatrix} 1 - c_{\text{off}} & c_{\text{off}} \\ c_{\text{off}} & 1 - c_{\text{off}} \end{pmatrix}, \quad (5)$$

$$\text{with } c_{\text{off}} \sim \text{Beta}(\alpha = 8, \beta = 8). \quad (6)$$

Here, we have the prior assumption that contacts between women, contacts between men, and contacts between women and men are equally probable. Hence, we chose the parameters for the Beta distribution such that c_{off} has a mean of 50% with a 2.5th and 97.5th percentile of [27%, 77%]. This prior is chosen such that

it is rather uninformative. As shown in Supplementary Fig. S17, this and other priors of auxiliary parameters do not affect the parameter of interest if their width is varied within a factor of 2 up and down.

$\mathbf{C}_{\text{match}}$ describes the contact behavior in the context of the Euro 2020 football matches (right purple box in Fig. 4). Here, we assume as a prior that the female participation in football-related gatherings accounts for $\simeq 33\%$ (95% percentiles [18%,51%] of the total participation). Hence, we get the following contact matrix

$$\mathbf{C}_{\text{match, unnorm.}} = \begin{pmatrix} (1 - \omega_{\text{gender}})^2 & \omega_{\text{gender}}(1 - \omega_{\text{gender}}) \\ \omega_{\text{gender}}(1 - \omega_{\text{gender}}) & \omega_{\text{gender}}^2 \end{pmatrix} \quad (7)$$

$$\mathbf{C}_{\text{match}} = \frac{\mathbf{C}_{\text{match, unnorm.}}}{\left\| \mathbf{C}_{\text{match, unnorm.}} \cdot \begin{pmatrix} 0.5 & 0.5 \end{pmatrix}^T \right\|_2} \quad (8)$$

$$\omega_{\text{gender}} \sim \text{Beta}(\alpha = 10, \beta = 20). \quad (9)$$

The prior beta distribution of ω_{gender} is bounded between at 0 and 1 and with the parameter values of $\alpha = 10$ and $\beta = 20$ has the expectation value of $1/3$. The robustness of the choice of this parameter is explored in Supplementary Fig. S15. $\mathbf{C}_{\text{match}}$ is normalized such that for balanced case numbers (equal case numbers for men and women) and an additive reproduction number $R_{\text{match}} = 1$ will lead to a unitary increase of total case numbers. The reproduction number of women will therefore increase by $2\omega_{\text{gender}}\Delta R_{\text{match}}(t)$ on match days whereas the one of men will increase by $2(1 - \omega_{\text{gender}})\Delta R_{\text{match}}$, assuming balanced case numbers beforehand.

$\mathbf{C}_{\text{noise}}$ describes the effect of an additional noise term, which changes gender balance without being related to football matches (middle purple box in Fig. 4). For simplicity, it is implemented as

$$\mathbf{C}_{\text{noise}} = \begin{pmatrix} 1 & 0 \\ 0 & -1 \end{pmatrix}, \quad (10)$$

whereby we center the diagonal elements such that the cases introduced by the noise term sum up to zero, i.e. $\sum_{i,j} R_{\text{noise}} \cdot C_{\text{noise},i,j} = 0$.

Football related effect

Our aim is to quantify the number of cases (or equivalently the fraction of cases) associated with the Euro 2020, Γ_g^{Euro} . To that end we assume that infections can occur at public or private football screenings in the two countries participating in the respective match m (parameterized by $\Delta R_{\text{match},m}$). Note that for the Euro 2020 not a single country, but a set of 11 countries hosted the matches. The participation of a team or the staging of a match in a country may have different effect sizes. Thus, we define the football related additive reproduction number as

$$\Delta R_{\text{football}}(t) := \sum_m \Delta R_{\text{match},m} \cdot \delta(t_m - t). \quad (11)$$

We assume the effect of each match to only be effective in a small time window centered around the day of a match m , t_m (light orange box in Fig. 4). Thus, we apply an approximate delta function $\delta(t_m - t)$. To guarantee differentiability and hence better convergence of the model, we did not use a delta distribution but instead a narrow normal distribution centered around t_m , with a standard deviation of one day:

$$\delta(t) = \frac{1}{\sqrt{2\pi}} \exp\left(-\frac{t^2}{2}\right). \quad (12)$$

We distinguish between the effect size of each match m on the spread of COVID-19. For modeling the effect $\Delta R_{\text{match},m}$, associated with public or private football screenings in the home country, we introduce one base effect $\Delta R_{\text{match}}^{\text{mean}}$ and a match specific offset $\Delta\alpha_m$ for a typical hierarchical modeling approach (dark orange box in Fig. 4). As prior we assume that the base effect $\Delta R_{\text{match}}^{\text{mean}}$ is centered around zero, which means that in principle also a negative effect of the football matches can be inferred:

$$\Delta R_{\text{match},m} = \alpha_{\text{prior},m} (\Delta R_{\text{match}}^{\text{mean}} + \Delta\alpha_m) \quad (13)$$

$$\Delta R_{\text{match}}^{\text{mean}} \sim \mathcal{N}(0, 5) \quad (14)$$

$$\Delta\alpha_m \sim \mathcal{N}(0, \sigma_\alpha) \quad (15)$$

$$\sigma_\alpha \sim \text{HalfNormal}(5). \quad (16)$$

$\alpha_{\text{prior},m}$ is the m -th element of the vector that encodes the prior expectation of the effect of a match on the reproduction number. If a country participated in a match, the entry is 1 and otherwise 0. The robustness of the results with respect to the hyperprior σ_α is explored in Supplementary Fig. S17.

For Supplementary Fig. S9, we expand the model by including the effect of infections happening in stadiums and in the vicinity of it as well as during travel towards the venue of the match. In detail, we add to the football related additive reproduction number (eq. (11)) an additive effect $\Delta R_{\text{stadium},m}$:

$$\Delta R_{\text{football}}(t) := \sum_m (\Delta R_{\text{match},m} + \Delta R_{\text{stadium},m}) \cdot \delta(t_m - t). \quad (17)$$

Analogously to the gathering-related effect we apply the same hierarchy to the effect caused by hosting a match in the stadium – but change the prior of the day of the effect:

$$\Delta R_{\text{stadium},m} = \beta_{\text{prior},m} (\Delta R_{\text{stadium}}^{\text{mean}} + \Delta\beta_m) \quad (18)$$

$$\Delta R_{\text{stadium}}^{\text{mean}} \sim \mathcal{N}(0, 5) \quad (19)$$

$$\Delta\beta_m \sim \mathcal{N}(0, \sigma_\beta) \quad (20)$$

$$\sigma_\beta \sim \text{HalfNormal}(5). \quad (21)$$

$\beta_{\text{prior},m}$ encodes whether or not a match was *hosted* by the respective country, i.e. equates 1 if the match took place in the country and otherwise equates 0.

Non-football related reproduction number

To account for effects not related to the football matches, e.g. non-pharmaceutical interventions, vaccinations, seasonality or variants, we introduce a slowly changing reproduction number $R_{\text{base}}(t)$, which is identical for both genders and should map all other not specifically modeled gender independent effects (left yellow box in Fig. 4):

$$R_{\text{base}}(t) = R_0 \exp\left(\sum_n \gamma_n(t)\right) \quad (22)$$

$$R_0 \sim \text{LogNormal}(\mu = 1, \sigma = 1) \quad (23)$$

This base reproduction number is modeled as a superposition of logistic change points $\gamma(t)$ every 10 days, which are parameterized by the transient length of the change points l , the date of the change point d and the effect of the change point $\Delta\gamma_n$. The subscripts n denotes the discrete enumeration of the change points:

$$\gamma_n(t) = \frac{1}{1 + e^{-4/l_n \cdot (t - d_n)}} \cdot \Delta\gamma_n \quad (24)$$

$$\Delta\gamma_n \sim \mathcal{N}(0, \sigma_{\Delta\gamma}) \quad \forall n \quad (25)$$

$$\sigma_{\Delta\gamma} \sim \text{HalfCauchy}(0.5) \quad (26)$$

$$l_n = \log(1 + \exp(l_n^\dagger)) \quad (27)$$

$$l_n^\dagger \sim \mathcal{N}(4, 1) \quad \forall n \quad (\text{unit is days}) \quad (28)$$

$$d_n = 27^{\text{th}} \text{ May } 2021 + 10 \cdot n + \Delta d_n \quad \text{for } n = 0, \dots, 9 \quad (29)$$

$$\Delta d_n \sim \mathcal{N}(0, 3.5) \quad \forall n \quad (\text{unit is days}). \quad (30)$$

The idea behind this parameterization is that $\Delta\gamma_n$ models the change of R-value, which occurs at times d_n . These changes are then summed in equation (24). Change points that have not occurred yet at time t do not

contribute in a significant way to the sum as the sigmoid function tends to zero for $t \ll d_n$. The robustness of the results regarding the spacing of the change-points d_n is explored in Supplementary Fig. S14 and the robustness of the choice of the hyperprior $\sigma_{\Delta\gamma}$ is explored in Supplementary Fig. S17.

Similarly, to account for small changes in the gender imbalance, the noise on the ratio between infections in men and women is modeled by a slowly varying reproduction number (middle yellow box in Fig. 4), parameterized by series of change points every 10 days:

$$\Delta R_{\text{noise}}(t) = \Delta R_{0,\text{noise}} + \left(\sum_n \tilde{\gamma}_n(t) \right) \quad (31)$$

$$\Delta R_{0,\text{noise}} \sim \mathcal{N}(\mu = 0, \sigma = 0.1) \quad (32)$$

$$\tilde{\gamma}_n(t) = \frac{1}{1 + e^{-4/\tilde{l}_n \cdot (t - \tilde{d}_n)}} \cdot \Delta \tilde{\gamma}_n \quad (33)$$

$$\Delta \tilde{\gamma}_n \sim \mathcal{N}(0, \sigma_{\Delta \tilde{\gamma}}) \quad (34)$$

$$\sigma_{\Delta \tilde{\gamma}} \sim \text{HalfCauchy}(0.2) \quad (35)$$

$$\tilde{l}_n = \log(1 + \exp(\tilde{l}_n^\dagger)) \quad (36)$$

$$\tilde{l}_n^\dagger \sim \mathcal{N}(4, 1) \quad \forall n \quad (\text{unit is days}) \quad (37)$$

$$\tilde{d}_n = 27^{\text{th}} \text{ May } 2021 + 10 \cdot n + \Delta \tilde{d}_n \quad \text{for } n = 0, \dots, 9 \quad (38)$$

$$\Delta \tilde{d}_n \sim \mathcal{N}(0, 3.5) \quad \forall n \quad (\text{unit is days}). \quad (39)$$

Delay

Modeling the delay between the time of infection and the reporting of it is an important part of the model (blue boxes in Fig. 4); it allows for a precise identification of changes in the infection dynamics because of football matches and the reported cases. We split the delay into two different parts: First we convolved the number of newly infected people with a kernel, which delays the cases between 4 and 7 days. Second, to account for delays that occur because of the weekly structure (some people might delay getting tested until Monday if they have symptoms on Saturday or Sunday), we added a variable fraction that delays cases depending on the day of the week.

Constant delay: To account for the latent period and an eventual apparition of symptoms we apply a discrete convolution, a Gamma kernel, to the infected pool (right blue box in Fig. 4). The prior delay distribution D is defined by incorporating knowledge about the country specific reporting structure: If the reported date corresponds to the moment of the sample collection (which is the case in England, Scotland and France) or if the reported date corresponds to the onset of symptoms (which is the case in the Netherlands), we assumed 4 days as the prior median of the delay between infection and case. If the reported date corresponds to the transmission of the case data to the authorities, we assumed 7 days as prior median of the delay. If we do not know what the published date corresponds to, we assumed a median \bar{D}_{country} of 5 days, with a larger prior standard deviation $\sigma_{\log \bar{D}}$ (see tab. 4):

$$C_g^\dagger(t) = \sum_{\tau=1}^T E_g(t - \tau) \cdot \text{Gamma}(\tau; \mu = D, \sigma = \sigma_D) \quad (40)$$

$$D = \log(D^\dagger) \quad (41)$$

$$D^\dagger \sim \mathcal{N}(\mu = \exp(\bar{D}_{\text{country}}), \sigma = \sigma_{\log \bar{D}}) \quad (42)$$

$$\sigma_D \sim \mathcal{N}(\mu = 0.2 \cdot \bar{D}_{\text{country}}, \sigma = 0.08 \cdot \bar{D}_{\text{country}}). \quad (43)$$

Here, Gamma represents the delay kernel. We obtain a delayed number of infected persons C_g^\dagger by delaying the newly infected number of persons $I_g(t)$ of gender g from eq. (1). The robustness of the choice of the width of the delay kernel σ_D is explored in Supplementary Fig. S17.

Weekday dependent delay: Because of the different availability of testing resources during a week, we further delay a fraction of persons, depending on the day of the week (left blue box in Fig. 4). We model the fraction η_t of delayed tests on a day t in a recurrent fashion, meaning that if a certain fraction gets delayed on Saturday, these same individuals can still get delayed on Sunday (eq. (44)). The fraction η_t is drawn separately for each individual day. However, the prior is the same for certain days of the week d (eq. (45)): We assume that few tests get delayed on Tuesday, Wednesday and Thursday, using a prior with mean 0.67% (eq. (48)), whereas we assume that more tests might be delayed on Monday, Friday, Saturday and Sunday. Hence compared to C_g^\dagger , we obtain slightly more delayed numbers of cases \hat{C}_g , which now include a weekday dependent delay:

$$\hat{C}_g(t) = (1 - \eta_t) \cdot \left(C_g^\dagger(t) + \eta_{t-1} \hat{C}_g(t-1) \right) \quad \text{with } \hat{C}_g(0) = C_g^\dagger(0) \quad (44)$$

$$\eta_t \sim \text{Beta} \left(\alpha = \frac{r_d}{e}, \beta = \frac{1 - r_d}{e} \right) \quad \text{with } d = \text{Monday}, \dots, \text{Sunday} \quad (45)$$

$$r_d = \text{sigmoid} \left(r_d^\dagger \right) \quad (46)$$

$$r_d^\dagger = r_{\text{base},d}^\dagger + \Delta r_d^\dagger \quad (47)$$

$$r_{\text{base},d}^\dagger \sim \mathcal{N}(-5, 1) \quad \text{for } d = \text{Tuesday}, \text{Wednesday}, \text{Thursday} \quad (48)$$

$$r_{\text{base},d}^\dagger \sim \mathcal{N}(-3, 2) \quad \text{for } d = \text{Friday}, \text{Saturday}, \text{Sunday}, \text{Monday} \quad (49)$$

$$\Delta r_d^\dagger \sim \mathcal{N}(0, \sigma_r) \quad (50)$$

$$\sigma_r \sim \text{HalfNormal}(1) \quad (51)$$

$$e \sim \text{HalfCauchy}(0.2). \quad (52)$$

The parameter r_d is defined such that it models the mean of the Beta distribution of eq. (45), whereas e models the scale of the Beta distribution. r_d is then transformed to an unbounded space by the sigmoid $f(x) = \frac{1}{1 + \exp(-x)}$ (eq. (46)). This allows to define the hierarchical prior structure for the different weekdays. We chose the prior of $r_{\text{base},d}^\dagger$ for Tuesday, Wednesday and Thursday such that only a small fraction of cases are delayed during the week. The chosen prior in equation (48) corresponds to a 2.5th and 97.5th percentile of r_d of [0%; 5%]. For the other days (Friday, Saturday, Sunday, Monday), the chosen prior leaves a lot of freedom for inferring the delay. Equation (49) corresponds to a 2.5th and 97.5th percentile of r_d of [0%; 72%]. The robustness of the other priors σ_r and e is explored in Supplementary Fig. S17.

Likelihood

Next we want to define the goodness of fit of our model to the sample data. The likelihood of that is modeled by a Student-t distribution, which allows for some outliers because of its heavier tails compared to a normal distribution (green box in Fig. 4). The error of the Student-t distribution is proportional to the square root of the number of cases, which corresponds to the scaling of the errors in a Poisson or Negative Binomial distribution:

$$C_g(t) \sim \text{StudentT}_{\nu=4} \left(\mu = \hat{C}_g(t), \sigma = \kappa \sqrt{\hat{C}_g(t) + 1} \right) \quad \text{with} \quad (53)$$

$$\kappa \sim \text{HalfCauchy}(\sigma = 30). \quad (54)$$

Here $C_g(t)$ is the measured number of cases in the population of gender g as reported by the respective health authorities, whereas $\hat{C}_g(t)$ is the modeled number of cases (eq. (44)). The robustness of the prior κ is explored in Supplementary Fig. S17.

Average effect across countries

In order to calculate the mean effect size across countries (Fig. 1 B, C), we average the individual effects of each country. To be consistent in our approach, we build an hierarchical Bayesian model accounting for the individual uncertainties of each country estimated from the width of the posterior distributions. As effect size, we use the fraction of primary cases associated with football matches during the championship. Then our estimated mean effect size \hat{I}_g across all countries c (except the Netherlands) for the gender g is inferred with the following model:

$$\hat{I}_g \sim \text{Normal}(\mu = 0, \sigma = 2) \quad \text{with } g = \{\text{male, female}\} \quad (55)$$

$$\tau_g \sim \text{HalfCauchy}(\beta = 10) \quad (56)$$

$$I_{c,g}^\dagger \sim \text{Normal}(\mu = \hat{I}_g, \sigma = \tau_g) \quad (57)$$

$$\hat{\sigma}_{c,g} \sim \text{HalfCauchy}(\beta = 10) \quad (58)$$

$$I_{s,c,g} \sim \text{StudentT}_{\nu=4}(\mu = I_{c,g}^\dagger, \sigma = \hat{\sigma}_{c,g}). \quad (59)$$

The estimated effect size of each country (the fraction of primary cases) is denoted by $I_{c,g}^\dagger$ and the effect size of individual samples s from the posterior of the main model is denoted by $I_{s,c,g}$.

We applied a similar hierarchical model but without gender dimensions and with slightly different priors to calculate the average mean match effect $\Delta R_{\text{match}}^{\text{mean}}$ (Fig. 1 A). Here by reusing the same notation:

$$\hat{I} \sim \text{Normal}(\mu = 0, \sigma = 10) \quad (60)$$

$$\tau \sim \text{HalfCauchy}(\beta = 10) \quad (61)$$

$$I_c^\dagger \sim \text{Normal}(\mu = \hat{I}, \sigma = \tau) \quad (62)$$

$$\hat{\sigma}_c \sim \text{HalfCauchy}(\beta = 10) \quad (63)$$

$$\Delta R_{\text{match},c,s}^{\text{mean}} \sim \text{StudentT}_{\nu=4}(\mu = I_c^\dagger, \sigma = \hat{\sigma}_c), \quad (64)$$

where $\Delta R_{\text{match},c,s}^{\text{mean}}$ are the posterior samples from the main model runs of the $\Delta R_{\text{match}}^{\text{mean}}$ variable.

Calculating the primary and subsequent cases

We compute the number of primary football related infected $I_{\text{primary},g}(t)$ as the number of infections happening at football related gathering. The percentage of primary cases f_g is then computed by dividing by the total number of infected $I_g(t)$.

$$I_{\text{primary},g}(t) = \frac{S(t)R_{\text{football}}(t)}{N} \sum_{g'} I_{g'}(t) \mathbf{C}_{\text{football},g',g} \quad (65)$$

$$f_g = \sum_t \frac{I_{\text{primary},g}(t)}{I_g(t)} \quad t \in [\text{11th June, 31st July}] \quad (66)$$

To obtain the subsequent infected $I_{\text{subsequent},g}(t)$ we subtract infected obtained from a hypothetical scenario without football games $I_{\text{none},g}(t)$ from the total number of infected.

$$I_{\text{subsequent},g} = I_g(t) - I_{\text{primary},g}(t) - I_{\text{none},g}(t) \quad (67)$$

$$(68)$$

Specific, we consider a counterfactual scenario, where we sample from our model leaving all inferred parameters the same expect for the football related reproduction number $R_{\text{football},g}(t)$, which we set to zero.

Sampling

The sampling was done using PyMC3 [49]. We use a NUTS sampler [50], which is a Hamiltonian Monte-Carlo sampler. As random initialization often leads to some chains getting stuck in local minima, we run 32

chains for 500 initialization steps and chose the 8 chains with the highest unnormalized posterior to continue tuning and sampling. We then let these chains tune for additional 2,000 steps and draw 4,000 samples. The maximum tree depth was set to 12.

The quality of the mixing was tested with the \mathcal{R} -hat measure [51] (Table 5). The \mathcal{R} -hat value measures how well chains with different starting values mix; optimal are values near one. We measured twice: (1) for all variables and (2) for the subset of variables encoding the reproduction number. Variables modeling the reproduction number are the central part of our model (lower half of Fig. 4). As such, we are satisfied if the \mathcal{R} -hat values is sufficiently good for these variables, which it is (≤ 1.07). The high \mathcal{R} -hat when calculated over all variables is mostly due to the weekday-dependent delay, which we assume is not central to the results we are interested in.

Robustness tests

In the base model for each country, we only consider the matches in which the respective country participated. It is reasonable to ask whether the matches of foreign countries occurring in local stadium have an effect on the case numbers, caused by transmission in and around the stadium and related travel. To investigate this question we ran a model with an additional parameter (in-country effect) associating the case numbers to the in-country matches (eq. (17)). In some countries the in-country effect parameter and the original fan gathering effect are covariant, as a large number of matches are played by the country at home whereas in other countries the additional parameter had no significant effect (Supplementary Fig. S9).

We checked that the inferred fractions of football related cases are robust against changes in the priors of the width σ_D of the delay parameter D (see Supplementary Fig. S13) and the intervals of change points of R_{base} (Supplementary Fig. S14). The results are also, to a very large degree, robust against a more uninformative prior on the fraction of female participants in the fan activities dominating the additional transmission ω_{gender} (Supplementary Fig. S15). To reduce CO2-emissions we performed fewer runs for these robustness tests: We only ran the models for which the original posterior distributions might indicate that one could find a significant effect. Each country required eight cores for about 10 days to finish sampling.

In order to further test the robustness of the association between individual matches and infections, we varied the dates of the matches, i.e. shifted them forward and backward in time. The results for the twelve countries under investigation are shown in Supplementary Fig. S10 and S12. In the countries where sensitivity to a championship-related case surge exists, a stable association is obtained for shifts by up to 2 days. As shown for the examples of England and Scotland in Fig. S19, such a shift is compensated by the model by a complementary adjustment of the delay parameter D . For larger shifts, the model might associate other matches to the increase of cases, as matches took place approximately every 4 days.

Correlations

In order to calculate the correlation between the effect size and various explainable variables (Fig. 3, Supplementary Fig. S4 and S6), we built a Bayesian regression model, using the previously computed posterior samples from the individual runs of each country. Let us denote the previously computed cumulative primary and subsequent cases related to the Euro 2020 by $Y_{s,c}$, for every sample s and analyzed country c , and the explainable variable from auxiliary data by X_c . We used a simple linear model to check for pairwise correlation between $Y_{s,c}$ and X_c :

$$\hat{Y}_c = \beta_0 + \beta_1 \hat{X}_c \quad (69)$$

$$\beta_0 \sim \text{Normal}(\mu = 0, \sigma = 10000) \quad (70)$$

$$\beta_1 \sim \text{Normal}(\mu = 0, \sigma = 100000) \quad (71)$$

We used every sample s obtained from the main analysis to incorporate uncertainties on the variable Y_c from our prior results. The auxiliary data X_c might also have errors ϵ_c , which we model using a Normal distribution. Additionally we allow our estimate for the effect size \hat{Y}_c to have an error for each country c in a typical hierarchical manner and choose uninformative priors for the scale hyper-parameter τ . As prior we considered 10k a reasonable choice for the β parameter as our data X_c is normally in a range multiple

magnitudes smaller:

$$\hat{X}_c \sim \text{Normal}(\mu = X_c, \sigma = \epsilon_c) \quad \forall c \quad (72)$$

$$\tau \sim \text{HalfCauchy}(\beta = 10000) \quad (73)$$

$$Y_c^\dagger \sim \text{Normal}(\mu = \hat{Y}_c, \sigma = \tau) \quad \forall c. \quad (74)$$

Again using uninformative priors for the error, the likelihood to obtain our results given the individual country effect size estimate Y_c^\dagger from the hierarchical linear model is

$$Y_{s,c} \sim \text{StudentT}_{\nu=4}(\mu = Y_c^\dagger, \sigma = \hat{\sigma}_c) \quad \text{with} \quad (75)$$

$$\hat{\sigma}_c \sim \text{HalfCauchy}(\beta = 10000). \quad (76)$$

Therefore our regression model includes the ‘‘measurement error’’ $\hat{\sigma}_c$ which models the heteroscedastic effect size of every country, and an additional model error τ which models the homoscedastic deviations of the country effect sizes from the linear model. In the plots, we plot the regression line \hat{Y}_c with its shaded 95% CI, and data points (\hat{X}_c, Y_c^\dagger) where the whiskers correspond to the one standard deviation, modeled here by ϵ_c and $\hat{\sigma}_c$.

The coefficient of determination, R^2 , is calculated following the procedure suggested by Gelman and colleagues [52]. Their R^2 measure is intended for Bayesian regression models as it notably uses the expected data variance given the model instead of the observed data variance. For our model it is defined as

$$R^2 = \frac{\text{Explained variance}}{\text{Residual variance} + \text{Explained variance}} = \frac{\frac{1}{n_c-1} \sum_c \hat{Y}_c^2}{\tau^2 + \frac{1}{n_c-1} \sum_c \hat{Y}_c^2}, \quad (77)$$

where n_c is the number of countries. With this formula, one obtains the posterior distribution of R^2 by evaluating it for every sample.

As auxiliary data we used:

1. *Mobility Data*: We use the mobility index $m_{c,t}$ provided by the ‘‘Google COVID-19 Community Mobility Reports’’ [53] for each country c at day t during the Euro 2020 ($t \in [11\text{th June } 2021, 11\text{th July } 2021]$), where N denotes the number of days in the interval. The error is the standard deviation of the mean:

$$X_c = \frac{1}{N} \sum_t m_{c,t} \quad (78)$$

$$\epsilon_c = \sqrt{\frac{1}{N^2} \sum_t (m_{c,t} - X_c)^2} \quad (79)$$

2. *Reproduction Number*: We use the base reproduction number $R_{\text{pre},c}$ for each country c as inferred from our model two weeks prior to the Euro 2020 ($t \in [28\text{th May } 2021, 11\text{th June } 2021]$).

$$X_c = \frac{1}{N} \sum_t R_{\text{pre},c}(t) \quad (80)$$

$$\epsilon_c = \sqrt{\frac{1}{N} \sum_t (R_{\text{pre},c}(t) - X_c)^2} \quad (81)$$

3. *Cumulative reported cases*: From the daily reported cases $C(t)$ two weeks prior to the Euro 2020 ($t \in [28\text{th May } 2021, 11\text{th June } 2021]$), we computed the cumulative reported cases normalized by the number of inhabitants p_c in each country c . Note: We also used reported cases without gender assignment here.

$$X_c = \frac{\sum_t C(t)}{p_c} \quad (82)$$

$$\epsilon_c = \vec{0} \quad (83)$$

4. *Potential for COVID-19 spread:* As for the cumulative cases we used the daily reported cases $C(t)$ two weeks prior to the Euro 2020 ($t \in [28\text{th May } 2021, 11\text{th June } 2021]$), and we computed the cumulative reported cases normalized by the number of inhabitants p_c in each country c . Furthermore, we used the base reproduction number $R_{\text{base}}(t)$ two weeks prior to the Euro 2020, as well as the duration of a country participating in the championship T_c (Table S5) to compute the potential for spread:

$$N_0 = \frac{\sum_t C(t)}{p_c} \quad (84)$$

$$X_c = N_0 \cdot \frac{\sum_t R_{\text{pre},c}^{T_c/4}(t)}{N} \quad (85)$$

$$\epsilon_c = \vec{0} \quad (86)$$

5. *Proxy for popularity:* To represent popularity of the Euro 2020 in country c , we used the union of the number of matches played by each country $n_{\text{match},c}$ and the number of matches hosted by each country $n_{\text{hosted},c}$ (Table S5). By “union” we mean the sum without the overlap, i.e., we take the sum of these numbers and subtract the number of home matches $n_{\text{home},c}$

$$X_c = n_{\text{match},c} + n_{\text{hosted},c} - n_{\text{home},c} \quad (87)$$

$$\epsilon_c = \vec{0} \quad (88)$$

Tables

Variable	Meaning	Equation
$R_{\text{eff},g,g'}(t)$	Effective reproduction number between genders g and g'	(4)
$S_g(t)$	Number of susceptible persons of gender g	(2)
$I_g(t)$	Number of infected persons of gender g	(1)
N	Population size	
$G(\tau)$	Generation interval (Gamma kernel)	(3)
$R_{\text{base}}(t)$	Base reproduction number	(22)
$\Delta R_{\text{football}}(t)$	Time dependent additive reproduction number due to football matches	(11)
$\Delta R_{\text{noise}}(t)$	Time dependent additive reproduction number due other non-balanced transmission	(31)
$\Delta R_{\text{match},m}$	Additive reproduction number of match m	(13)
\mathbf{C}_{base}	Base contact matrix between genders	(5)
$\mathbf{C}_{\text{match}}$	Contact matrix for football related gatherings	(8)
$\mathbf{C}_{\text{noise}}$	Contact matrix for other non-balanced transmission	(10)
t_m	Day of match m	
α_{prior}	Vector encoding country participation in matches	
β_{prior}	Vector encoding whether country hosted matches	
$\Delta\alpha_m$	Difference of the effect of individual matches m (the country participated in) to mean effect of such matches	(15)
$\Delta\beta_m$	Difference of the effect of individual matches m (the country hosted) to mean effect of such matches	(20)
$\gamma_n(t)$	Time-dependent base reproduction number in log-space between change point n and $n + 1$	(24)
$\Delta\gamma_n$	Effect of the change point n	(25)
$\tilde{\gamma}_n(t)$	Additive reproduction number due other non-balanced transmission between change point n and $n + 1$	(33)
$\Delta\tilde{\gamma}_n$	Effect of the change point n on the non-balanced transmission	(34)
$C_g^\dagger(t)$	Delayed number of infected persons of gender g	(40)
\bar{D}_{country}	Country dependent reporting delay	Table 4
$\hat{C}_g(t)$	Modeled number of cases of gender g	(44)
η_t	Fraction of daily delayed cases	(45)
r_d	Average value of the fraction of delayed cases on weekday d	(46)
r_d^\dagger	Logit-transformed average value of the fraction of delayed cases on weekday d	(47)
Δr_{d^\dagger}	Deviation from the prior value of the fraction of delayed cases on weekday d	(50)
$C_g(t)$	Measured number of cases of gender g	(53)
R_{pre}	Reproduction number two weeks prior to the start of the Euro 2020	Used in 3
I_{primary}	Number of primary infected persons due to football matches	(65)
$I_{\text{subsequent}}$	Number of subsequent infected persons due to football matches	(67)
I_{none}	Number of infected persons without considering football matches	(67)

Table 1: **The intermediate variables of the model and their meaning.**

Variable	Meaning	Prior distribution	Equation
c_{off}	Off-diagonal term of non-football related interaction matrix	Beta ($\alpha = 8, \beta = 8$)	(6)
ω_{gender}	The fraction of female participation in football related gatherings compared to the total participation	Beta ($\alpha = 10, \beta = 20$)	(9)
$\Delta R_{\text{match}}^{\text{mean}}$	Mean gathering-related match effect	$\mathcal{N}(\mu = 0, \sigma = 5)$	(14)
$\Delta R_{\text{stadium}}^{\text{mean}}$	Mean effect of hosting a match at the stadium	$\mathcal{N}(\mu = 0, \sigma = 5)$	(19)
σ_{α}	Prior value of the deviation from the mean match effect	HalfNormal ($\sigma = 5$)	(16)
σ_{β}	Prior value of the deviation from the mean stadium effect	HalfNormal ($\sigma = 5$)	(21)
R_0	Value of $R_{\text{base}}(t)$ at $t = 0$	LogNormal ($\mu = 1, \sigma = 1$)	(23)
$\sigma_{\Delta\gamma}$	Prior value of the effect of the change points of the base reproduction number	HalfCauchy (0.5)	(26)
l_n	Length of the change point n	$\log(1 + \exp(\mathcal{N}(4, 1)))$	(27)
d_n	Date of the change point n	27th May 2021 + $10 \cdot n + \mathcal{N}(0, 3.5)$	(29)
$\Delta R_{0,\text{noise}}$	Value of $\Delta R_{\text{noise}}(t)$ at $t = 0$	$\mathcal{N}(\mu = 0, \sigma = 0.1)$	(32)
$\sigma_{\Delta\tilde{\gamma}}$	Prior value of the effect of the change points of the reproduction number of other non-balanced transmission	HalfCauchy (0.2)	(35)
\tilde{l}_n	Length of the non-balanced transmission change point n	$\log(1 + \exp(\mathcal{N}(4, 1)))$	(36)
\tilde{d}_n	Date of the non-balanced transmission change point n	27th May 2021 + $10 \cdot n + \mathcal{N}(0, 3.5)$	(38)
D	Median of the latent period and reporting delay kernel	$\log(\mathcal{N}(\mu = \exp(\bar{D}_{\text{country}}), \sigma = \sigma_{\log \bar{D}}))$	(41)
σ_D	Standard deviation of the delay kernel	$\mathcal{N}(\mu = 0.2 \cdot \bar{D}_{\text{country}}, \sigma = 0.08 \cdot \bar{D}_{\text{country}})$	(43)
$r_{\text{base},d}^{\dagger}$	Prior fraction of the logit-transformed weekday dependent delay		(48),(49)
σ_r	Prior deviation of the different weekdays from the prior of the fraction of delayed cases	HalfCauchy (1)	(51)
e	Prior deviation of each day from the weekday dependent delay	HalfCauchy (0.2)	(52)
κ	Overdispersion of the observed cases around the expected number of cases	HalfCauchy (20)	(54)

Table 2: **Prior distributions.** These are all the prior distributions and their meaning in our main model.

Index	Meaning	Values
\cdot_g	Gender	1 = male 2 = female
\cdot_m	Match	
\cdot_n	Change point	
\cdot_t	Time (in days)	
\cdot_d	Weekday	Monday, ..., Sunday

Table 3: **Indices.** We use these standardized indices in our model.

Country	Reporting convention	Prior delay (\bar{D}_{country})	Scale of prior delay ($\sigma_{\log \bar{D}}$)
England	symptom onset	4 days	0.1
Scotland	symptom onset	4 days	0.1
Germany	reporting date	7 days	0.1
France	symptom onset	4 days	0.1
Austria	unknown	5 days	0.15
Belgium	unknown	5 days	0.15
The Czech Republic	unknown	5 days	0.15
Italy	unknown	5 days	0.15
The Netherlands	symptom onset	4 days	0.1
Portugal	unknown	5 days	0.15
Slovakia	unknown	5 days	0.15
Spain	unknown	5 days	0.15

Table 4: **Country dependent priors on the delay structure.** These priors depend on the definition of the date in the daily case numbers, which for some countries refers to symptom onset, sample collection or sample analysis.

Country	Max. \mathcal{R} -hat of relevant variables	Max. \mathcal{R} -hat of all variables
England	1.07	1.98
The Czech Republic	1.00	1.16
Scotland	1.01	1.10
Spain	1.05	2.24
Italy	1.01	1.10
Slovakia	1.00	1.15
Germany	1.01	1.42
Austria	1.00	1.15
Belgium	1.01	1.22
France	1.01	1.82
Portugal	1.00	1.14
The Netherlands	1.03	1.83

Table 5: **Maximal \mathcal{R} -hat values** [51]. The convergence is good (≈ 1) for the relevant variables, which are the variables that encode the reproduction number.

Data availability

The data from our model runs, i.e., from the sampling is available on G-node https://gin.g-node.org/semohr/covid19_soccer_data.

The daily case numbers stratified by age and gender were acquired from the local health authorities (see also Supplementary section S1) from the following sources: Robert Koch Institut, Germany; Santé publique, France; National Health Service, England; Österreichische Agentur für Gesundheit und Ernährungssicherheit GmbH, Austria; Sciensano, Belgium Ministerstvo zdravotnictví, Czech Republic; National Institute for Public Health and the Environment, The Netherlands; and COVERAGE-DB

Code availability

All code to reproduce the analysis and figures shown in the manuscript as well as in the supplementary information is available online on GitHub https://github.com/Priesemann-Group/covid19_soccer or via DOI <https://doi.org/10.5281/zenodo.7386313> [54].

Acknowledgments

We thank the Priesemann group for exciting discussions and for their valuable input. We also thank Arne Gottwald and Cornelius Grunwald for their continuous input during the conceptual and finalizing stage of the manuscript. We thank Piklu Mallick for proofreading. All authors received support from the Max-Planck-Society. JD, SBM received funding from the "Netzwerk Universitätsmedizin" (NUM) project egePan (01KX2021). SBM received funding from the "Infrastructure for exchange of research data and software" (crc1456-inf) project. SC and PD received funding by the German Federal Ministry for Education and Research for the RESPINOW project (031L0298) and ENI for the infoXpand project (031L0300A). VP was supported by the Deutsche Forschungsgemeinschaft (DFG, German Research Foundation) under Germany's Excellence Strategy - EXC 2067/1-390729940. This work was partly performed in the framework of the PUNCH4NFDI consortium supported by DFG fund "NFDI 39/1", Germany.

Author Contributions Statement

Conceptualization: VP, SBM, JD, SC, PD

Methodology: SBM, JD, VP, PB, OS

Software: SBM, JD

Validation: SBM, JD

Formal analysis: SBM, JD

Investigation: SBM, JD, OS, PB

Data curation: SBM, JD, PD, OS

Writing - Original Draft: all

Writing - Review & Editing: all

Visualization: SBM, JD, PD, SC, EI

Supervision: VP, PB, OS, JD

Funding acquisition: VP, PB, OS

Competing interests Statement

VP is a member of the ExpertInnenrat of the German federal government on COVID and is also advising other governmental and non-governmental entities. The remaining authors declare no competing interests.

References

- [1] Chau, N. V. V. *et al.* Superspreading Event of SARS-CoV-2 Infection at a Bar, Ho Chi Minh City, Vietnam. *Emerging infectious diseases* **27**, 310 (2021).
- [2] Bernheim, B. D., Buchmann, N., Freitas-Groff, Z. & Otero, S. The effects of large group meetings on the spread of COVID-19: the case of Trump rallies. *SSRN* (2020).
- [3] Wang, L. *et al.* Inference of person-to-person transmission of COVID-19 reveals hidden super-spreading events during the early outbreak phase. *Nature communications* **11**, 1–6 (2020).
- [4] Dave, D., McNichols, D. & Sabia, J. J. The contagion externality of a superspreading event: The Sturgis Motorcycle Rally and COVID-19. *Southern economic journal* **87**, 769–807 (2021).
- [5] Leclerc, Q. J. *et al.* What settings have been linked to SARS-CoV-2 transmission clusters? *Wellcome open research* **5** (2020).
- [6] Nordsiek, F., Bodenschatz, E. & Bagheri, G. Risk assessment for airborne disease transmission by poly-pathogen aerosols. *PloS one* **16**, e0248004 (2021).
- [7] Fischer, K. Thinning out spectators: Did football matches contribute to the second COVID-19 wave in Germany? *German Economic Review* **23**, 595–640 (2022).
- [8] Toumi, A., Zhao, H., Chhatwal, J., Linas, B. P. & Ayer, T. The Effect of NFL and NCAA Football Games on the Spread of COVID-19 in the United States: An Empirical Analysis. *medRxiv* (2021). URL <https://doi.org/10.1101/2021.02.15.21251745>.
- [9] Olczak, M., Reade, J. & Yeo, M. Mass outdoor events and the spread of an airborne virus: English football and Covid-19. *Available at SSRN 3682781* (2021). URL <https://dx.doi.org/10.2139/ssrn.3682781>.
- [10] Alfano, V. COVID-19 Diffusion Before Awareness: The Role of Football Match Attendance in Italy. *Journal of Sports Economics* **23**, 503–523 (2022).
- [11] Gómez, J.-P. & Mironov, M. Using soccer games as an instrument to forecast the spread of covid-19 in europe. *Finance Research Letters* **43**, 101992 (2021).
- [12] Jones, B. *et al.* SARS-CoV-2 transmission during rugby league matches: do players become infected after participating with SARS-CoV-2 positive players? *British Journal of Sports Medicine* **55**, 807–813 (2021).
- [13] Schumacher, Y. O. *et al.* Resuming professional football (soccer) during the COVID-19 pandemic in a country with high infection rates: a prospective cohort study. *British Journal of Sports Medicine* **55**, 1092–1098 (2021).
- [14] Egger, F., Faude, O., Schreiber, S., Gärtner, B. C. & Meyer, T. Does playing football (soccer) lead to SARS-CoV-2 transmission? - A case study of 3 matches with 18 infected football players. *Science and Medicine in Football* **5**, 2–7 (2021).
- [15] Oh, T., Sung, H. & Kwon, K. D. Effect of the stadium occupancy rate on perceived game quality and visit intention. *International Journal of Sports Marketing and Sponsorship* **18**, 166–179 (2017).
- [16] Herold, E., Boronczyk, F. & Breuer, C. Professional Clubs as Platforms in Multi-Sided Markets in Times of COVID-19: The Role of Spectators and Atmosphere in Live Football. *Sustainability* **13** (2021).
- [17] Horky, T. No sports, no spectators – no media, no money? the importance of spectators and broadcasting for professional sports during covid-19. *Soccer & Society* **22**, 96–102 (2021). URL <https://doi.org/10.1080/14660970.2020.1790358>.
- [18] Yim, B. H., Byon, K. K., Baker, T. A. & Zhang, J. J. Identifying critical factors in sport consumption decision making of millennial sport fans: mixed-methods approach. *European Sport Management Quarterly* **21**, 484–503 (2021).
- [19] Cuschieri, S., Grech, S. & Cuschieri, A. An observational study of the covid-19 situation following the first pan-european mass sports event. *European Journal of Clinical Investigation* **52**, e13743 (2022).
- [20] Feder, T. Soccer obeys Bessel-function statistics. *Physics Today* **59**, 26 (2006).

- [21] Dehning, J. *et al.* Inferring change points in the spread of COVID-19 reveals the effectiveness of interventions. *Science* (2020).
- [22] Brauner, J. M. *et al.* Inferring the effectiveness of government interventions against COVID-19. *Science* (2020).
- [23] Sharma, M. *et al.* Understanding the effectiveness of government interventions against the resurgence of COVID-19 in Europe. *Nature communications* **12**, 1–13 (2021).
- [24] Lagaert, S. & Roose, H. The gender gap in sport event attendance in Europe: The impact of macro-level gender equality. *International Review for the Sociology of Sport* **53**, 533–549 (2018).
- [25] Shah, S. A. *et al.* Predicted COVID-19 positive cases, hospitalisations, and deaths associated with the Delta variant of concern, June–July, 2021. *The Lancet Digital Health* (2021).
- [26] Marsh, K., Griffiths, E., Young, J. J., Gibb, C.-A. & McMenamin, J. Contributions of the EURO 2020 football championship events to a third wave of SARS-CoV-2 in Scotland, 11 June to 7 July 2021. *Eurosurveillance* **26** (2021).
- [27] Riley, S. *et al.* REACT-1 round 13 interim report: acceleration of SARS-CoV-2 Delta epidemic in the community in England during late June and early July 2021. *medRxiv* (2021). URL <https://doi.org/10.1101/2021.07.08.21260185>.
- [28] Roxby, P. Covid: Watching Euros may be behind rise in infections in men. *BBC News* (2021). URL <https://www.bbc.com/news/health-57754938>.
- [29] Fraser, C. Estimating Individual and Household Reproduction Numbers in an Emerging Epidemic. *PLoS ONE* **2** (2007).
- [30] Riffe, T. & Acosta, E. Data Resource Profile: COVerAGE-DB: a global demographic database of COVID-19 cases and deaths. *International Journal of Epidemiology* **50**, 390–390f (2021).
- [31] Wilkinson, M. D. *et al.* The fair guiding principles for scientific data management and stewardship. *Scientific data* **3**, 1–9 (2016).
- [32] Government of The Netherlands. Reopening society step by step. <https://web.archive.org/web/20210627222056/https://www.government.nl/topics/coronavirus-covid-19/plan-to-reopen-society>.
- [33] Hale, T. *et al.* A global panel database of pandemic policies (Oxford COVID-19 Government Response Tracker). *Nature Human Behaviour* **5**, 529–538 (2021).
- [34] Zierenberg, J., Spitzner, F. P., Priesemann, V., Weigel, M. & Wilczek, M. How contact patterns destabilize and modulate epidemic outbreaks. *arXiv preprint arXiv:2109.12180* (2021). URL <https://arxiv.org/abs/2109.12180>.
- [35] Iftekhhar, E. N. *et al.* A look into the future of the COVID-19 pandemic in Europe: an expert consultation. *The Lancet Regional Health-Europe* **8**, 100185 (2021).
- [36] Heese, H. *et al.* Results of the enhanced COVID-19 surveillance during UEFA EURO 2020 in Germany. *Epidemiology & Infection* **150**, 1–7 (2022).
- [37] Euro 2020 players affected by COVID-19. Reuters: <https://www.reuters.com/article/soccer-euro-coronavirus-idUKL5N2NS2ED>. (2021).
- [38] Kretzschmar, M. E., Rozhnova, G. & van Boven, M. Isolation and Contact Tracing Can Tip the Scale to Containment of COVID-19 in Populations With Social Distancing. *Frontiers in Physics* **8** (2021).
- [39] Kerr, C. C. *et al.* Controlling COVID-19 via test-trace-quarantine. *Nature communications* **12**, 1–12 (2021).
- [40] Contreras, S. *et al.* The challenges of containing SARS-CoV-2 via test-trace-and-isolate. *Nature communications* **12**, 1–13 (2021).
- [41] Contreras, S. *et al.* Low case numbers enable long-term stable pandemic control without lockdowns. *Science advances*
- [42] Salathé, M. *et al.* COVID-19 epidemic in Switzerland: on the importance of testing, contact tracing and isolation. *Swiss medical weekly* **150**, w20225 (2020).

- [43] Flaxman, S. *et al.* Estimating the effects of non-pharmaceutical interventions on COVID-19 in Europe. *Nature* 1–8 (2020).
- [44] Meier, H. E., Strauss, B. & Riedl, D. Feminization of sport audiences and fans? Evidence from the German men’s national soccer team. *International Review for the Sociology of Sport* **52**, 712–733 (2017).
- [45] Zhang, M. *et al.* Transmission Dynamics of an Outbreak of the COVID-19 Delta Variant B.1.617.2 — Guangdong Province, China, May–June 2021. *China CDC Weekly* **3**, 584–586 (2021).
- [46] Hart, W. S. *et al.* Generation time of the alpha and delta SARS-CoV-2 variants: an epidemiological analysis. *The Lancet Infectious Diseases* **22**, 603–610 (2022).
- [47] Hu, S. *et al.* Infectivity, susceptibility, and risk factors associated with SARS-CoV-2 transmission under intensive contact tracing in Hunan, China. *Nature Communications* **12**, 1533 (2021).
- [48] Ferretti, L. *et al.* Quantifying SARS-CoV-2 transmission suggests epidemic control with digital contact tracing. *Science* **368**, eabb6936 (2020).
- [49] Salvatier, J., Wiecki, T. V. & Fonnesbeck, C. Probabilistic programming in Python using PyMC3. *PeerJ Computer Science* **2**, e55 (2016).
- [50] Hoffman, M. D. & Gelman, A. The No-U-Turn Sampler: Adaptively Setting Path Lengths in Hamiltonian Monte Carlo. *arXiv:1111.4246 [cs, stat]* (2011). URL <http://arxiv.org/abs/1111.4246>.
- [51] Vehtari, A., Gelman, A., Simpson, D., Carpenter, B. & Bürkner, P.-C. Rank-normalization, folding, and localization: An improved \hat{R} for assessing convergence of MCMC. *Bayesian Analysis* **16** (2021).
- [52] Gelman, A., Goodrich, B., Gabry, J. & Vehtari, A. R-squared for Bayesian Regression Models. *The American Statistician* **73**, 307–309 (2019).
- [53] COVID-19 Community Mobility Reports. <https://www.google.com/covid19/mobility/>.
- [54] Dehning, J. *et al.* Software: Impact of the Euro 2020 championship on the spread of COVID-19. https://github.com/Prieseemann-Group/covid19_soccer (2022). <https://doi.org/10.5281/zenodo.7386313>
- [55] E. O.-O. Max Roser, Hannah Ritchie, J. Hasell, Coronavirus Pandemic (COVID-19), *Our World in Data* (2020). <https://ourworldindata.org/coronavirus>, (Europe, America, and Oceania and Asia).
- [56] A systematic approach to monitoring and analysing public health and social measures (PHSM) in the context of the COVID-19 pandemic: underlying methodology and application of the PHSM database and PHSM Severity Index (2020).
- [57] E. Dong, H. Du, L. Gardner, An interactive web-based dashboard to track COVID-19 in real time, *The Lancet Infectious Diseases* **20**, 533 - 534 (2020).
- [58] Google Trends, <https://trends.google.de/trends>.
- [59] Oxford COVID-19 Government Response Tracker, Blavatnik School of Government and University of Oxford, <https://covidtracker.bsg.ox.ac.uk/>.

Supplementary Information

S1 Data sources

We used the daily COVID-19 case numbers, resolved by age and country, as reported publicly by the state health institute or equivalent of each country covered in this work. The data was retrieved either directly or taken from COVERAGE-DB [30]:

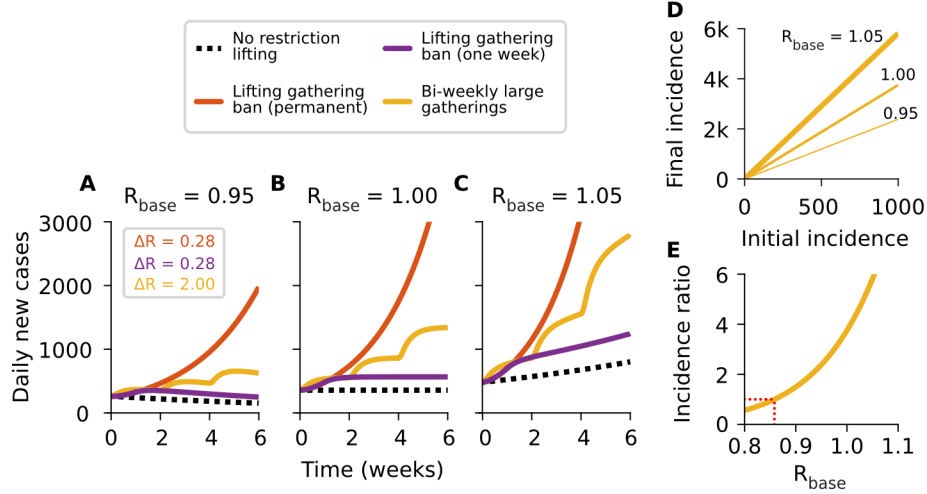
- Germany: Robert Koch Institut
<https://www.arcgis.com/home/item.html?id=f10774f1c63e40168479a1feb6c7ca74>
- France: Santé publique France
<https://www.data.gouv.fr/fr/datasets/taux-dincidence-de-lepidemie-de-covid-19>
- England: National Health Service
<https://coronavirus.data.gov.uk/details/download>
- Scotland: Public Health Scotland
<https://www.opendata.nhs.scot/dataset/covid-19-in-scotland>
- Austria: Österreichische Agentur für Gesundheit und Ernährungssicherheit GmbH
<https://covid19-dashboard.ages.at/>
- Belgium: Sciensano
<https://epistat.wiv-isp.be/covid/>
- The Czech Republic: Ministerstvo zdravotnictví
<https://onemocneni-aktualne.mzcr.cz/covid-19>
- Italy: Istituto Superiore di Sanità
Aggregated by COVERAGE-DB from
<https://www.epicentro.iss.it/coronavirus/sars-cov-2-sorveglianza-dati>
- The Netherlands: National Institute for Public Health and the Environment
<https://data.rivm.nl/covid-19/>
- Slovakia: The Institute for Healthcare Analyses (IZA) of the Ministry of Health
Aggregated by COVERAGE-DB from
<https://github.com/Institut-Zdravotnych-Analyz/covid19-data>
- Spain: Ministry of Public Health
Aggregated by COVERAGE-DB from
<https://cnecovid.isciii.es/covid19/>

To estimate the deaths associated with the Euro 2020 cases we calculate the case fatality risk by using the number of deaths and number of cases as reported by Our World in Data (OWD) [55].

For showcasing the stringency of governmental measures (panel C in Fig. S24-S36), we used data from the Oxford COVID-19 Government Response Tracker [33] and the public health and social measures (PHSM) severity index [56] from the World Health Organization (WHO). For our correlational analysis of cases and human mobility (Fig. 3B and S4), we used data from the COVID-19 Community Mobility Reports [53] provided by Google. For correlation with pre-Euro 2020 incidences (Fig.S6B) we use case numbers as reported by the Johns Hopkins University (JHU) [57]. Lastly, we used data from Google Trends [58] to investigate people’s interest in the Euro 2020 (Fig. S20).

S2 Supplementary analysis: our results in context

To put our results in context, we compare the impact that different hypothetical scenarios of lifting of restrictions would have on case numbers (Fig. S1). Using a linear SEIS model for illustrative purposes, we evaluate three scenarios: i) Recurrent, bi-weekly (period $T = 2$ weeks) large events that strongly increase the reproduction number over its base level R_{base} for one day by $\Delta R_s = 2.0$ (yellow curves). This effect



Supplementary Figure S1: **Our results in context: How much of an effect do short but strong increases of transmission have?** **A–C:** Understanding Euro 2020 matches as point interventions where the reproduction number is allowed to increase drastically from its base level R_{base} for one day ($\Delta R = 2.0$, yellow curve), we compare its cumulative effect with different scenarios of lifting restrictions. These effects are in the order of magnitude of those reported in the literature [23]. The purple lines represent the same effect as a single increase but distributed over one week ($\Delta R = 0.28 \approx 2/7$), while the red curve represents a permanent lifting of those restrictions. The effect of the yellow and purple interventions is similar for $t \leq 2$ weeks because the product between ΔR and the duration of the intervention is the same. **D:** We observe long-term effects of consecutive interventions even when R_{base} is lower than one (red dotted line). The impact of these effects increases exponentially with R_{base} . **E:** Similarly, the final incidence (after six weeks) increases with R_{base} . The red dotted line indicates that an incidence ratio larger than one can already result from values of R_{base} smaller than one. Altogether, the cumulative effect of short but strong interventions (such as Euro 2020 matches) can be compared to lifting all bans on gatherings for a certain period of time. Curves were generated using a linear SEIS model without immunity for illustrative purposes.

size is comparable to what we inferred for some heated matches (e.g., Scotland - England for Scotland: $\Delta R_{\text{match}} = 3.5 [2.9, 4.2]$, England - Italy for England: $\Delta R_{\text{match}} = 2.0 [1.6, 3.5]$, England - Italy for Italy: $\Delta R_{\text{match}} = 0.9 [-0.7, 4.4]$, and the Czech Republic - Denmark for the Czech Republic: $\Delta R_{\text{match}} = 2.7 [0.8, 4.4]$).
 ii) A temporary one-week lifting of restrictions, with an effect equal to a single-day large event by distributing the increase in R_{base} over a week: $\Delta R_w = 0.28 \approx 2/7$ (purple curves).
 iii) A permanent lifting of restrictions to the level of the second scenario: $\Delta R_p = 0.28$ for the considered time span (red curves). The value for ΔR_s in the first scenario is comparable to the largest effects found for the England-Scotland matches, while those in the second and third scenarios are similar to the effect of banning all private gatherings of 2 people or more as reported in [23].

The effect of interventions is comparable whenever the products between ΔR and the duration of the interventions are the same (e.g., yellow and purple curves for $t \leq 2$ weeks in Fig. S1A, B). In other words, the cumulative effect of short but strong interventions (such as Euro 2020 matches), can be compared to lifting all bans on gatherings for a certain period of time. However, for regularly recurring interventions of size ΔR_s , we observe permanent long-term effects when $R_{\text{base}} + \Delta R_s/T \geq 1$; the impact of recurring interventions increases disproportionately over time (Fig. S1A–C). Controlling the long-term effect of recurrent increases of the reproduction number is possible if the underlying reproduction number R_{base} is small enough. Small changes of R_{base} substantially impact the outcome, even below the $R_{\text{base}} = 1$ threshold, and in an exponential manner (Fig. S1D, E). This underlines the importance of control strategies if large-scale events are expected to temporally increase the spread of COVID-19.

On the other hand, quantitatively, the expected size z of an infection chain depends on the effective reproduction number R_{eff} . As long as R_{eff} is larger than one, the infection chains can become arbitrarily large. But even if $R_{\text{eff}} < 1$, one single infection is expected to cause $z = (1 - R_{\text{eff}})^{-1}$ infections before the chain dies out. For example, if $R_{\text{eff}} = 0.9$, a single infection caused by the Euro 2020 implies $z = 10$ infections

in the total chain. Thus, in comparison, the primary cases have only a small contribution; the majority of the impact of an event like the Euro 2020 is the spread of subsequent infections into the general population (e.g., Fig. 2A).

S3 Supplementary Tables

Country	Median percentage of primary cases	Median percentage of subsequent cases	Median percentage of primary and subsequent cases	Probability that football increased cases
Avg.	3.2% [1.3%, 5.2%]	-	-	> 99.9%
England	12.4% [5.6%, 22.5%]	36.0% [27.9%, 44.7%]	47.8% [36.0%, 62.9%]	> 99.9%
Czech Republic	9.7% [3.3%, 16.2%]	47.8% [24.2%, 58.7%]	57.7% [28.7%, 72.6%]	> 99.9%
Scotland	3.3% [1.3%, 8.1%]	36.6% [28.6%, 43.9%]	40.8% [30.9%, 50.3%]	> 99.9%
Spain	2.8% [-1.1%, 9.2%]	24.1% [-16.3%, 60.6%]	26.9% [-16.9%, 69.2%]	91.8%
Italy	2.1% [-5.8%, 10.9%]	16.1% [-230.2%, 69.5%]	18.7% [-235.6%, 78.4%]	74.1%
Slovakia	1.6% [-7.7%, 10.2%]	15.5% [-88.2%, 50.6%]	17.3% [-95.7%, 60.0%]	70.8%
Germany	1.4% [-1.8%, 4.2%]	22.1% [-36.3%, 44.8%]	23.6% [-38.0%, 48.6%]	86.7%
Austria	1.2% [-2.2%, 4.8%]	24.0% [-62.9%, 60.8%]	25.2% [-65.0%, 65.2%]	79.4%
Belgium	0.6% [-2.3%, 4.2%]	9.2% [-60.0%, 47.9%]	9.8% [-62.2%, 51.8%]	67.6%
France	0.5% [-0.2%, 1.4%]	23.1% [-8.4%, 45.8%]	23.6% [-8.6%, 47.0%]	94.1%
Portugal	0.3% [-2.6%, 2.7%]	-4.4% [-55.1%, 24.5%]	-4.1% [-57.4%, 26.9%]	60.6%
The Netherlands	-1.5% [-3.3%, -0.2%]	-49.1% [-111.7%, -1.4%]	-50.6% [-114.6%, -1.7%]	1.5%

Supplementary Table S1: **Credible intervals from the posterior distribution** of the number of football related cases divided by the total number of cases during the championship. CI denotes 95% credible interval.

Country	Primary cases per mil. people (male)	Primary cases per mil. people (female)	Primary and subsequent cases per mil. people
Avg.	-	-	2228 [986, 3308]
England	3595 [2661, 5729]	1686 [1143, 3453]	10600 [8185, 13875]
Czech Republic	94 [40, 142]	65 [22, 108]	459 [229, 577]
Scotland	1352 [940, 1758]	351 [222, 517]	7897 [6136, 9529]
Spain	594 [-217, 1722]	387 [-160, 1346]	4518 [-2840, 11595]
Italy	55 [-121, 227]	27 [-77, 131]	319 [-4001, 1335]
Slovakia	8 [-30, 38]	4 [-19, 25]	57 [-313, 196]
Germany	15 [-16, 36]	7 [-11, 24]	174 [-280, 359]
Austria	42 [-70, 141]	23 [-45, 100]	642 [-1646, 1661]
Belgium	34 [-112, 198]	18 [-81, 155]	411 [-2611, 2174]
France	43 [-12, 95]	27 [-8, 76]	1515 [-552, 3008]
Portugal	41 [-331, 340]	25 [-247, 251]	-449 [-6294, 2960]
Netherlands	-186 [-328, -31]	-98 [-222, -13]	-4805 [-10851, -166]

Supplementary Table S2: **Cases attributed to the Euro 2020 per million inhabitants** and related 95% credible intervals in the male and female population. Primary and primary plus secondary cases are shown separately. Subsequent cases are almost gender-symmetric in all countries (see also Fig. S2). This indicates that also possible unobserved characteristics of the primary football-related infections in terms of other factors – such as age – are most likely distributed over the whole population in the course of subsequent infections.

Country	Primary cases (male)	Primary cases (female)	Primary and subsequent cases	Estimated deaths associated with primary and subsequent cases
England	93619 [69591, 145127]	43872 [29946, 87030]	567280 [436870, 747399]	1227 [945, 1616]
Czech Republic	494 [215, 753]	346 [116, 558]	4920 [2455, 6182]	60 [30, 75]
Scotland	3478 [2444, 4481]	908 [574, 1320]	41720 [31766, 50146]	90 [69, 108]
Spain	13570 [-4463, 40212]	8870 [-3339, 31389]	211952 [-122694, 546650]	503 [-291, 1298]
Italy	1535 [-3399, 6718]	750 [-2219, 3824]	17810 [-243916, 79338]	170 [-2327, 757]
Slovakia	21 [-87, 100]	11 [-47, 67]	320 [-1809, 1087]	4 [-24, 14]
Germany	618 [-629, 1460]	306 [-440, 944]	14626 [-23538, 29644]	304 [-489, 616]
Austria	178 [-308, 626]	97 [-179, 436]	6078 [-15534, 15387]	34 [-86, 85]
Belgium	191 [-600, 1091]	101 [-441, 834]	5352 [-31477, 24778]	14 [-84, 66]
France	1357 [-331, 2920]	857 [-219, 2325]	95929 [-40644, 190114]	423 [-179, 838]
Portugal	202 [-1683, 1667]	122 [-1229, 1255]	-5205 [-72249, 29231]	-22 [-300, 121]
Netherlands	-1573 [-2756, -277]	-838 [-1859, -106]	-82805 [-181983, -3149]	-75 [-164, -3]
Total	114769 [81915, 167796]	56781 [36247, 100400]	844609 [396860, 1253494]	1689 [794, 2507]

Supplementary Table S3: **Total cases attributed to the Euro 2020** and related 95% credible intervals. The associated deaths are calculated under the assumption that the cases were equally distributed among age-groups and using the case fatality risk for the respective country in the time window of the Euro 2020.

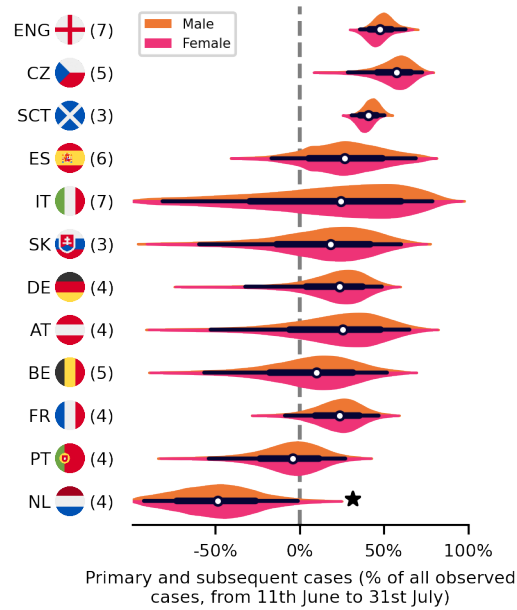
Country	$\Delta R_{\text{match}}^{\text{mean}}$	Delay D
Avg.	0.46 [0.18, 0.75]	
England	0.75 [0.01, 1.66]	4.55 [4.36, 4.94]
Czech Republic	1.26 [-0.50, 3.19]	5.53 [4.75, 6.32]
Scotland	1.09 [-2.77, 4.69]	3.52 [3.35, 3.74]
Spain	0.37 [-0.72, 1.83]	6.91 [5.43, 7.82]
Italy	0.28 [-1.11, 1.79]	5.51 [3.96, 7.11]
Slovakia	0.32 [-2.27, 2.56]	5.00 [3.67, 7.28]
Germany	0.33 [-0.62, 1.12]	6.82 [5.69, 8.43]
Austria	0.28 [-0.90, 1.45]	4.58 [3.46, 6.37]
Belgium	0.11 [-0.61, 0.92]	5.09 [3.71, 6.69]
France	0.30 [-0.46, 0.97]	3.68 [3.13, 4.46]
Portugal	-0.02 [-1.33, 1.34]	5.49 [4.30, 6.55]
Netherlands	-0.74 [-3.30, 1.36]	5.70 [4.28, 6.00]

Supplementary Table S4: **Average effect of Euro 2020 matches on the spread of COVID-19, per country.**

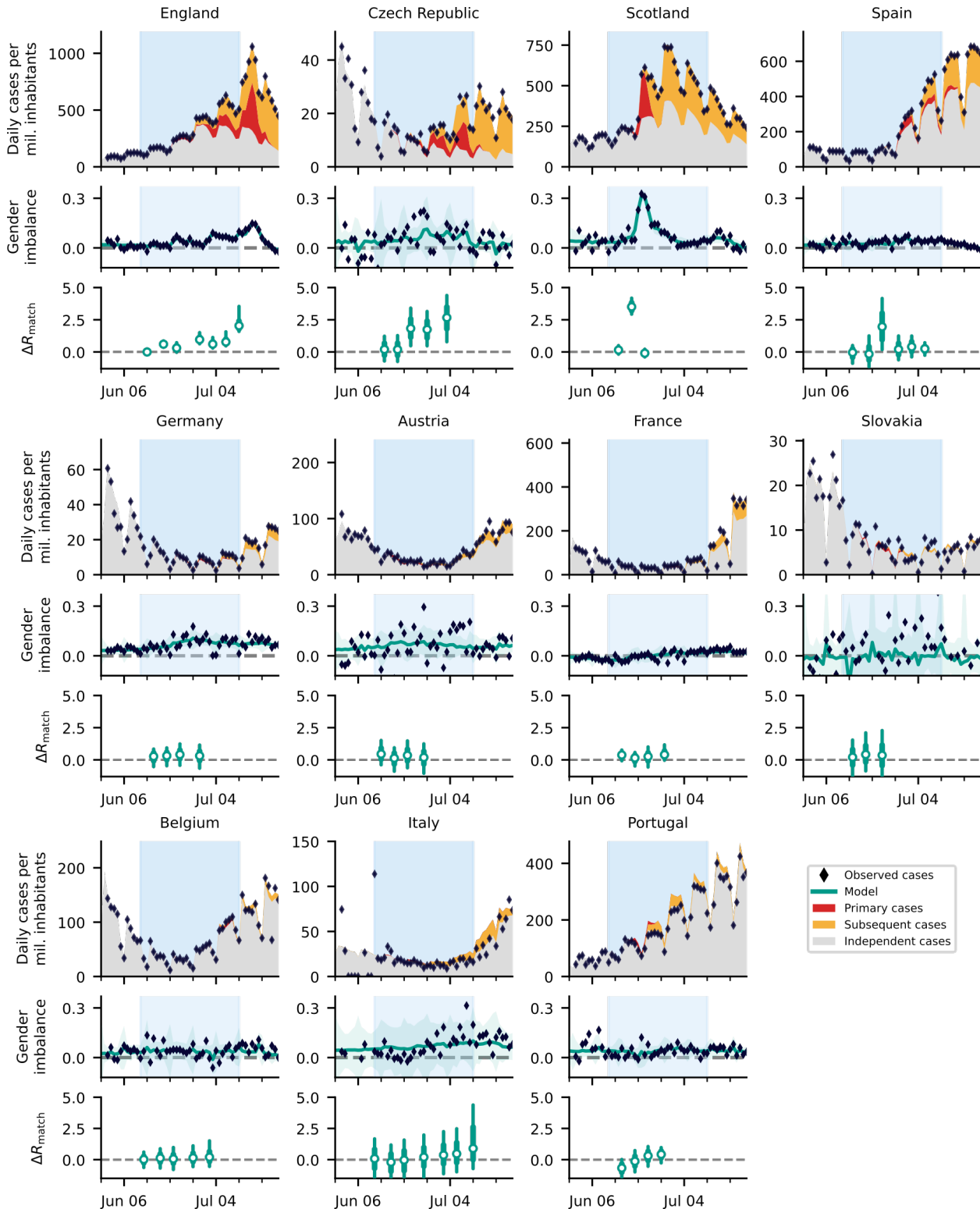
Country	Matches played	Matches hosted	Union	Time between first and last match of the country (days)
England	7	8	9	28
Czech Republic	5	0	5	19
Scotland	3	4	5	8
Spain	6	4	7	22
Italy	7	4	8	30
Slovakia	3	0	3	9
Germany	4	4	5	14
Austria	4	0	4	13
Belgium	5	0	5	20
France	4	0	4	13
Portugal	4	0	4	12
Netherlands	4	4	5	14

Supplementary Table S5: **Number of matches** played by the national team in the Euro 2020, matches played in the country and the union of the two categories. The union denotes the sum of the first two numbers without the overlapping matches.

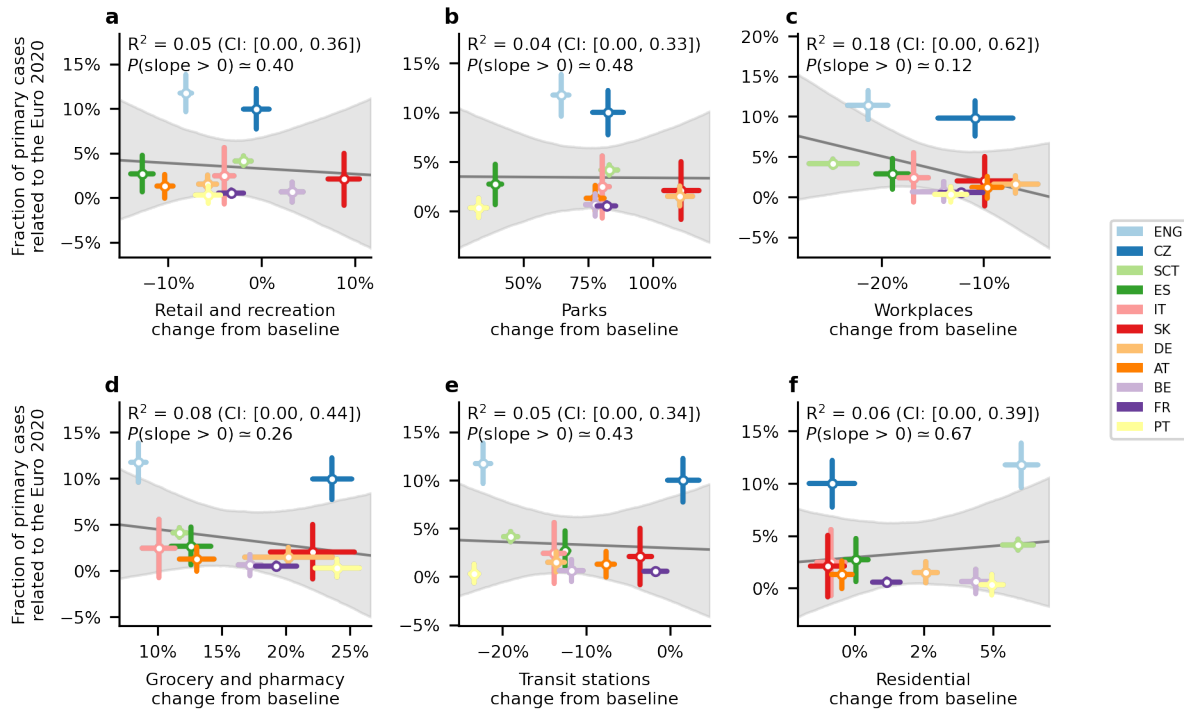
S4 Supplementary Figures



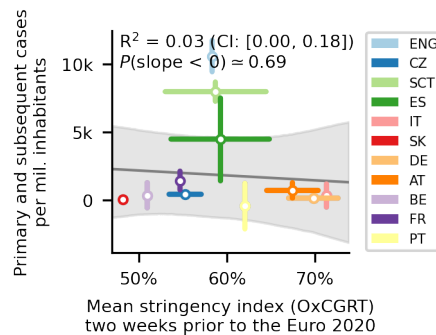
Supplementary Figure S2: **Overview of the sum of primary and subsequent cases accountable to the Euro 2020.** Calculations account for cases until July 31st, i.e., about three weeks after the championship finished. In the Netherlands (★) the “freedom day” occurred on the same time as the Euro 2020. This effect also had a gender imbalance, thus, making it hard for our model to extract the Euro 2020 effect (see. Fig. S31). White dots represent median values, black bars and whiskers correspond to the 68% and 95% credible intervals (CI), respectively, and the distributions in color (truncated at 99% CI) represent the differences by gender ($n = 12$ countries).



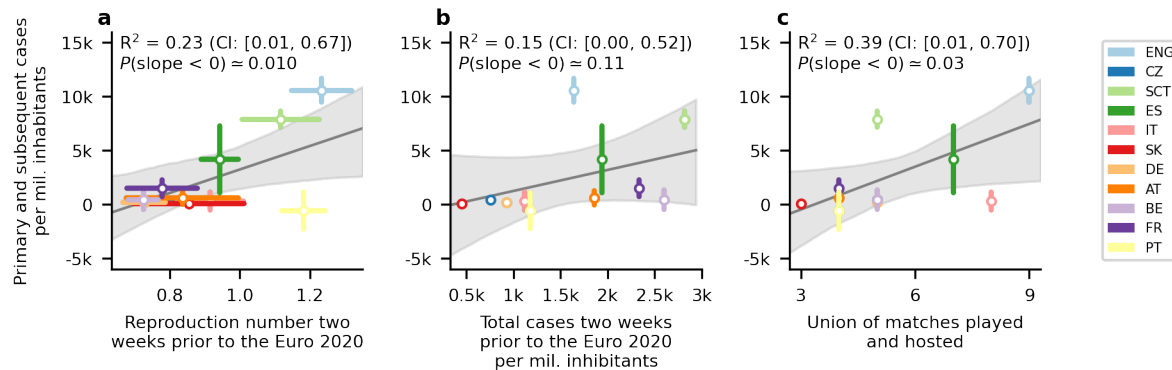
Supplementary Figure S3: **Overview of cases in all considered countries apart from the Netherlands** We split the observed incidence (black diamonds) of the three countries with the largest effect size into i) cases independent of Euro 2020 matches (gray area), ii) primary cases (directly associated with Euro 2020 matches, red area), and iii) subsequent cases (additional infection chains started by primary cases, orange area). See Figure 2 for more details. The turquoise shaded areas correspond to 95% CI. In the box plots, white dots represent median values, turquoise bars and whiskers correspond to the 68% and 95% credible intervals (CI), respectively.



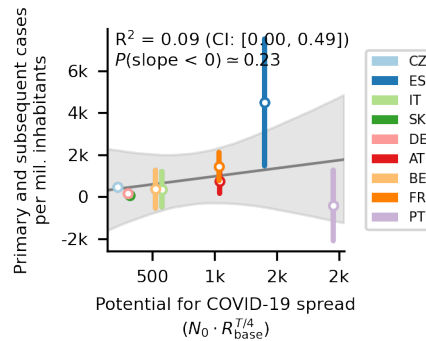
Supplementary Figure S4: **We found no significant correlation between cases arising from the Euro 2020 and human mobility.** Using mobility data from the “Google COVID-19 Community Mobility Reports” [53], we tested for correlation against the fraction of Euro 2020 related cases. Using the different categories (A-F) from the Mobility Report we found no significant correlation in either. The gray line and area are the median and 95% credible interval of the linear regression ($n = 11$ countries; The Netherlands was excluded for this analysis). Whiskers denote one standard deviation.



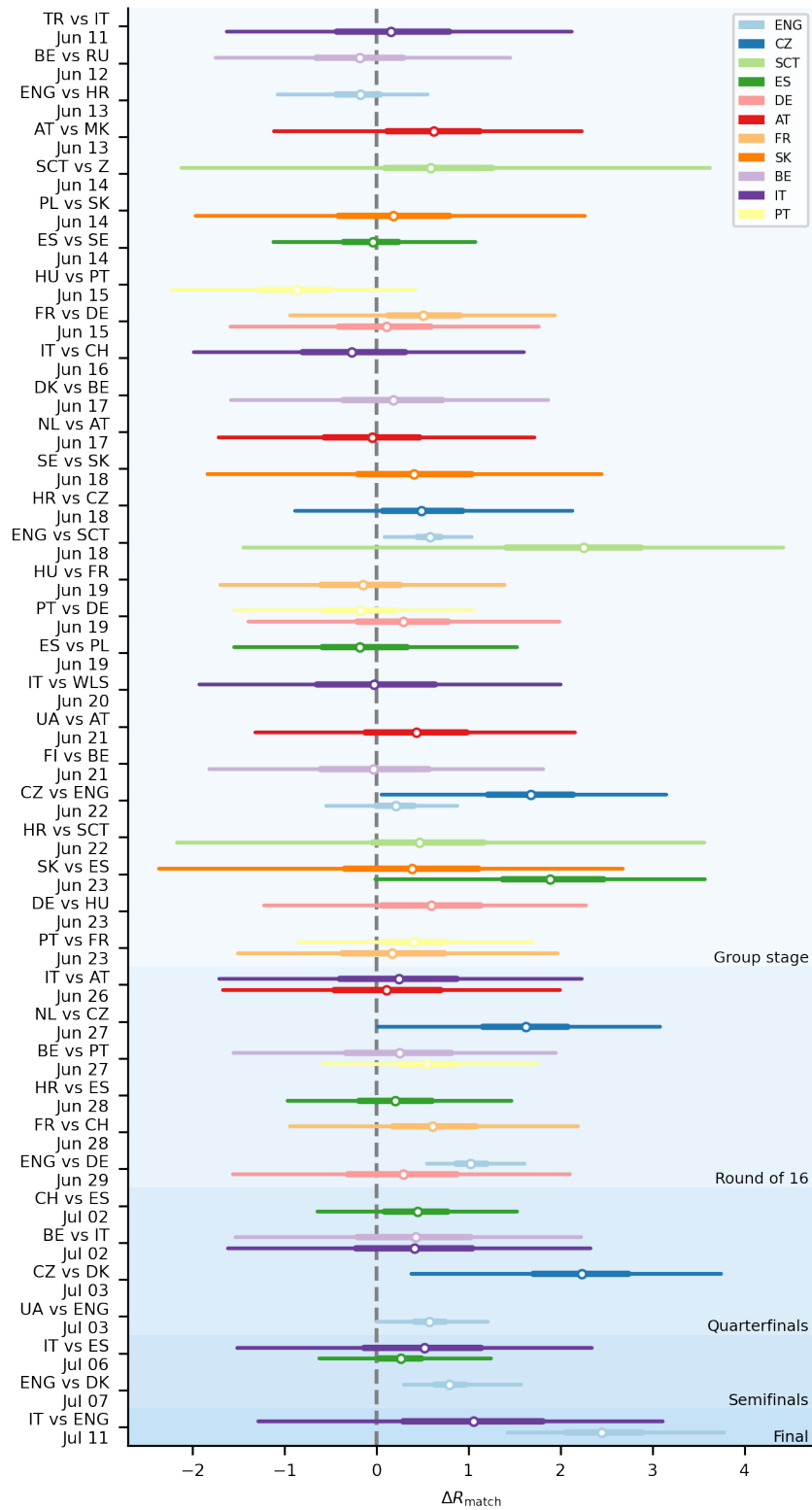
Supplementary Figure S5: **We found no significant correlation between cases arising from the Euro 2020 and the stringency of governmental interventions.** We correlated the average Oxford governmental response tracker [33] in the two weeks before the championship with the total number of cases per million inhabitants related to football gatherings. The gray line and area are the median and 95% credible interval of the linear regression ($n = 11$ countries; The Netherlands was excluded for this analysis). Whiskers denote one standard deviation.



Supplementary Figure S6: **We found slight trends in the correlations between the impact of Euro 2020 and the base reproduction number and country popularity.** While these correlations are below the classical significance threshold of 0.05, they are less explanatory than the potential for spread (defined in Fig. 3). There was no significant correlation between the initial COVID-19 incidence and the impact of the Euro 2020. The gray line and area are the median and 95% credible intervals of the linear regression ($n = 11$ countries; The Netherlands was excluded for this analysis). Whiskers denote one standard deviation.

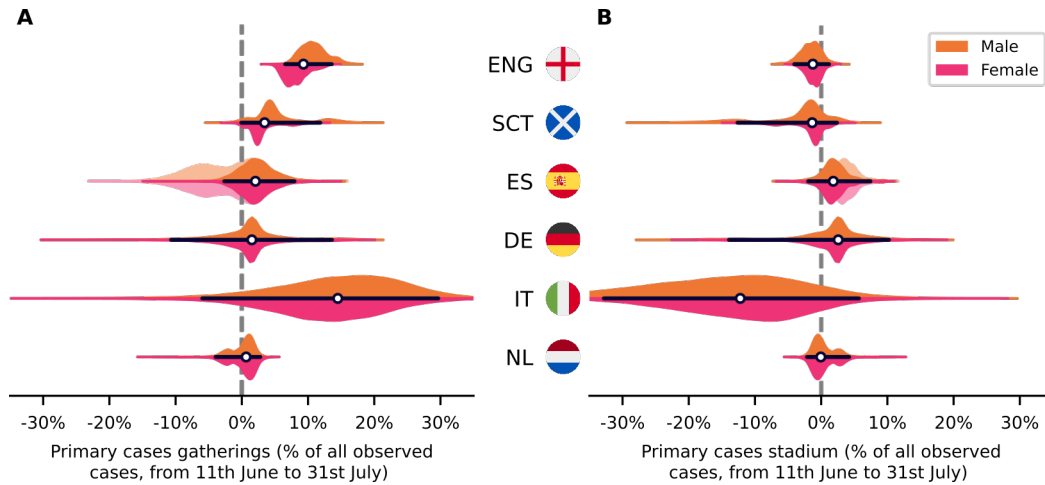


Supplementary Figure S7: **Prediction of the impact of Euro 2020 matches without the two most significant countries in the main model (England and Scotland).** The potential for spread, i.e., the number of COVID-19 cases that would be expected during the time T a country is playing in the Euro 2020 ($N_0 \cdot R_{pre}^{T/4}$) is still correlated with the number of Euro 2020-related cases after removing the two most significant entries from the analysis but not significantly. The observed slope without the most significant countries (median: 0.76, 95% CI: [-1.46, 3.04]) is consistent within its uncertainties with the slope including all countries (median: 1.62, 95% CI: [1.0, 2.26]). Due to the post-hoc nature of the removal of the most significant entries, this result is only shown for information. The gray line and area are the median and 95% credible interval of the linear regression ($n = 9$ countries; The Netherlands, England and Scotland were excluded for this analysis). Whiskers denote one standard deviation.



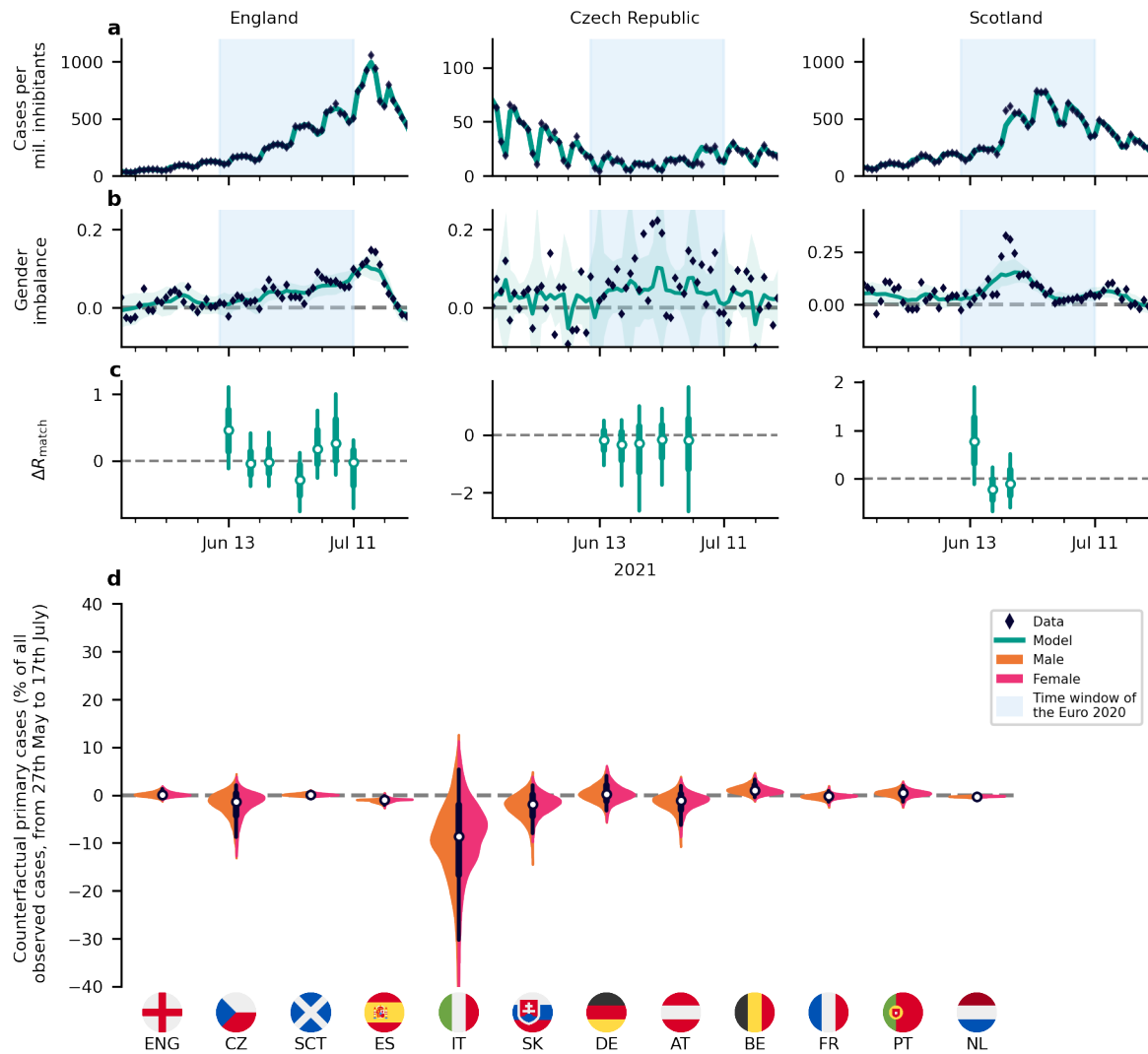
Supplementary Figure S8: **Effect of single Euro 2020 matches on the spread of COVID-19 across competing countries.** White dots represent median values, colored bars and whiskers correspond to the 68% and 95% credible intervals (CI).

S4.1 Model including the effect of stadiums

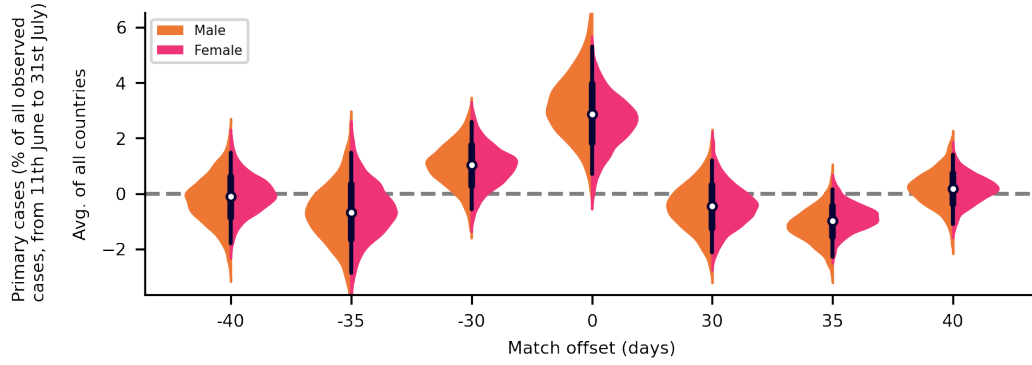


Supplementary Figure S9: **Including in our model the potential local transmission around the stadium where the matches occur does not significantly increase the overall effect.** In addition to the effect of football-related gatherings (A), we extended our model to include an additive effect on the reproduction number when a country hosted a match (B) (for those countries that hosted matches, i.e. $n = 6$ countries). We assume that local transmissions in and around the stadium would be detected mainly in the venue's country. However, football-related cases in a country where matches have a significant contribution to COVID-19 spread are tied to the dates of matches played by the country's team (A) and not to the country of the stadium venue (B), which is especially visible for England and Scotland. This also explains why previous attempts at measuring Euro 2020-related cases focusing on stadium venues were inconclusive. For Spain, an increase in the base reproduction number close to the date of a match makes the model inconclusive. In transparent is the region of the posterior of which we suppose that the model identifies the increase incorrectly; that is, where the posterior delay is smaller than 5.5 days. White dots represent median values, black bars and whiskers correspond to the 68% and 95% credible intervals (CI), respectively, and the distributions in color (truncated at 99% CI) represent the differences by gender.

S4.2 Testing the detection of a null-effect

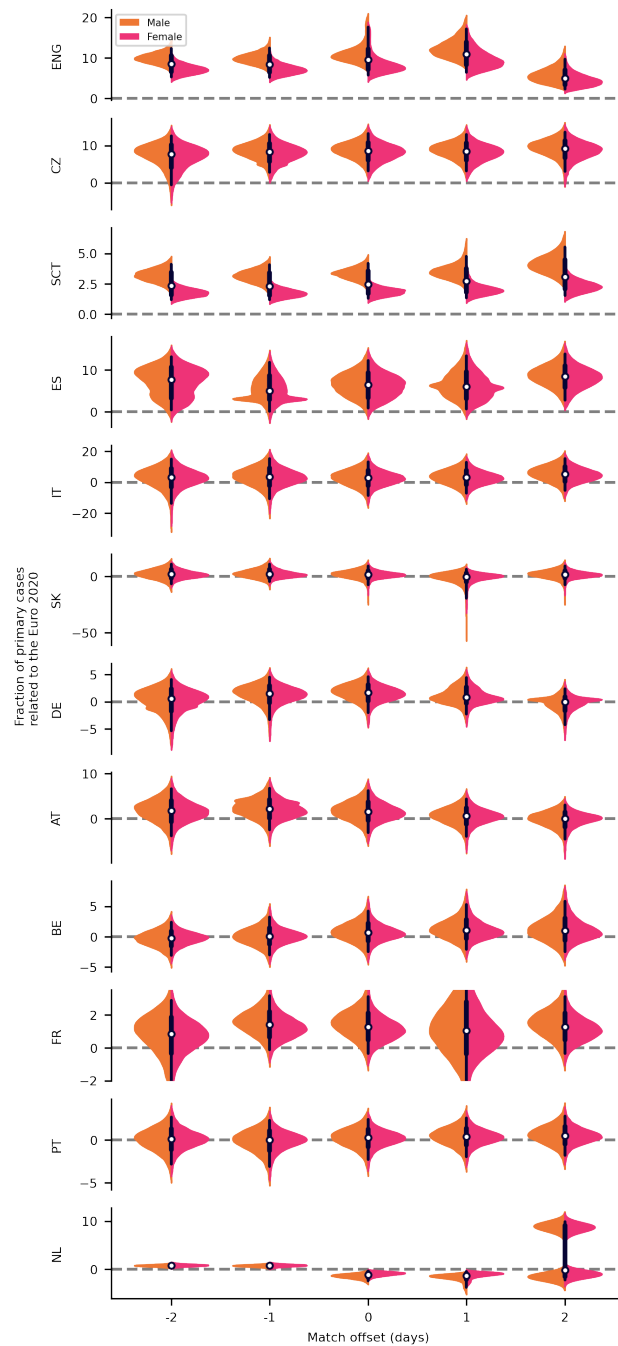


Supplementary Figure S10: **A temporal offset of 14 days leads to no inferred effect.** An artificial offset of the match data of 14 days decouples the gender ratio changes and the matches. This leads to no inferred effect of the championship – even in the three countries with the largest effect sizes in the main model (A-C). White dots represent median values, black bars and whiskers correspond to the 68% and 95% credible intervals (CI) ($n = 12$ countries). Shaded turquoise area denotes 95% CI.

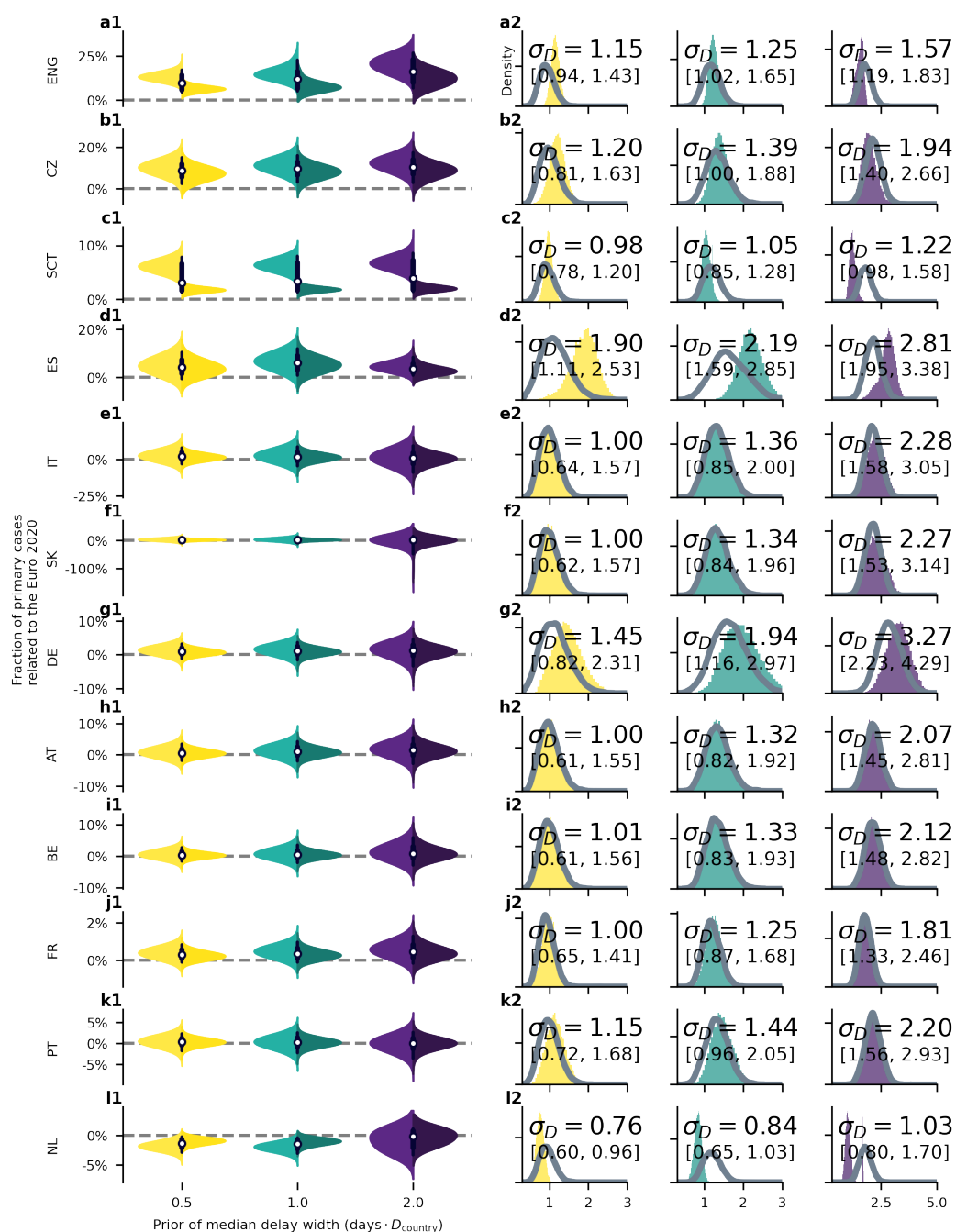


Supplementary Figure S11: **Changing the days of the match by a large offset results in a non-significant effect.** To test the reliability of our results, we ran counterfactual scenarios where the date of the matches was moved to lie outside the championship period. As expected, such offsets lead non-significant results of the average effect size across countries. White dots represent median values, black bars and whiskers correspond to the 68% and 95% credible intervals (CI) ($n = 11$ countries, The Netherlands was excluded for this analysis).

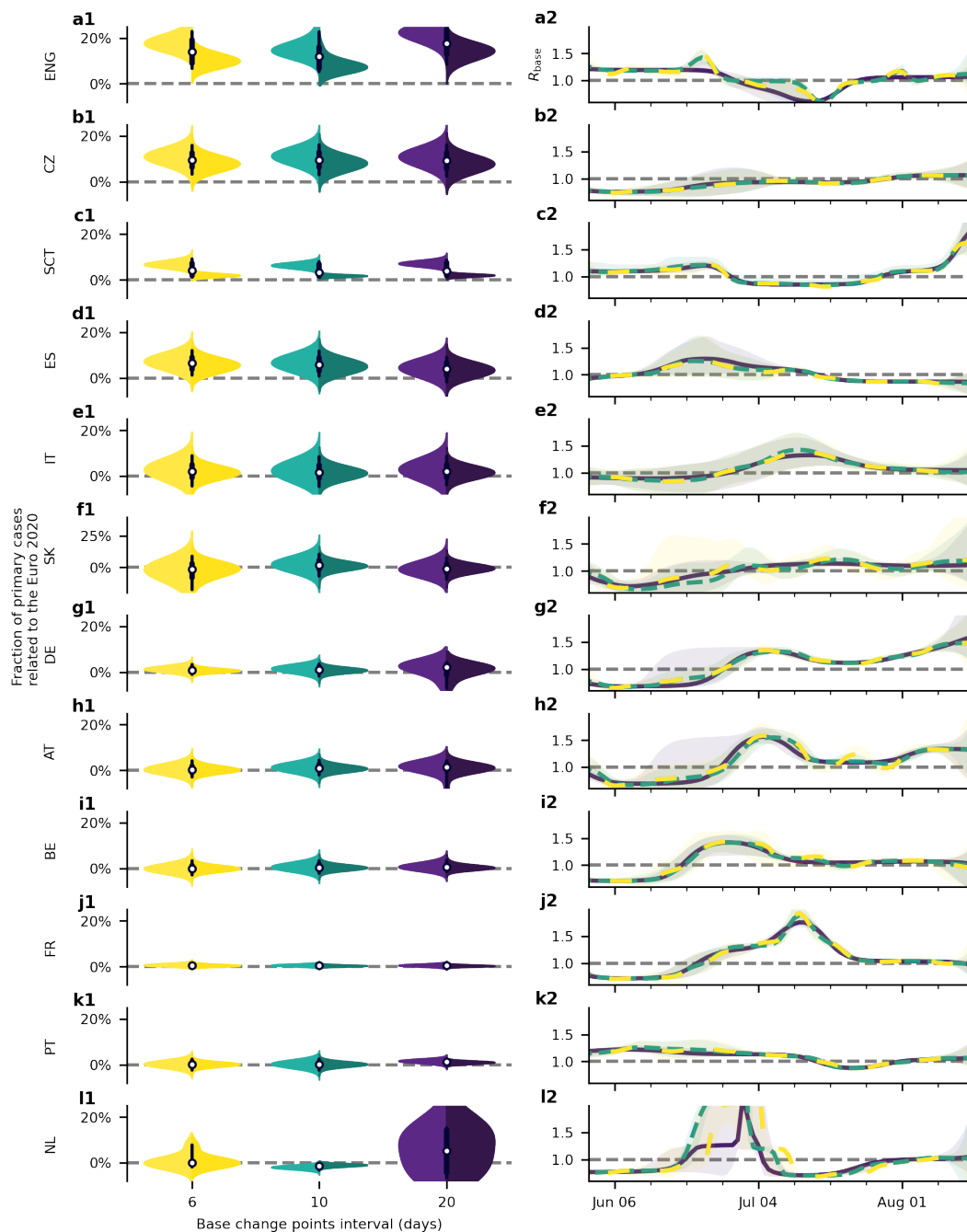
S4.3 Robustness of parameters



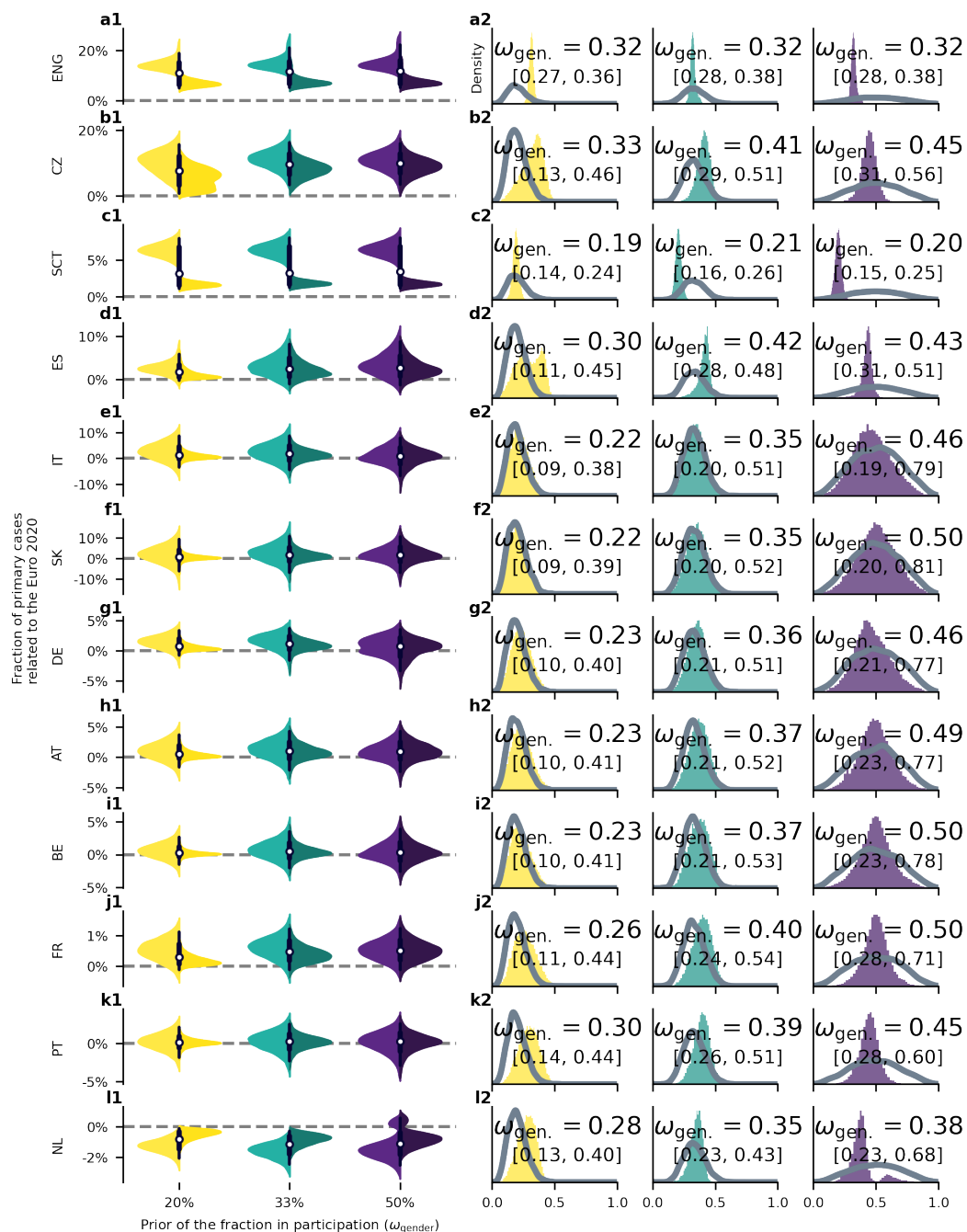
Supplementary Figure S12: **Robustness test for the effect of the temporal association between matches and cases by varying the effective delay.** We applied an artificial variation of all match days in a positive or negative direction. Under these relatively small variations of the delay, the gender imbalance is strong enough to lead to a stable effect size as the prior of the delay still allows for a sufficient shift of the posterior delay. The model run for France with a 1-day offset is missing because of an unknown, sampling-based error. White dots represent median values, black bars and whiskers correspond to the 68% and 95% credible intervals (CI), respectively, and the distributions in color (truncated at 99% CI) represent the differences by gender ($n = 11$ countries, The Netherlands was excluded for this analysis).



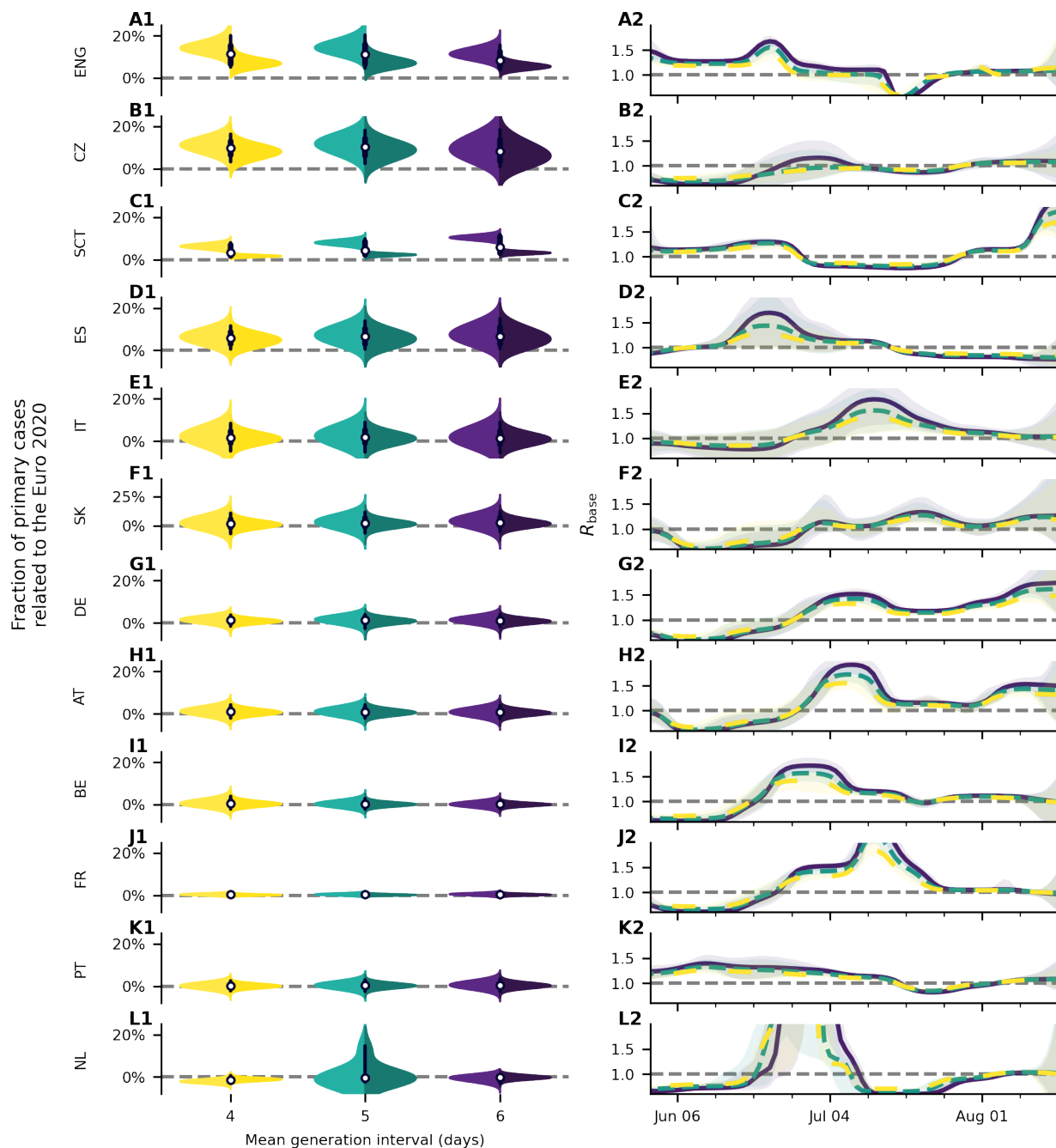
Supplementary Figure S13: **Robustness test for the effect of the width of the delay kernel.** In this robustness test, we varied the prior for the width of the delay kernel from the country-specific default (green) towards smaller (yellow) and larger (purple) widths (left column). In the violin plots, the left side is the prior for men; the right side for women. The right column shows the priors and resulting posterior of the standard deviation of the delay kernel σ_D . Except for England and Scotland (**A2**, **D2**), the data does not constrain this parameter. The results are not significantly modified in any country by changing the prior assumptions on this parameter (left column). On average, allowing for larger widths increases the effect size over the reported results. White dots represent median values, black bars and whiskers correspond to the 68% and 95% credible intervals (CI), respectively, and the distributions in color (truncated at 99% CI) represent the differences by gender.



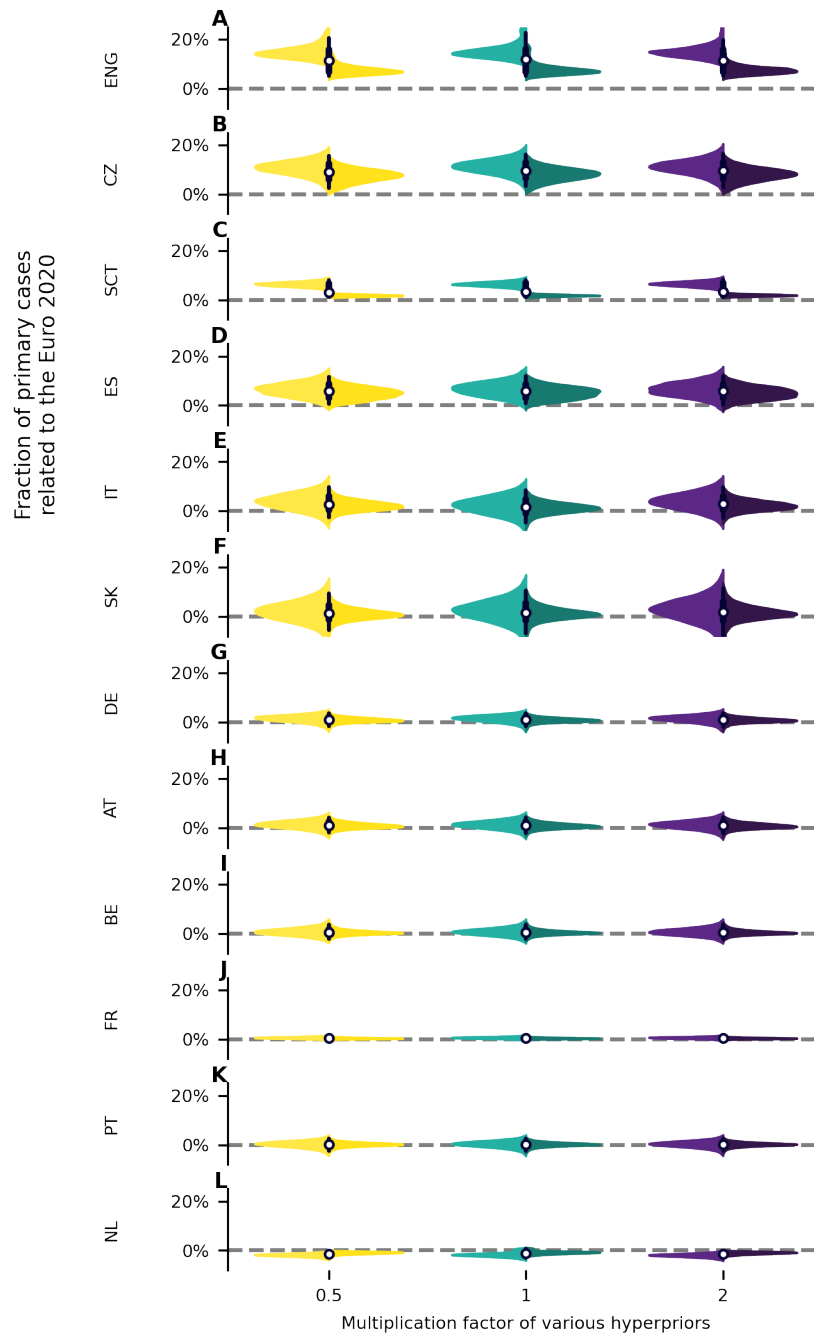
Supplementary Figure S14: **Robustness test for the effect of the allowed base reproduction number variability.** We propose models with three different base change point intervals: 6 days (yellow), 10 days (green), and 20 days (purple). In the violin plots, the left side is the distribution for men; the right side for women. We do not find significant differences in the fraction of football-related cases (left column) nor in the base reproduction numbers R_{base} (right column). On average, allowing less variation in R_{base} – i.e., removing the freedom of the model to absorb potential gender-symmetric and non-time-resolved cases related to football matches into short-timescale variations of R_{base} – increases the effect size over the reported baseline results. Shaded areas in panels *2 correspond to 95% CI. White dots represent median values, black bars and whiskers correspond to the 68% and 95% credible intervals (CI), respectively, and the distributions in color (truncated at 99% CI) represent the differences by gender.



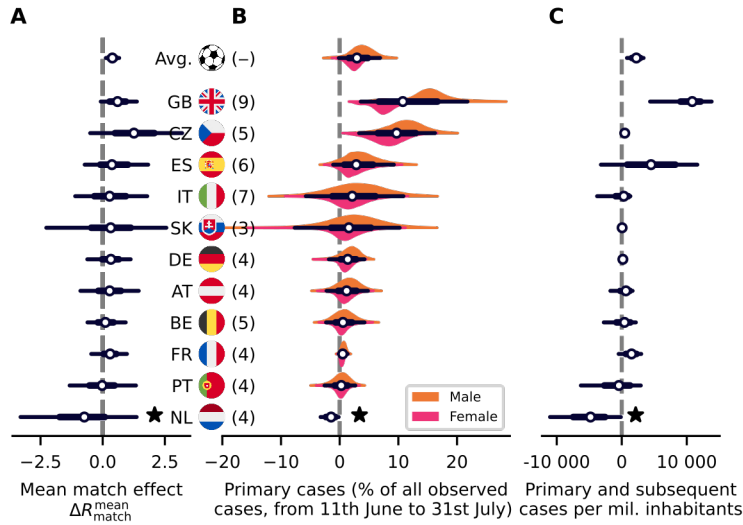
Supplementary Figure S15: **Robustness test for the effect of the fraction of female participation in football related gatherings** The default model employs a relatively constraining prior for the fraction of female participation in football-related gatherings (green) motivated by [24]. To check for the influence of this assumption, in an alternative model, we assume a more uninformative prior with mean female participation of 50% participation (purple) instead of 20% (green) (**A2-G2**). We do not find large differences in the results. On average, the total fraction of cases attributed to football matches grows when allowing the assumption of larger female participation in the fan gatherings. Hence, more cases are attributed to the Euro 2020 overall than in the baseline model. At the same time, a constraint used by the model for associating cases and matches is relieved. Thus, on average, the uncertainty of the posterior slightly grows (**A1-G1**). White dots represent median values, black bars and whiskers correspond to the 68% and 95% credible intervals (CI), respectively, and the distributions in color (truncated at 99% CI) represent the differences by gender.



Supplementary Figure S16: **Robustness test for the effect the generation interval.** We propose models with three different generation intervals: with a mean of 4 days (yellow), 5 days (green), and 6 days (purple). The lack of significant difference in the fraction of football-related cases (left column) shows that if we assume a longer generation intervals than our base assumption of 4 days our conclusions do not change. One remarks that the the base reproduction numbers R_{base} (right column) increases with a longer assumed generation interval, which is expected because a the increase of cases that needs to be modeled stays fixed. In the violin plots, the left side is the distribution for men; the right side for women. Shaded areas in the right column correspond to 95% CI. White dots represent median values, black bars and whiskers correspond to the 68% and 95% credible intervals (CI), respectively, and the distributions in color (truncated at 99% CI) represent the differences by gender.

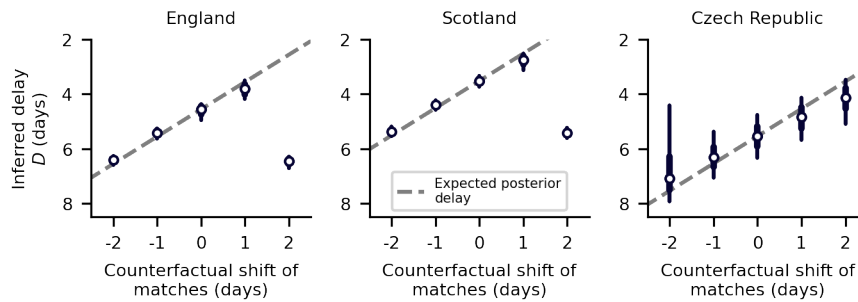


Supplementary Figure S17: **Robustness test for the remaining priors not studied in the previous figures.** Many of the priors in the model are relatively uninformative for the model. In these runs, we increased and decreased the prior value of the equations (16), (26), (35), (51), (52) and (54) by a factor of 2. In the violin plots, the left side is the distribution for men; the right side for women. White dots represent median values, black bars and whiskers correspond to the 68% and 95% credible intervals (CI), respectively, and the distributions in color (truncated at 99% CI) represent the differences by gender.

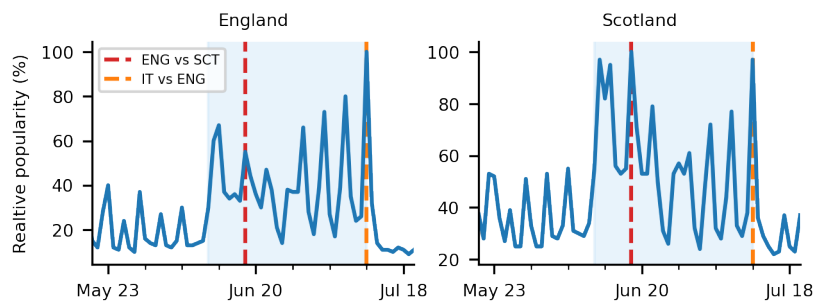


Supplementary Figure S18: **The combination of the case numbers of England and Scotland leads to similar results.** Because England and Scotland had each a team participating in the Euro 2020 we analyzed them separately, even if both are part of the United Kingdom. Here we added the case numbers of both (denoted as GB) and combined their matches for a new model run. The overall results do not change much in this alternative parametrization. White dots represent median values, black bars and whiskers correspond to the 68% and 95% credible intervals (CI), respectively, and the distributions in color (truncated at 99% CI) represent the differences by gender ($n = 11$ countries).

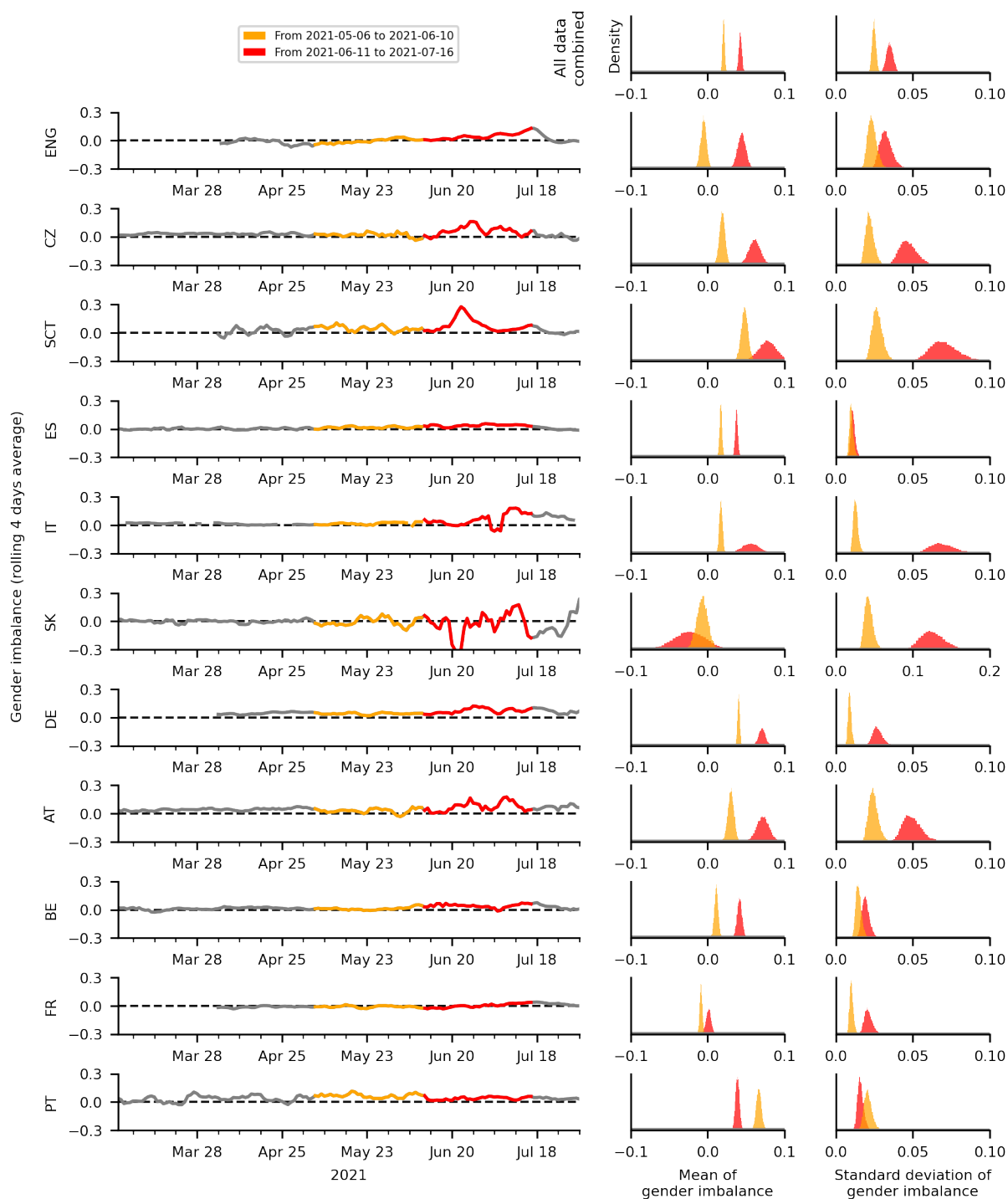
S4.4 Further analyses



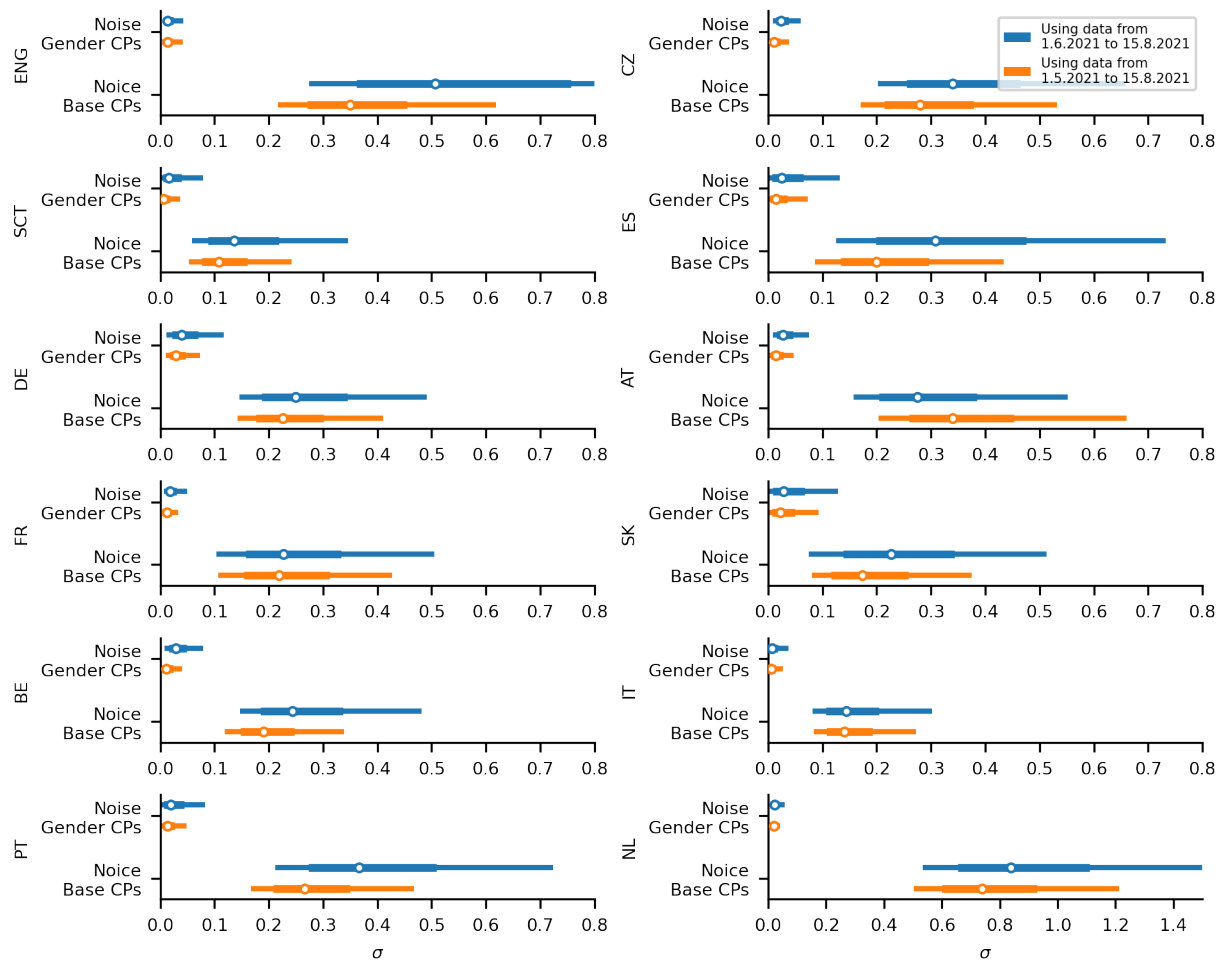
Supplementary Figure S19: **Our model is able to identify the delay between infection and reporting of it.** We tested counterfactual scenarios for England, Scotland and the Czech Republic where the dates of the matches were changed. Despite the same prior delay, the model managed to adapt the inferred delay to match the expected delay from the original model. White dots represent median values, black bars and whiskers correspond to the 68% and 95% credible intervals (CI).



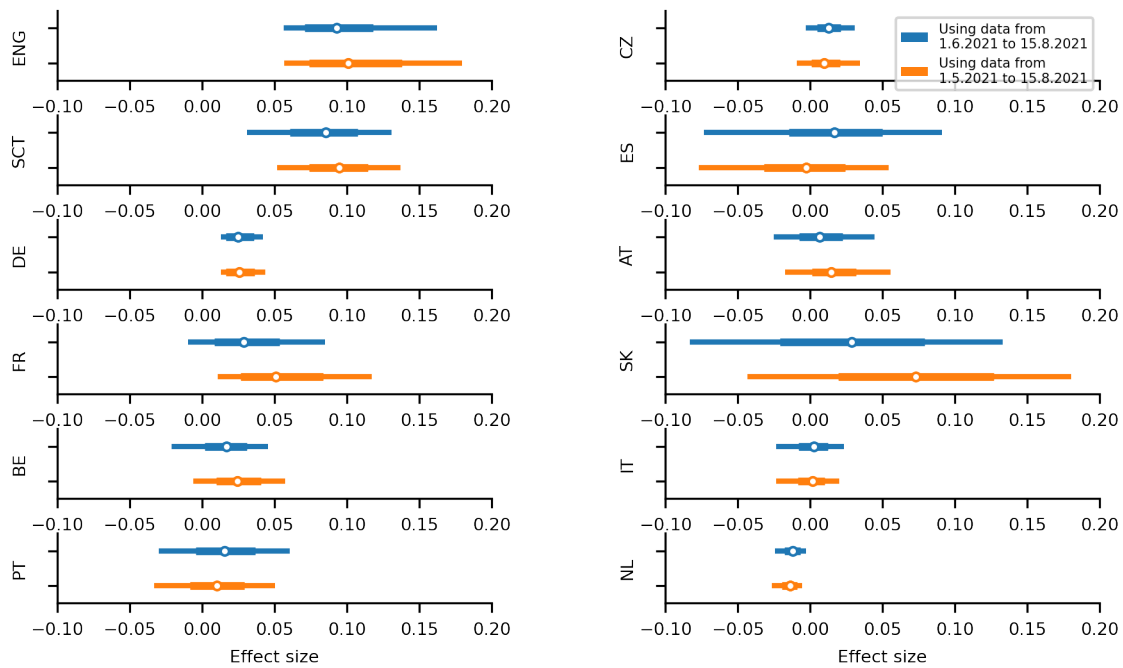
Supplementary Figure S20: **Relative popularity of the search term “football” in England and Scotland** measured using “Google Trends” [58] in the category “sport news”. Vertical red lines represent the final and match of Scotland vs England, respectively.



Supplementary Figure S21: **Male-female imbalance over time shows the largest deviations during championship.** We plotted the gender imbalance directly from our data (left column). All countries which showed significant effects had their largest imbalance change during or slightly after the championship (red), and also a number of non-significant countries display this behavior. In addition, the standard deviation of the imbalance during the championship (red) was on average larger than before the championship (orange, right column). This indicates that the large changes in imbalance during the championship were highly unusual and can't be attributed to chance alone. The red time period are the 30 days of the tournament plus the 5 days after and the orange time period the ones up to 35 days before the tournament.

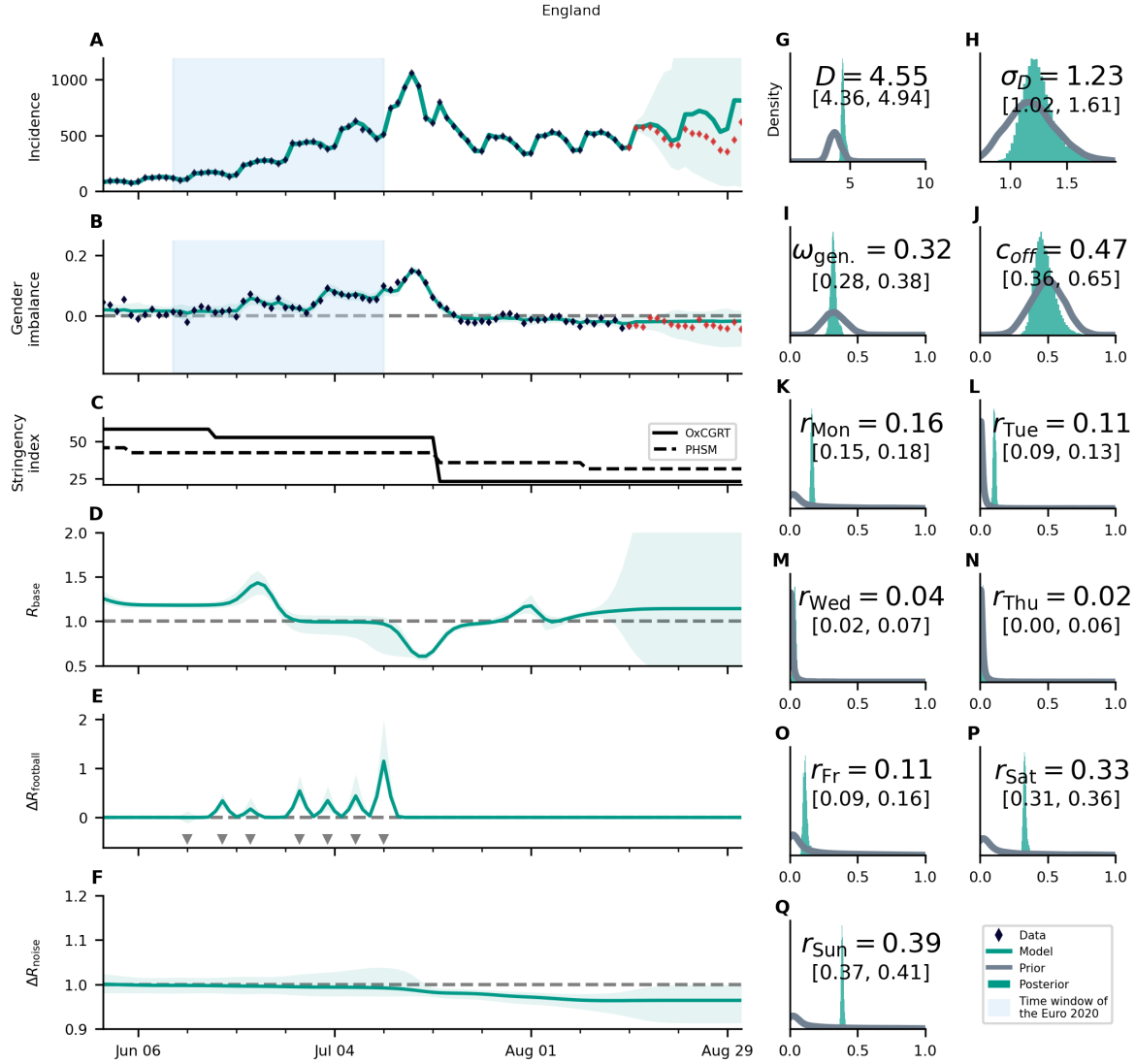


Supplementary Figure S22: **The inferred noise terms do not depend strongly on the length of the analyzed time-period.** We plotted the size of our gender noise term $\sigma_{\Delta\tilde{\gamma}}$ and the size of the change-points of the base reproduction number $\sigma_{\Delta\gamma}$. When beginning the run of our model a month earlier (blue), the noise terms do not change significantly compared to our base model (orange). White dots represent median values, colored bars and whiskers correspond to the 68% and 95% credible intervals (CI).

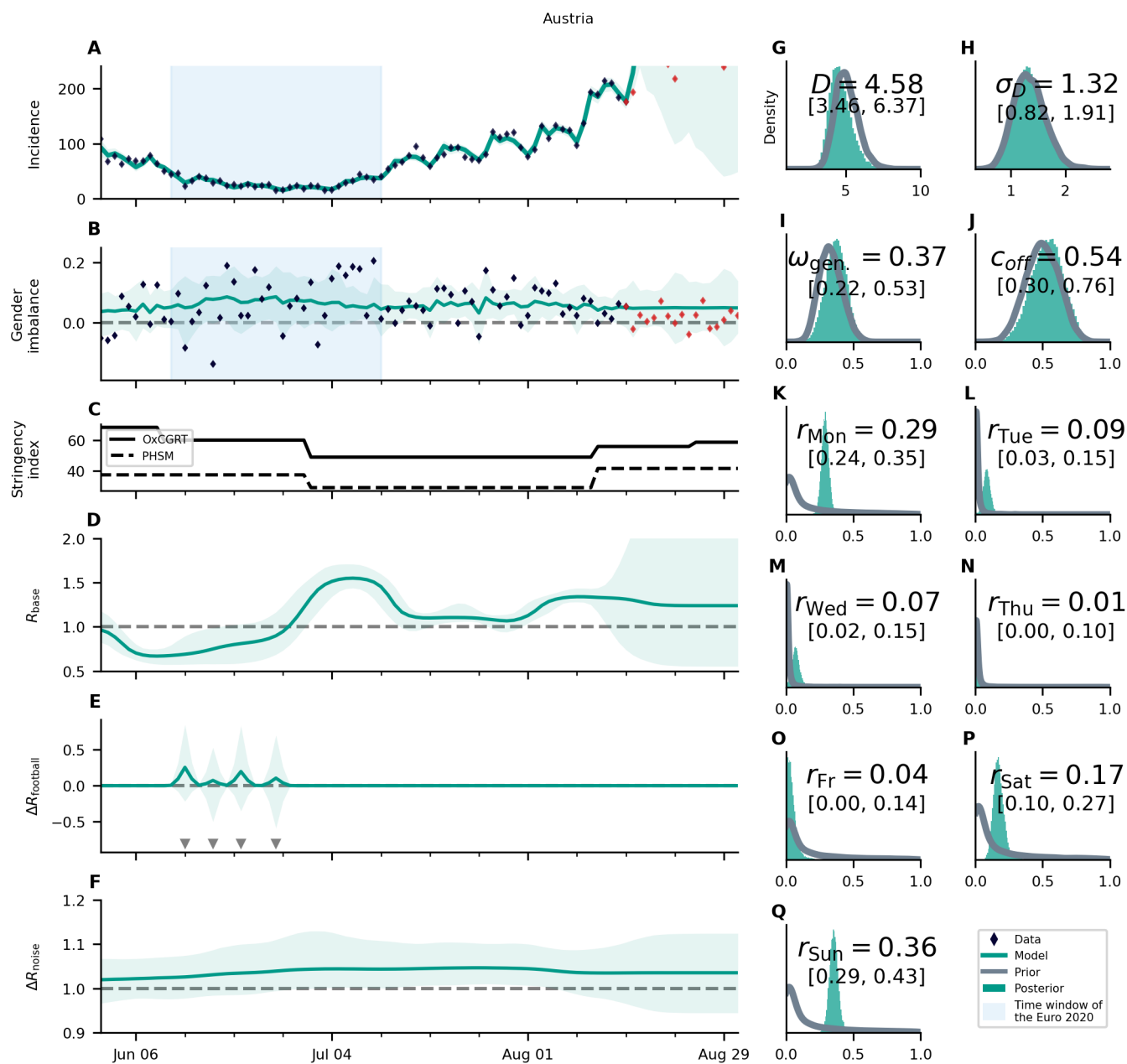


Supplementary Figure S23: **The inferred effect size (percentage of football-related primary infections) do not depend strongly on the length of the analyzed time-period.** To showcase that the total length of the analyzed period doesn't change significantly our results, we compare the percentage of football-related primary infections one-month-longer runs (blue) compared to our base model (orange). White dots represent median values, colored bars and whiskers correspond to the 68% and 95% credible intervals (CI).

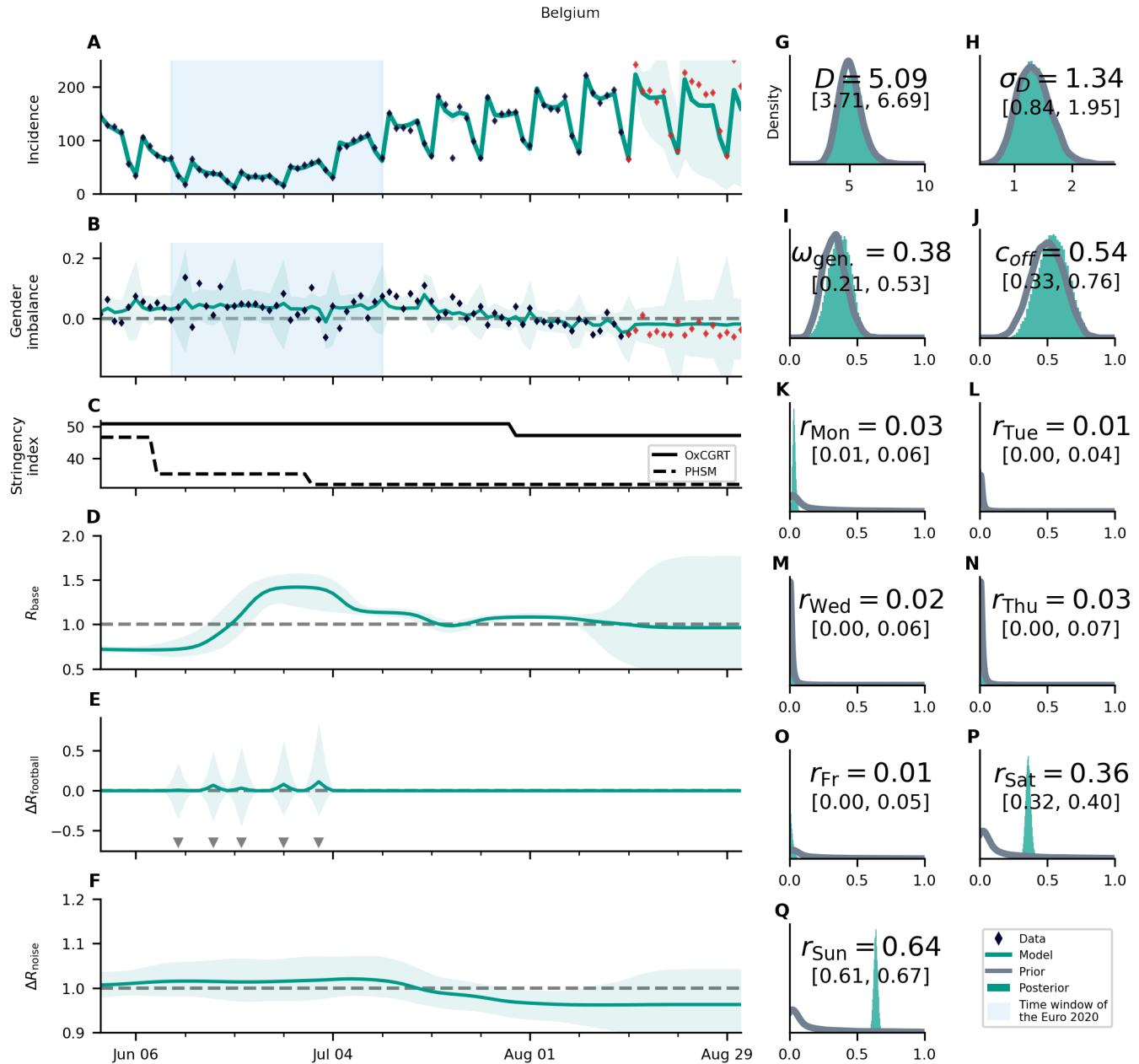
S4.5 Posterior of parameters



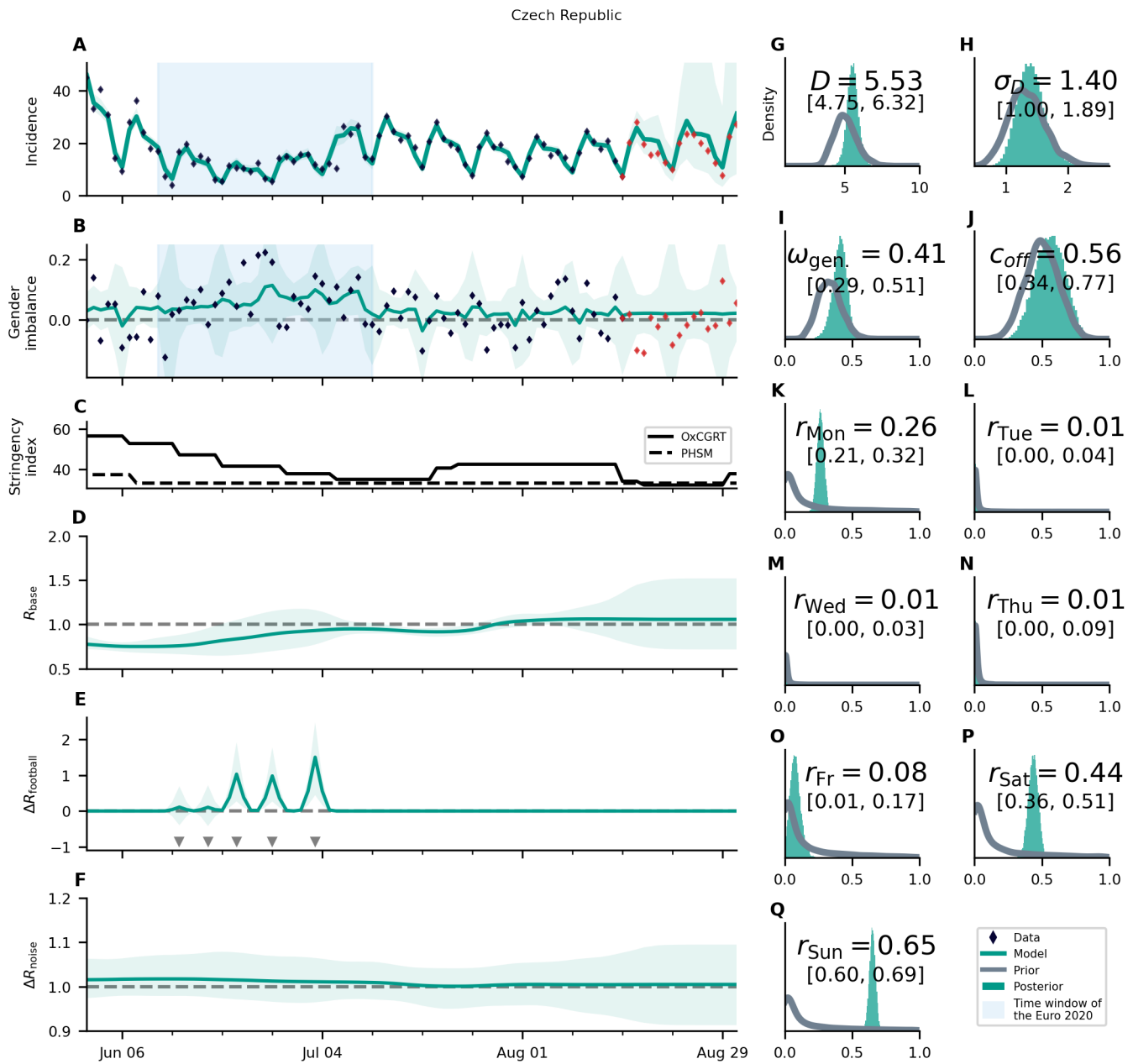
Supplementary Figure S24: **Overview of the posterior for England.** We compare (A) the time-dependence of the incidence before, during (blue shaded area) and after the championship; (B) the gender imbalance of observed cases; (C) Oxford governmental response tracker (OxCGRT) [33] and public health and social measures severity index (PHSM) [56] (not part of the model); (D) the gender-symmetric base reproduction number R_{base} ; (E) the gender-asymmetric football reproduction number R_{football} ; (F) gender-asymmetric noise related reproduction number R_{noise} ; and (G) to (Q) the prior and posterior of various parameters. In mid July the incidence starts dropping. In contrast, the number of deaths continues to increase. Together, this indicates that the testing policy was changed around that time. England is one of the two countries where the delay D and the female participation in fan activities dominating the additional transmission can be measured and significantly constrained with the data compared to the prior distribution (G and I). Red diamonds show data not used for the analysis. This comes with an increase in the uncertainty in the model prediction. One notes two slight bumps of the base reproduction number: one during and one after the end of the championship. The first bump may indicate that our model is not able to fully attribute a part of the effective reproduction number to $\Delta R_{\text{football}}$ and is attributing the effect of England's matches in the group phase to the base reproduction number instead. The second bump might be explained hereby: During the championship there may be generally more social contacts, which are not in temporal synchronization with the matches, and therefore not explained by $\Delta R_{\text{football}}$ but by R_{base} instead. Hence, after the championship the base reproduction number decreases and increases again when measures are lifted (C). The turquoise shaded areas correspond to 95% credible intervals.



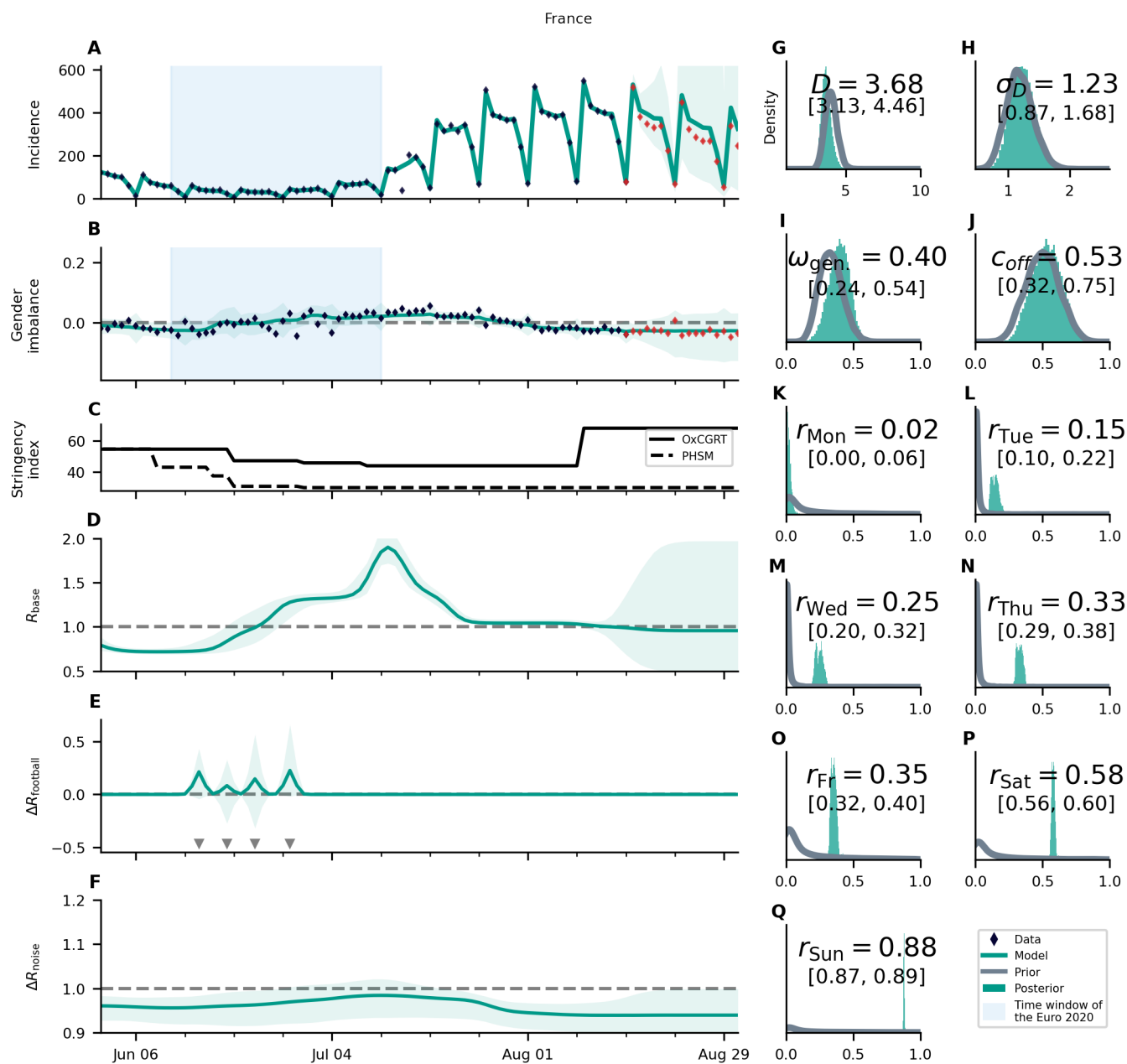
Supplementary Figure S25: **Overview of the posterior for Austria.** For an explanation of the panel structure, see supplementary Fig. S24. Austria shows a low significance for assigning cases to matches. The increase of R_{base} coincides with the relaxation of restrictions C, but the subsequent decrease is not explained. The turquoise shaded areas correspond to 95% credible intervals.



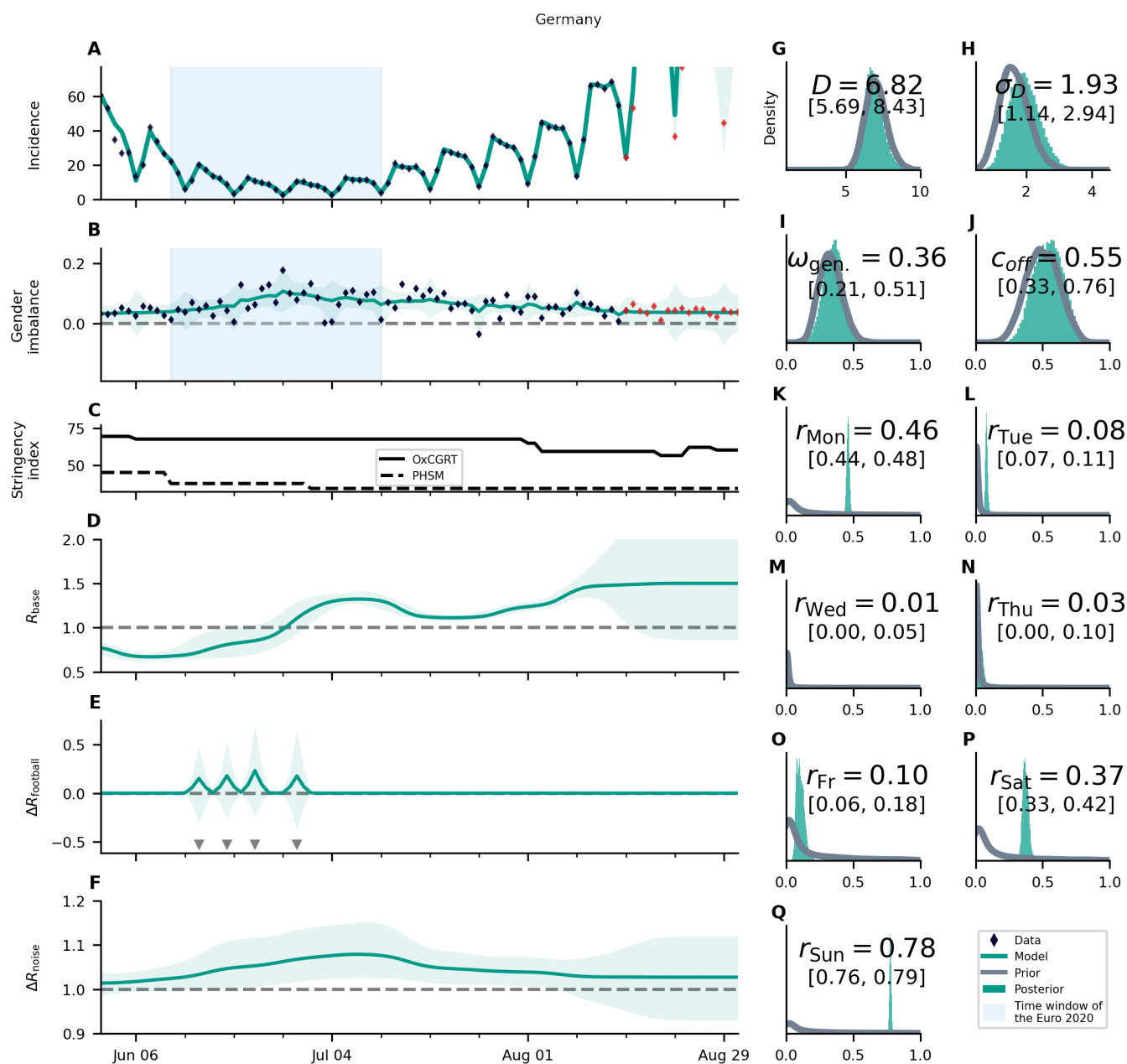
Supplementary Figure S26: **Overview of the posterior for Belgium.** For an explanation of the panel structure, see supplementary Fig. S24. Belgium shows a low significance for assigning cases to matches, but an intermittent increase of R_{base} during the championship. The turquoise shaded areas correspond to 95% credible intervals.



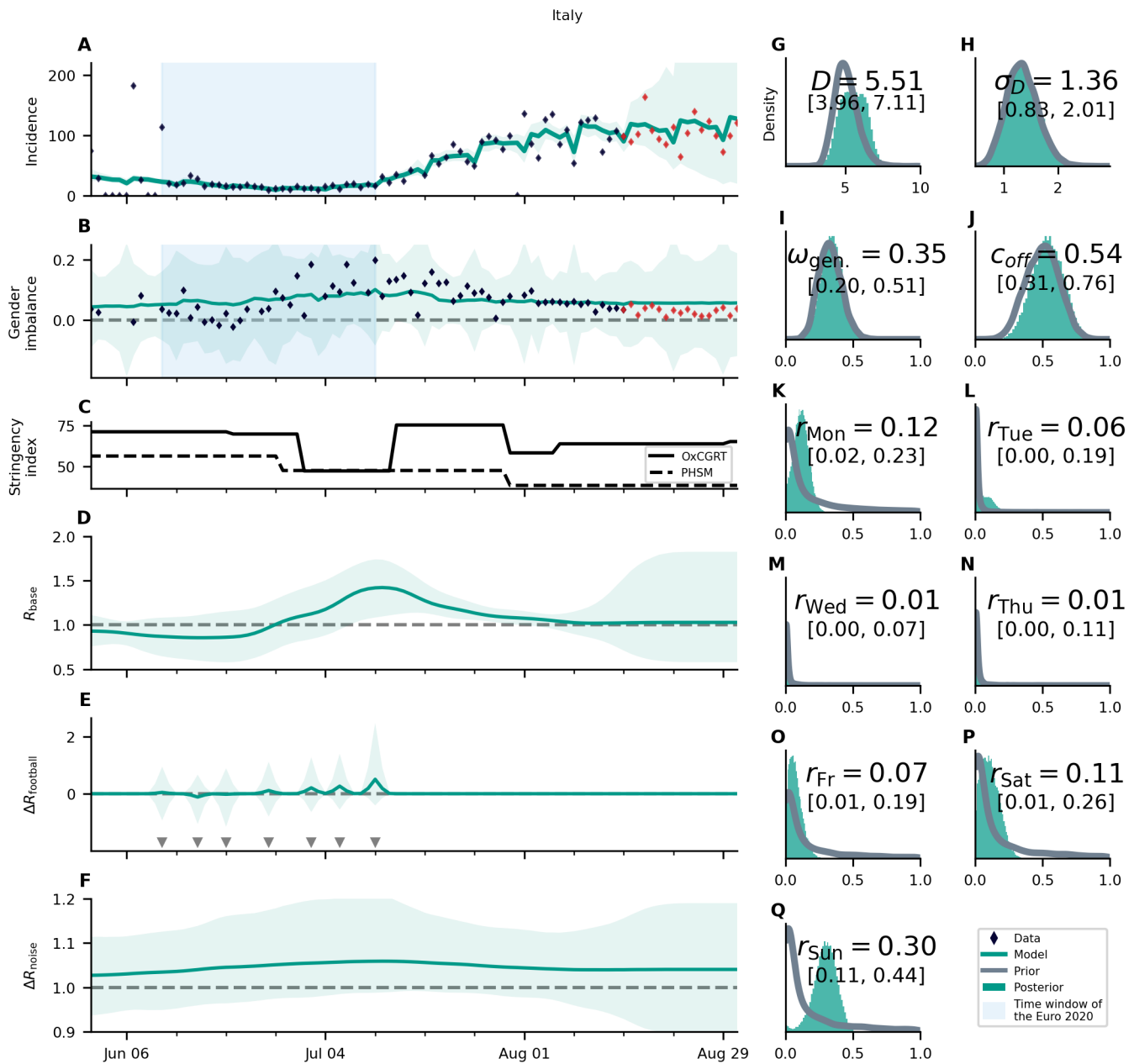
Supplementary Figure S27: **Overview of the posterior for the Czech Republic.** For an explanation of the panel structure, see supplementary Fig. S24. The overall incidence is relatively low, which increases the noisiness of the data. This is especially apparent in the gender imbalance (B). The base reproduction number is slowly increasing during the analyzed time-period, which can be partially explained by a decrease of the stringency index (C). The match effects are greater for later matches, beginning from the last group match until the quarterfinals (E), which is the expected variation. The turquoise shaded areas correspond to 95% credible intervals.



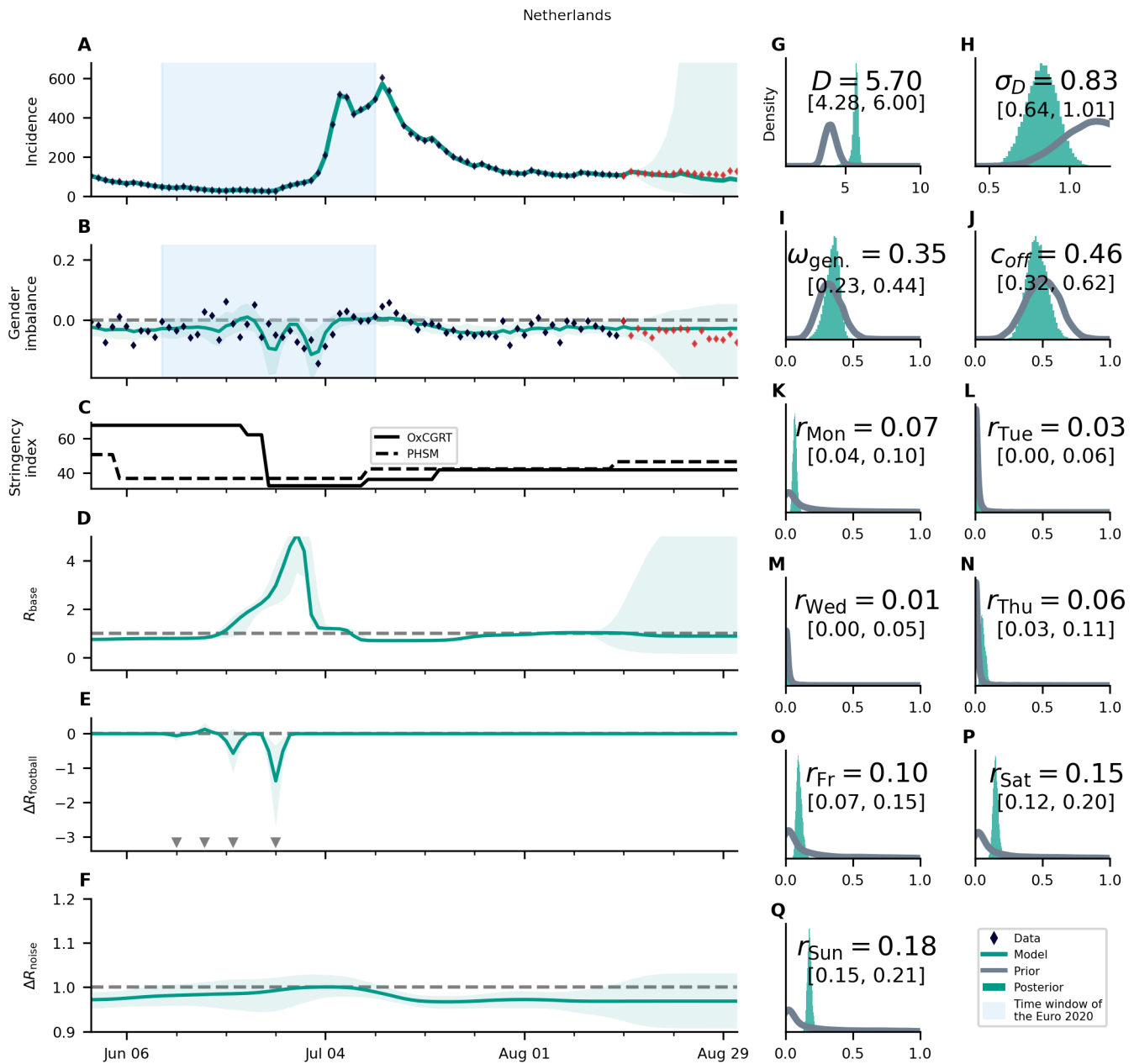
Supplementary Figure S28: **Overview of the posterior for France.** For an explanation of the panel structure, see supplementary Fig. S24. France shows a very pronounced increase of R_{base} over the course of the championship and a very small fraction of cases assigned to matches of the French team. This hints at a rather gender-neutral effect of match-induced infections in France, in agreement with the results shown in Fig. S15. The peak of R_{base} occurs on July 11th when clubs etc re-opened. It is unclear why the base reproduction number decreases this much again afterwards. The turquoise shaded areas correspond to 95% credible intervals.



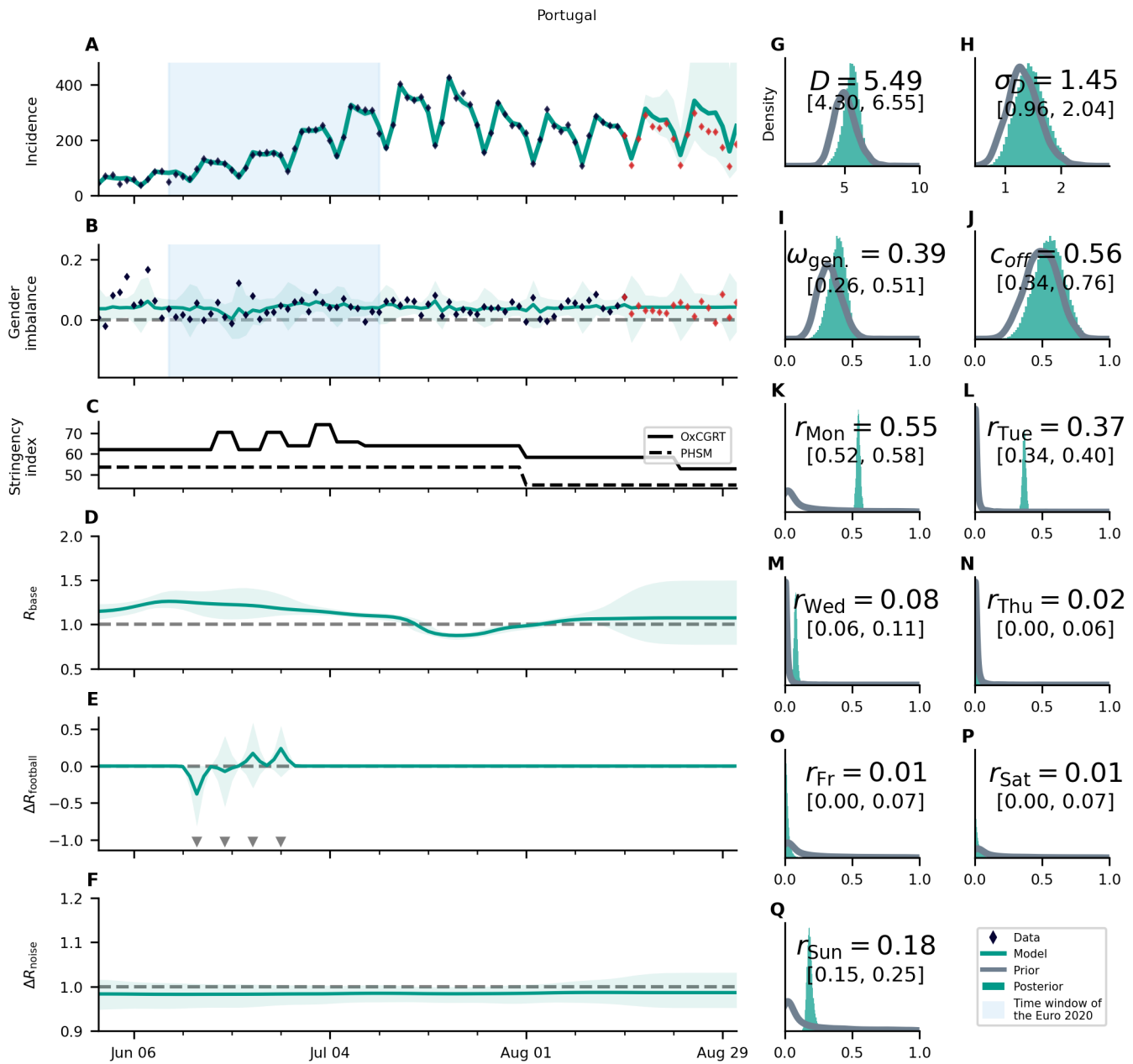
Supplementary Figure S29: **Overview of the posterior for Germany.** For an explanation of the panel structure, see supplementary Fig. S24. Germany shows an increase of R_{base} and of the gender imbalance over the course of the championship (**B**). It might be the case that the Euro 2020 contribution is not tightly tied to matches of the German team, prohibiting the model to explain the observed gender imbalance via the individual matches (**E**), leading to an increase of ΔR_{noise} instead (**F**). The turquoise shaded areas correspond to 95% credible intervals.



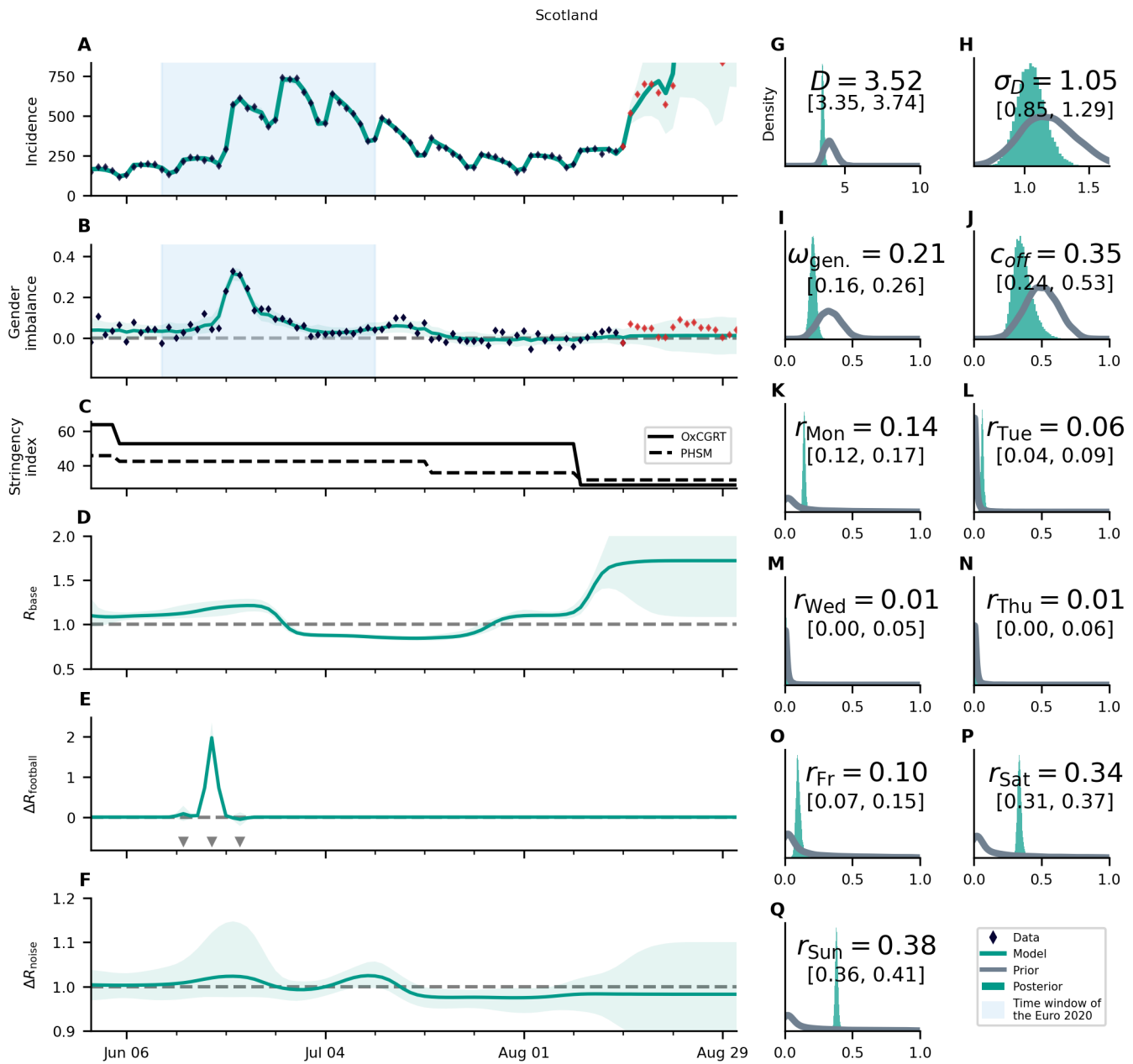
Supplementary Figure S30: **Overview of the posterior for Italy.** For an explanation of the panel structure, see supplementary Fig. S24. Italy is one of the countries where an intermittent increase in R_{base} is observed (D). The development of the base reproduction number also coincides well with the relaxations and reinstatement of restrictions (C). Match-related football effects are not clearly visible (E). The turquoise shaded areas correspond to 95% credible intervals.



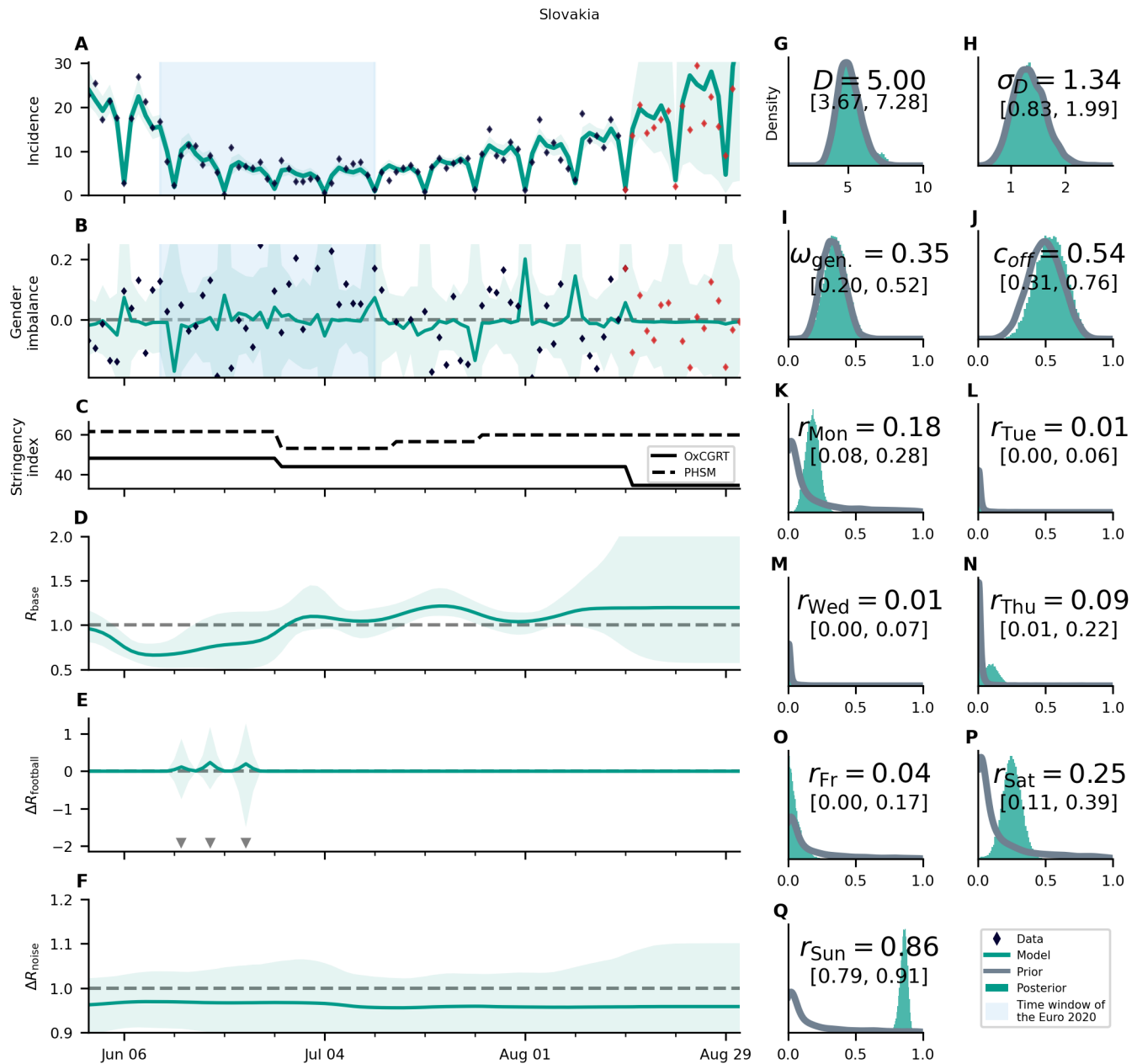
Supplementary Figure S31: **Overview of the posterior for the Netherlands.** For an explanation of the panel structure, see supplementary Fig. S24. The country wide “freedom day” on June 26th [59] is clearly visible in the incidence numbers **A** as well as the posterior base reproduction number **B**. Its effects overshadow possible effects from the Euro 2020 and we removed this country from subsequent analyses. The turquoise shaded areas correspond to 95% credible intervals.



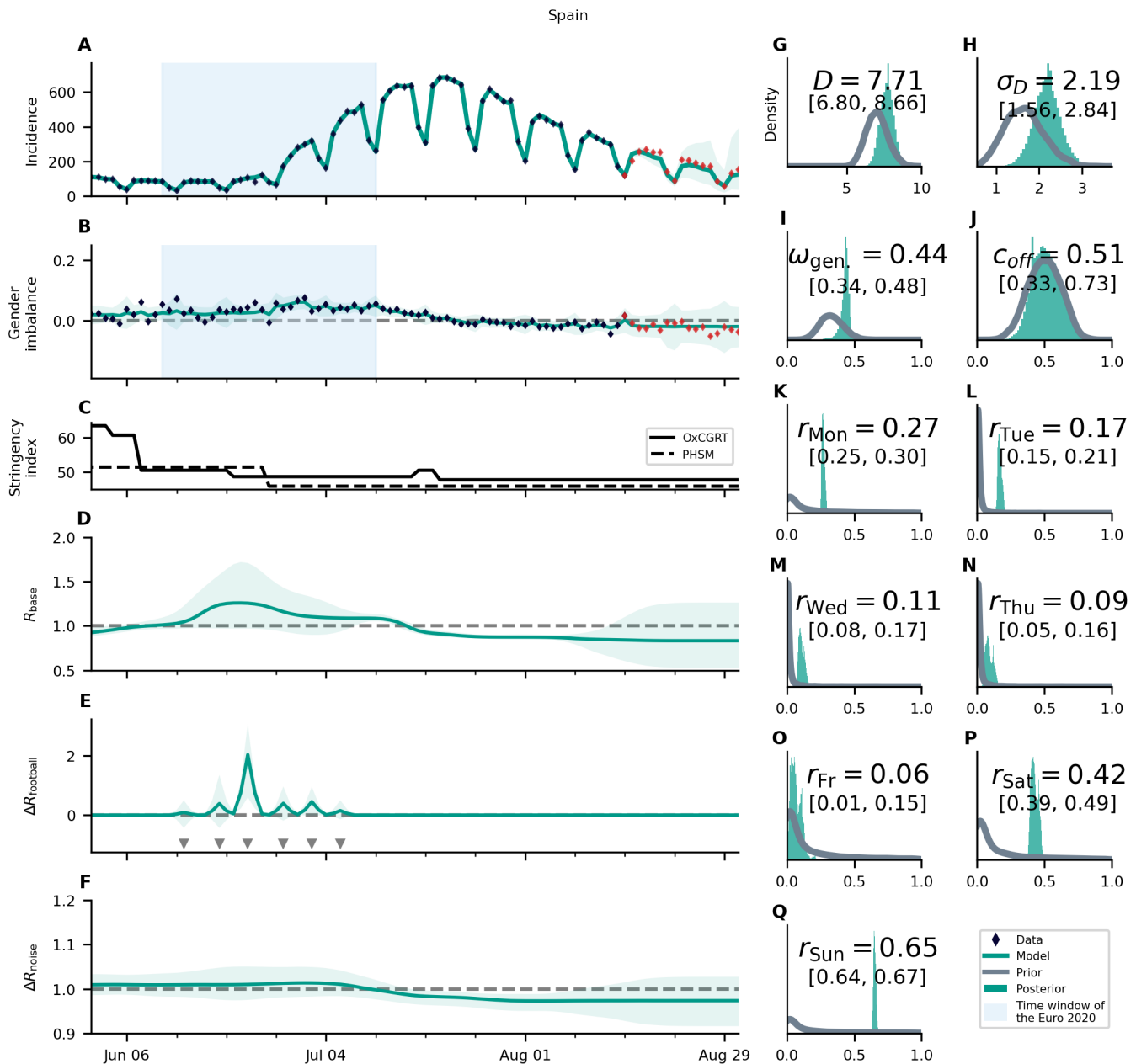
Supplementary Figure S32: **Overview of the posterior for Portugal.** For an explanation of the panel structure, see supplementary Fig. S24. Together with England, Portugal has the highest R_{base} before the championship. It is the only country in which a decrease of R_{base} over the course of the championship is observed. The fact that R_{base} remains low after the championship could be a hint that the possible increase of cases due to the Euro 2020 in Portugal is small compared to the reduction stemming from unrelated changes. The turquoise shaded areas correspond to 95% credible intervals.



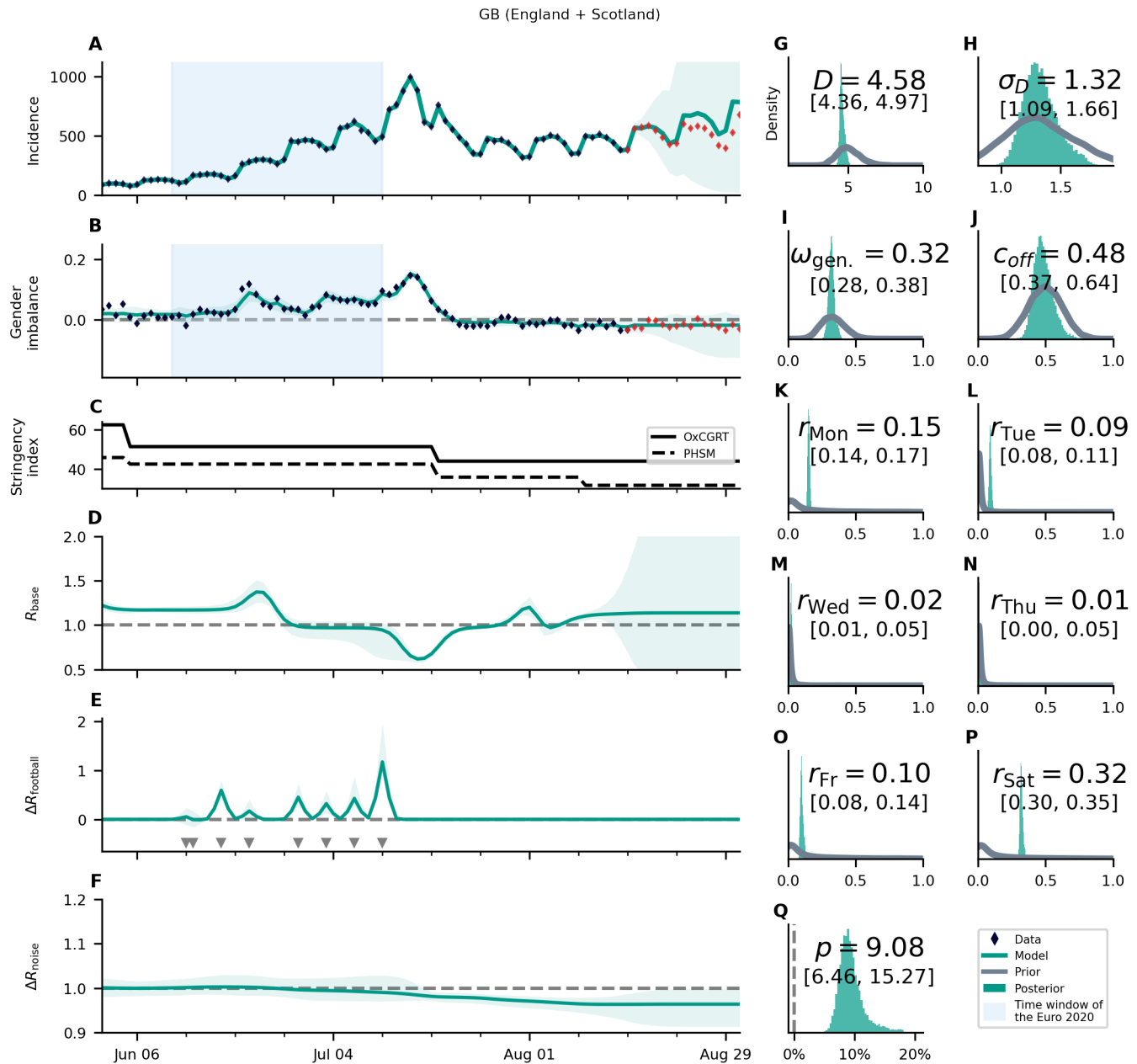
Supplementary Figure S33: **Overview of the posterior for Scotland.** For an explanation of the panel structure, see supplementary Fig. S24. Scotland is the country with the most significant effect of a single match, in this case against England. While this is in full agreement press reports (see also Fig. S20), the prior assumption of an exceptional large effect of this game is not built into the model. This clear association, thus, is a successful validation of the model functionality. The relaxation of governmental restrictions on August 9th is also well reflected in the development of the base reproduction number. The turquoise shaded areas correspond to 95% credible intervals.



Supplementary Figure S34: **Overview of the posterior for Slovakia.** For an explanation of the panel structure, see supplementary Fig. S24. Hardly any significant effects, apart from a small but long-lasting increase in R_{base} , are observed. The turquoise shaded areas correspond to 95% credible intervals.

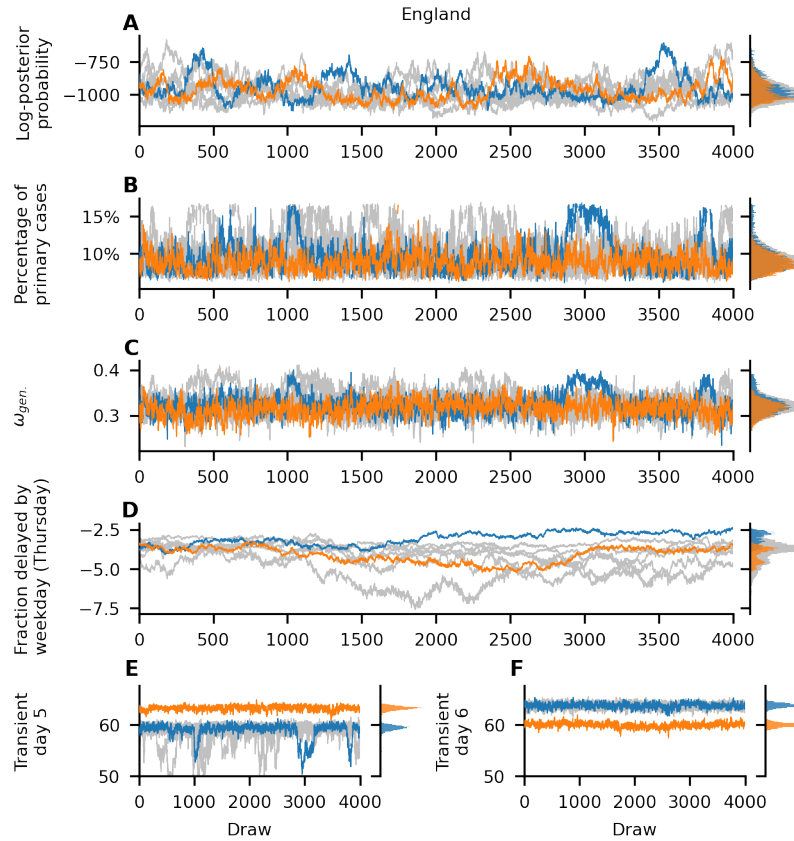


Supplementary Figure S35: **Overview of the posterior for Spain.** For an explanation of the panel structure, see supplementary Fig. S24. The national state of emergency ended in Spain on June 21st, in the middle of the championship. The model has therefore some difficulty to separate the effect of the relaxation of restrictions and the one of the matches, which translates into wide credible intervals in R_{base} (C) and $\Delta R_{\text{football}}$ (D). The turquoise shaded areas correspond to 95% credible intervals.

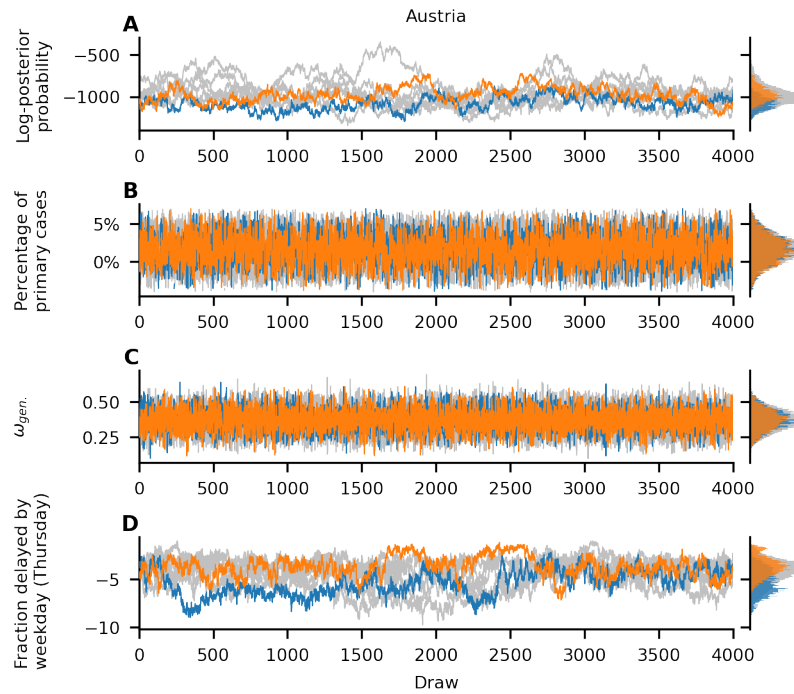


Supplementary Figure S36: **Overview of the posterior for the combined data of England and Scotland** For an explanation of the panel structure, see supplementary Fig. S24. The turquoise shaded areas correspond to 95% credible intervals.

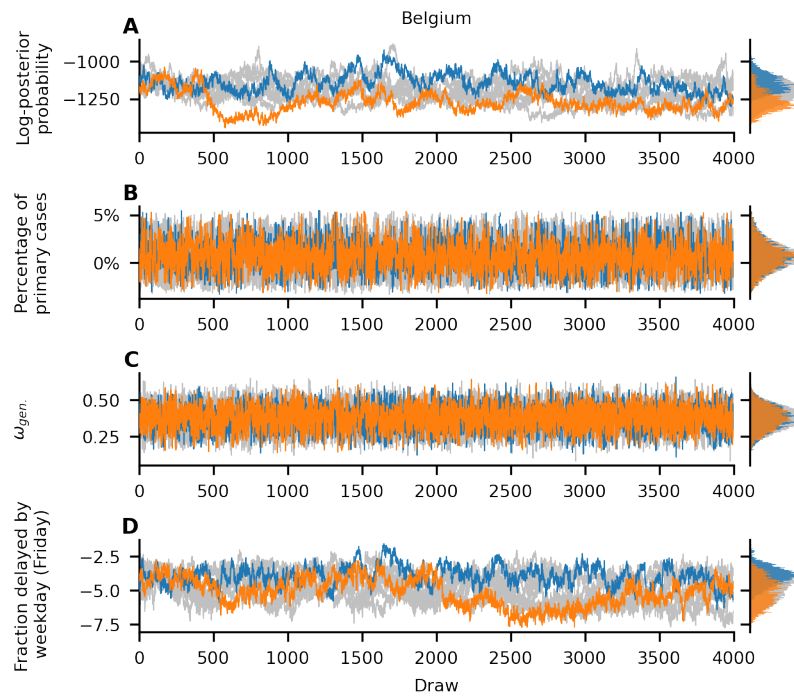
S4.6 Chain mixing of selected parameters



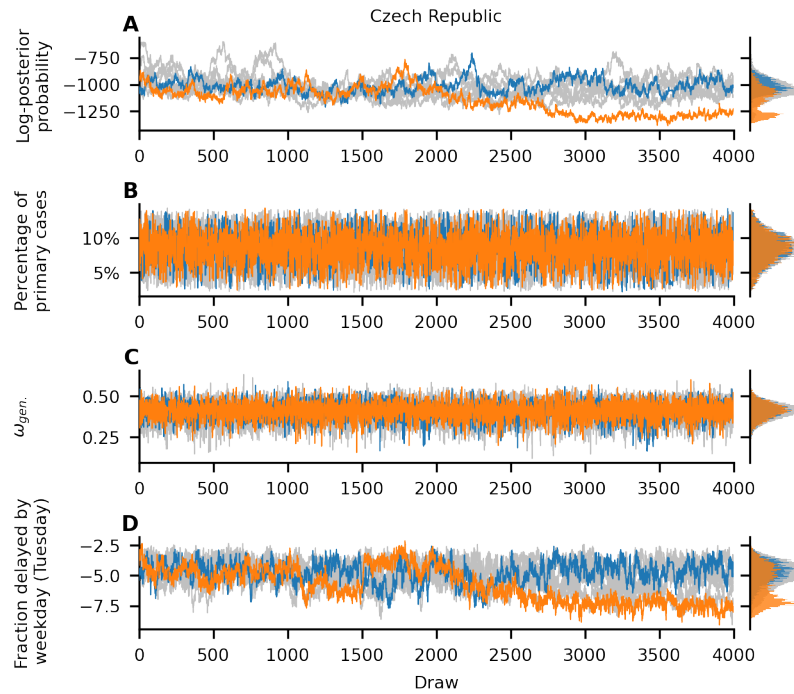
Supplementary Figure S37: **Chain mixing of selected parameters for England** Here we plot the unnormalized log-posterior probability (**A**) and selected parameters (**B – F**) as function for each draw and MCMC chain. Orange and blue depict two chains with the highest between-chain variance, the two least converging chains. The gray lines and histogram represent the ensemble of all chains. For our parameters of interest (**B**, **C**) the posterior distribution mixes well, even if the individual chains do not mix well in some other parameters (**D – F**), indicating that despite the degeneracy of some parameters, the inference of our parameters of interest is not affected. Panel **D** is a plot of the parameter with the worst mixing (the highest \mathcal{R} -hat value). Panels **E** and **F** show that the non-converging behavior can be explained as the exchange between two nearly degenerate solutions in two of the auxiliary parameters.



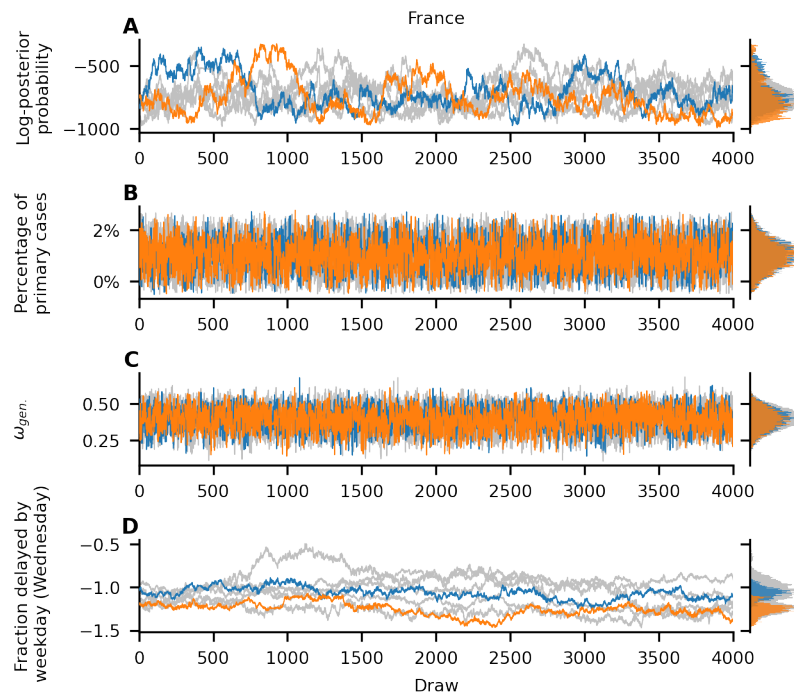
Supplementary Figure S38: **Chain mixing of selected parameters for Austria** Here the fraction of cases delayed by weekday on Thursdays is the parameter with the highest \mathcal{R} -hat values as seen in panel **D**. For a further detailed description of the panels see supplementary Fig. S37.



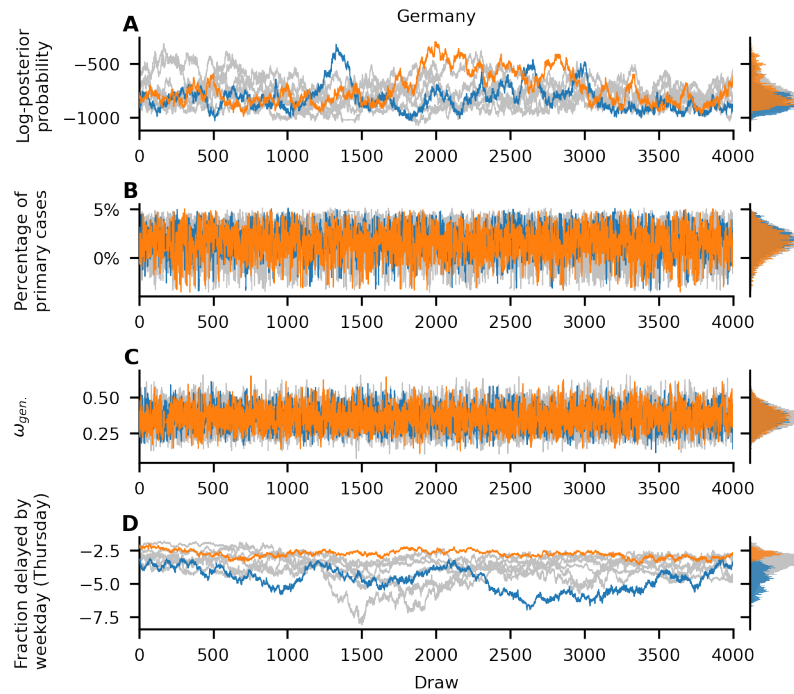
Supplementary Figure S39: **Chain mixing of selected parameters for Belgium** Here the fraction of cases delayed by weekday on Fridays is the parameter with the highest \mathcal{R} -hat values as seen in panel **D**. For a further detailed description of the panels see supplementary Fig. S37.



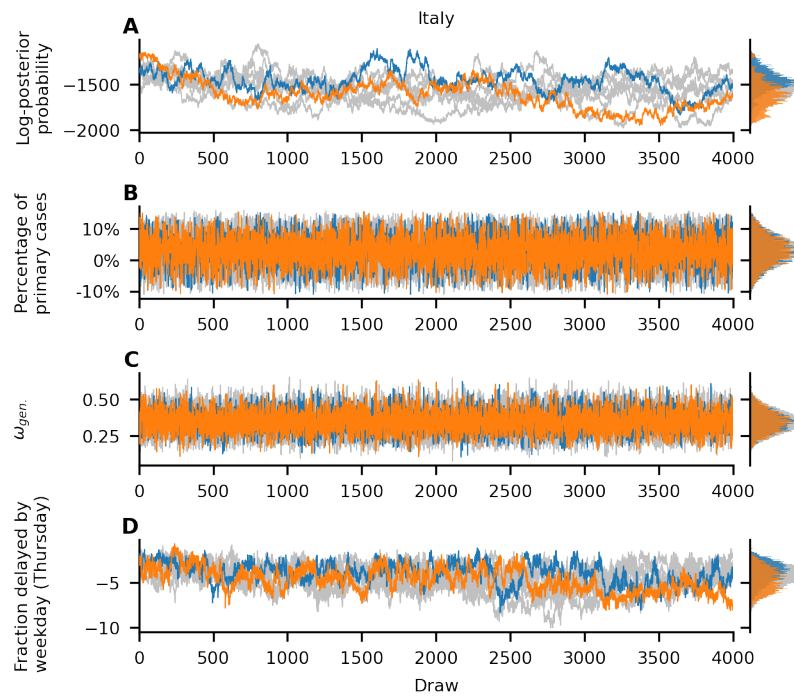
Supplementary Figure S40: **Chain mixing of selected parameters for Czech Republic** Here the fraction of cases delayed by weekday on Thursdays is the parameter with the highest \mathcal{R} -hat values as seen in panel **D**. For a further detailed description of the panels see supplementary Fig. S37.



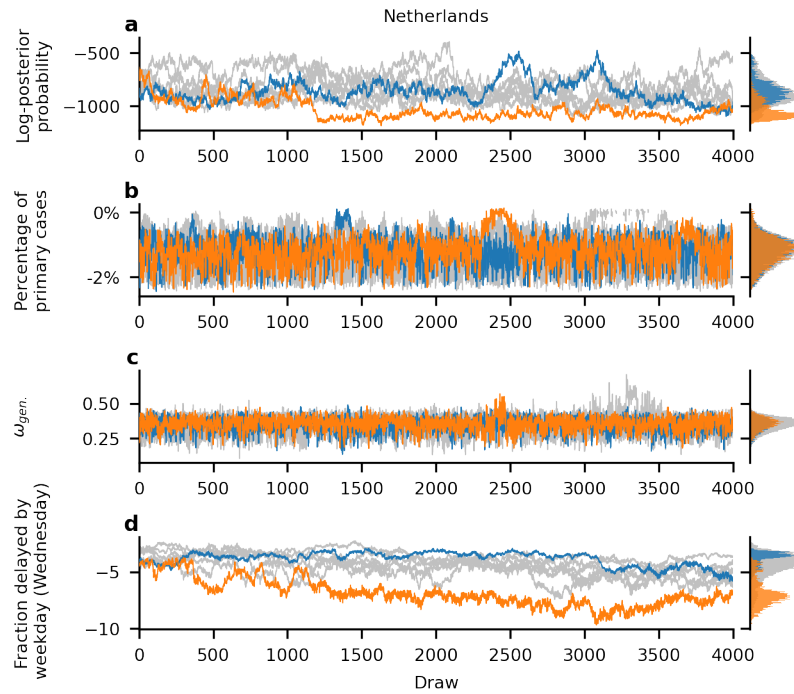
Supplementary Figure S41: **Chain mixing of selected parameters for France** Here the fraction of cases delayed by weekday on Wednesdays is the parameter with the highest \mathcal{R} -hat values as seen in panel **D**. For a further detailed description of the panels see supplementary Fig. S37.



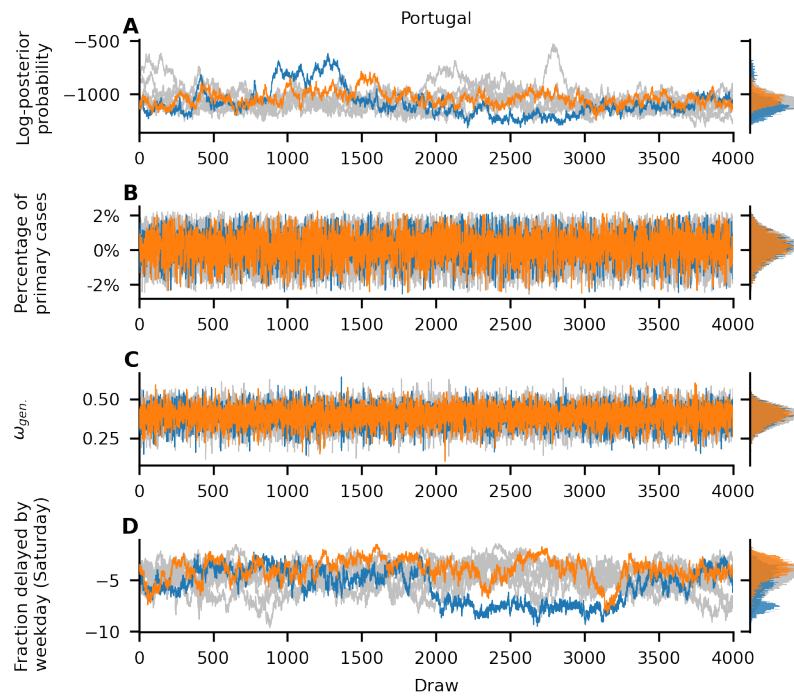
Supplementary Figure S42: **Chain mixing of selected parameters for Germany** Here the fraction of cases delayed by weekday on Thursdays is the parameter with the highest \mathcal{R} -hat values as seen in panel D. For a further detailed description of the panels see supplementary Fig. S37.



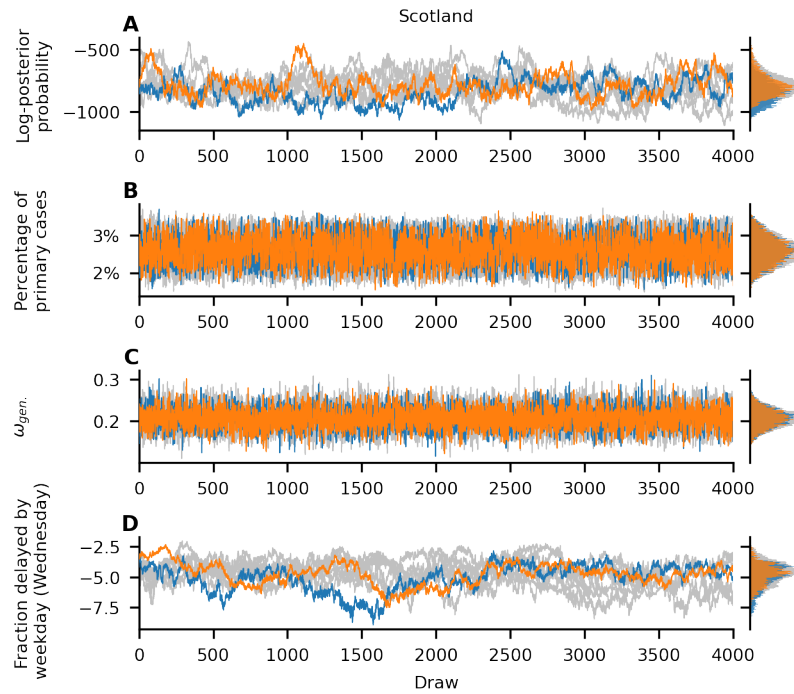
Supplementary Figure S43: **Chain mixing of selected parameters for Italy** Here the fraction of cases delayed by weekday on Thursdays is the parameter with the highest \mathcal{R} -hat values as seen in panel D. For a further detailed description of the panels see supplementary Fig. S37.



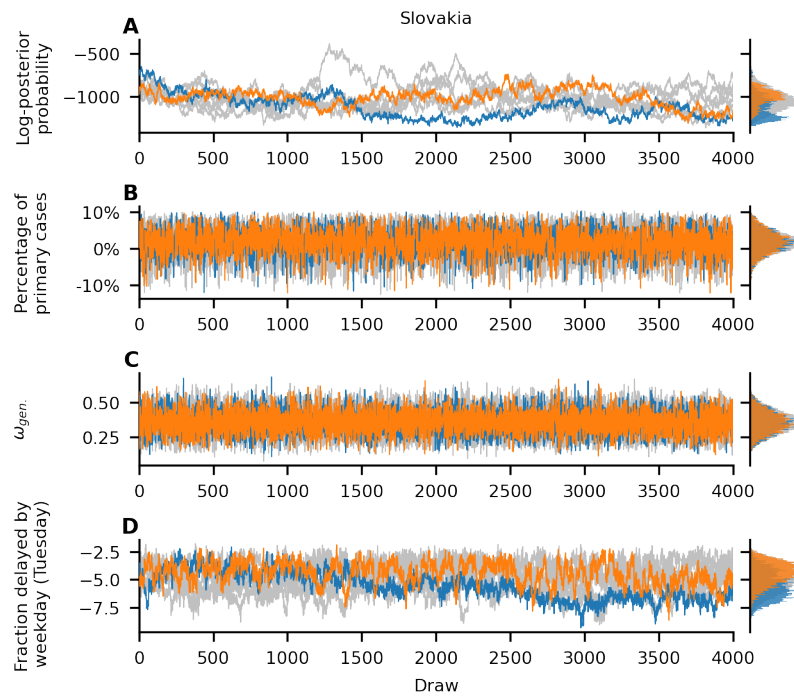
Supplementary Figure S44: **Chain mixing of selected parameters for Portugal** Here the fraction of cases delayed by weekday on Wednesdays is the parameter with the highest \mathcal{R} -hat values as seen in panel **D**. For a further detailed description of the panels see supplementary Fig. S37.



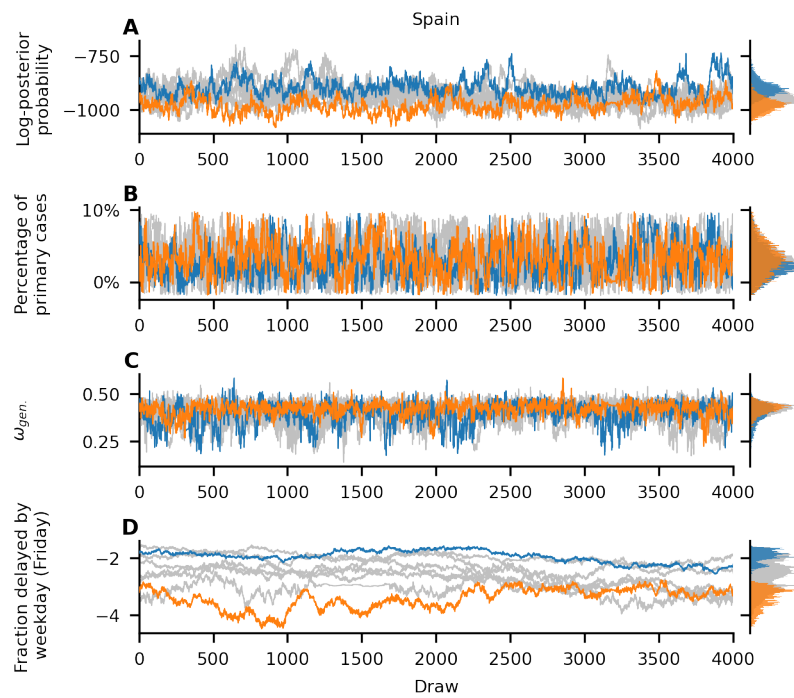
Supplementary Figure S45: **Chain mixing of selected parameters for Portugal** Here the fraction of cases delayed by weekday on Saturdays is the parameter with the highest \mathcal{R} -hat values as seen in panel **D**. For a further detailed description of the panels see supplementary Fig. S37.



Supplementary Figure S46: **Chain mixing of selected parameters for Scotland** Here the fraction of cases delayed by weekday on Wednesdays is the parameter with the highest \mathcal{R} -hat values as seen in panel **D**. For a further detailed description of the panels see supplementary Fig. S37.



Supplementary Figure S47: **Chain mixing of selected parameters for Slovakia** Here the fraction of cases delayed by weekday on Thursdays is the parameter with the highest \mathcal{R} -hat values as seen in panel **D**. For a further detailed description of the panels see supplementary Fig. S37.



Supplementary Figure S48: **Chain mixing of selected parameters for Spain** Here the fraction of cases delayed by weekday on Fridays is the parameter with the highest \mathcal{R} -hat values as seen in panel **D**. For a further detailed description of the panels see supplementary Fig. S37.